AWARD NUMBER: W81XWH-14-1-0006

TITLE: Preventing Ototoxic Synergy of Prior Noise Trauma during Aminoglycoside Therapy

PRINCIPAL INVESTIGATOR: Hongzhe Li, PhD

RECIPIENT:
VA Medical Center, Loma Linda, CA
Loma Linda, CA 92357

REPORT DATE: September 2021

TYPE OF REPORT: Final Technical Report

PREPARED FOR: U.S. Army Medical Research and Materiel Command
Fort Detrick, Maryland 21702-5012

REPORT DOCUMENTATION PAGE

Form Approved
OMB No. 0704-0188

1. REPORT DATE *(DD-MM-YYYY)*	2. REPORT TYPE	3. DATES COVERED *(From - To)*
SEPTEMBER 2021	Final Technical Report	1DEC2013 - 31MAY2021

4. TITLE AND SUBTITLE

Preventing Ototoxic Synergy of Prior Noise Trauma during Aminoglycoside Therapy

5a. CONTRACT NUMBER
W81XWH-14-1-0006

5b. GRANT NUMBER
11243004

5c. PROGRAM ELEMENT NUMBER

6. AUTHOR(S)

Hongzhe Li, PhD

E-Mail: Hongzhe.Li@va.gov

5d. PROJECT NUMBER

5e. TASK NUMBER

5f. WORK UNIT NUMBER

7. PERFORMING ORGANIZATION NAME(S) AND ADDRESS(ES)

VA Loma Linda Healthcare
System, Research (151)
11201 Benton Street
Loma Linda, CA 92357

8. PERFORMING ORGANIZATION REPORT NUMBER

9. SPONSORING / MONITORING AGENCY NAME(S) AND ADDRESS(ES)

U.S. Army Medical Research and Materiel Command
Fort Detrick, MD 21702-5012

10. SPONSOR/MONITOR'S ACRONYM(S)

11. SPONSOR/MONITOR'S REPORT NUMBER(S)

12. DISTRIBUTION / AVAILABILITY STATEMENT

Approved for Public Release; Distribution Unlimited

13. SUPPLEMENTARY NOTES

14. ABSTRACT

Upon the conclusion of the project, we have successfully identified two molecular targets among a handful candidates that contribute to an escalated inner ear ototoxicity. One is the Duffy antigen receptor for chemokines (Darc), and the other is the transient receptor potential vanilloid 1 (TrpV1). Both receptors actively mediate the process of cochlear inflammation, a lesser-previously researched condition resulting from exposure to moderate and intense noise stimulation, as well as other inner ear insults. In the present project, we used electrophysiology, immunohistochemistry, and cochlear perfusion techniques to conduct proposed experiments. The effect of inflammation on drug- or noise-induced ototoxicity was investigated in depth, such as using the applications of LPS and aminoglycosides. Acquired data were analyzed thoroughly, resulting in numerous conference abstracts and peer-reviewed publications.

15. SUBJECT TERMS
Noise trauma, combat injury, otoprotection, aminoglycoside antibiotic, gentamicin, loop diuretic, furosemide, bacterial infection, LPS, ototoxicity, auditory function, hearing loss

16. SECURITY CLASSIFICATION OF:			17. LIMITATION OF ABSTRACT	18. NUMBER OF PAGES	19a. NAME OF RESPONSIBLE PERSON
a. REPORT	b. ABSTRACT	c. THIS PAGE			USAMRMC
Unclassified	Unclassified	Unclassified	Unclassified	45	19b. TELEPHONE NUMBER *(include area code)*

Table of Contents

Background: Exposure to loud sounds causes temporary or permanent threshold shifts in auditory perception, with reversible or irreversible cellular damage in the cochlea. Noise trauma, or loud sound exposure, is particularly associated with military environments, especially when sustaining blast injuries. These injuries are frequently treated with aminoglycoside antibiotics that have broad-spectrum bactericidal activity for treating or preventing life-threatening infections. However, aminoglycosides are also toxic to the cochlea, leading to hearing loss and further degradation from pre-injury status. The combination of both prior noise trauma and aminoglycoside treatment can degrade auditory function greater than simple summation of the two insults. We have found that prior sound exposure enhances cochlear uptake of aminoglycosides, providing a mechanistic basis for the observed ototoxic synergy due to noise trauma and subsequent aminoglycoside treatment.

Objective/Hypothesis: The ultimate goal of this research is to prevent aminoglycoside-induced cochleotoxicity (as well as vestibulotoxicity and nephrotoxicity) that can severely debilitate the recovery of military personnel, including combatants and associated casualties to pre-injury effectiveness. In this proposal, we hypothesize that ***prior noise trauma induces synergistic ototoxicity with systemically-administered aminoglycosides by potentiating cochlear uptake of the drug.*** We also hypothesize that specific aminoglycoside-permeant cation channels directly facilitate noise trauma-enhanced uptake of aminoglycosides in the cochlea.

Specific Aims:

Aim 1: Determine the acoustic parameters that induce noise-enhanced aminoglycoside uptake in auditory sensory hair cells.

Aim 2: Determine if prior noise trauma modifies intra-cochlear trafficking of aminoglycosides.

Aim 3: Determine if aminoglycoside-permeant channels on the hair cell apical membrane contribute to aminoglycoside uptake by cochlear hair cells.

Aim 4: Determine if TRP channels on the basolateral membrane of cochlear hair cells also contribute to aminoglycoside uptake.

Study Design: In Aims 1, 3a and 4a, C57BL/6 mice, genetically-modified mice and Dunkin-Hartley guinea pigs will receive noise exposure followed by systemic aminoglycoside administration to determine the minimum and optimal acoustic paradigms that enhance hair cell uptake of aminoglycosides. Cochlear tissues will be examined by whole-mount preparation and confocal microscopy. In Aim 2 and 4b, cochlear perfusion will be performed with aminoglycosides administered either systemically or locally by scala tympani perfusion. In Aim 3b, noise-exposed organ of Corti will be prepared for scanning electron microscopy to correlate tip-link survival and drug uptake compared to control animals. In Aim 3c, cochlear explants will be prepared for MET blockade to determine if hair cells can take up aminoglycosides via TRPV4 and $P2X_2$ channels.

Relevance: Eliminating ototoxic synergy is not possible when prior loud or traumatic noise exposure is followed by treatment with aminoglycosides for blast, burns or penetrative injuries. The proposed research will test specific mechanisms to determine how noise trauma enhances aminoglycoside entry into cochlear hair cells to induce synergistic ototoxicity. This knowledge will enable the development of countermeasures to preserve auditory function during sequential and synergistic ototoxic insults in military environments.

1. INTRODUCTION

Exposure to loud sounds causes temporary or permanent threshold shifts in auditory perception, with reversible or irreversible cellular damage in the cochlea. Noise trauma, or loud sound exposure, is particularly associated with military environments, especially when sustaining blast injuries. These injuries are frequently treated with aminoglycoside antibiotics that have broad-spectrum bactericidal activity for treating or preventing life-threatening infections. However, aminoglycosides are also toxic to the cochlea, leading to hearing loss and further degradation from pre-injury status. The combination of both prior noise trauma and aminoglycoside treatment can degrade auditory function greater than simple summation of the two insults. We have found that prior sound exposure enhances cochlear uptake of aminoglycosides, providing a mechanistic basis for the observed ototoxic synergy due to noise trauma and subsequent aminoglycoside treatment.

In the mammalian inner ear – the cochlea, the auditory sensory cells, particularly outer hair cells (OHCs), are more susceptible to aminoglycoside-induced cytotoxicity than other cochlear cells, particularly at the base of the cochlea most sensitive to higher frequency sound. Once these OHCs are lost, these sensory cells cannot be endogenously regenerated, leading to life-long hearing loss and deafness. Thus, extensive efforts are underway to ameliorate and prevent aminoglycoside-induced hair cell death. Under normal physiological condition, aminoglycosides can rapidly cross the blood-labyrinth barrier (BLB) into the cochlear tissues and fluids and enter OHCs through a number of conduits. The best-characterized conduit is permeation through the mechanoelectrical transduction (MET) channel. The MET channel is mechanically-gated by the extracellular, heterodimeric tip links between two stereocilia. Other mechanisms by which aminoglycosides can enter hair cells include endocytosis, and/or other aminoglycoside cation channels (*e.g.* TRP channels) expressed by hair cells besides the MET channel, such as TRPV4 on the apical membranes, or TRPA1 on the basolateral membranes, of OHCs.

The ultimate goal of this research is to prevent aminoglycoside-induced cochleotoxicity (as well as vestibulotoxicity and nephrotoxicity) that can severely debilitate the recovery of military personnel, including combatants and associated casualties to pre-injury effectiveness. In this project, we hypothesize that prior noise trauma induces synergistic ototoxicity with systemically-administered aminoglycosides by potentiating cochlear uptake of the drug. We also hypothesize that specific aminoglycoside-permeant cation channels directly facilitate noise trauma-enhanced uptake of aminoglycosides in the cochlea.

2. KEYWORDS

Noise trauma, combat injury, otoprotection, aminoglycoside antibiotic, bacterial infection, ototoxicity, auditory function, hearing loss

3. OVERALL PROJECT SUMMARY

What were the major goals of the project?

Aim 1: Determine the acoustic parameters that induce noise-enhanced aminoglycoside uptake in auditory sensory hair cells.

This is completed at OHSU.

Aim 2: Determine if prior noise trauma modifies intra-cochlear trafficking of aminoglycosides.

Aim 2a: Use cochlear perfusion techniques to determine the contribution of endolymph or perilymph trafficking of aminoglycosides to hair cells with prior noise exposure. GTTR will be administrated either systemically or by scala tympani infusion to the animal.

This is completed at OHSU.

Aim 3: Determine if aminoglycoside-permeant channels on the hair cell apical membrane contribute to aminoglycoside uptake by cochlear hair cells.

Aim 3a: Determine if prior noise trauma enhances drug uptake in hair cells.

This is completed at Loma Linda.

Aim 3b: Examine tip-link integrity in noise-exposed rodents by scanning electron microscopy.

This is completed at Loma Linda.

Aim 3c: Confirm that hair cell $P2X_2$ and TRPV4 channels are aminoglycoside-permeant.

This is completed at Loma Linda.

Aim 4: Determine if TRP channels on the basolateral membrane of cochlear hair cells also contribute to aminoglycoside uptake.

Aim 4a: Determine if noise enhances drug uptake in TrpA1 or TrpV1 mice.

This is completed at Loma Linda.

Aim 4b: Verify that scala tympani perfusion of TRPA1 or TRPV1 antagonists in noise-exposed guinea pigs inhibit noise-enhanced uptake of GTTR.

This is completed at Loma Linda.

What was accomplished under these goals?

1) Major activities

During the entire span of the project, we performed research activities using electrophysiology, immunohistochemistry, and cochlear perfusion techniques to conduct proposed experiments. Substantial number of lab members contributed to the project, and most of them have left the lab and moved forward along their career path. The effect of inflammation on drug- or noise-induced ototoxicity was investigated in depth, including but not limited by using the applications of LPS and aminoglycosides. Acquired data were analyzed thoroughly, resulting in numerous conference abstracts and peer-reviewed publications.

2) Specific objectives

Objectives at OHSU

a) Confirm that prolonged prior noise exposure enhances GTTR uptake by sensory cochlear outer hair cells, with updated in-house software for noise exposure and newly sound calibration.

b) Determine the degree of hearing loss that is induced by each paradigm of noise exposure using separated batches of mice.

c) Acquire Dunkin-Hartley guinea pigs from Charles River Laboratory and establish hearing sensitivity standard by auditory brainstem response (ABR) measurement in this strain of guinea pigs, using a new ABR acquisition system.

d) Expose guinea pigs to wide band noise (WBN) and reliably produce hearing threshold shift, and document the cellular uptake of GTTR. That is, using our new ABR acquisition system, to investigate the effect of WBN on the hearing sensitivity of guinea pigs, as well as the intra-cochlear trafficking of GTTR.

e) Quantify the GTTR fluorescence signals in the cochlear tissue, including strial tissue (marginal cell layer, intermediate cell layer and basal cell layer) and organ of Corti (outer hair cells, inner hair cells and pillar cells). Additionally, measure the vessel diameter distributions of the strial capillaries in both sound-treated and control animals.

f) Establish image processing techniques for diameter measurement of strial capillaries.

g) Measure capillary diameters in control stria vascularis, and in sound-treated strial vascularis.

h) Examine the effect of cardiac perfusion on sound-induced vasodilation in strial capillaries.

i) Establish and expand *TrpV1* mouse cohort.

j) Immuno-label cochlear and kidney tissue from both heterozygous and mutant *TrpV1* mice, using TRPV1 antibodies from two different manufactures.

k) Characterized the effect of *TrpV1* deletion on auditory sensitivity at multiple postnatal ages, by measuring ABR.

l) Establish and expand *Myo7a* mouse cohort.

m) Quantify outer (OHC) and inner hair cell (IHC) survival in young adult mutant mice.

n) Systemically administer GTTR in mutant neonatal mice, or in adult mice.

o) Characterize the effect of *Myo7a* mutation on the uptake of GTTR, by examining OHC survival in the organ of Corti.

Objectives at Loma Linda

a) Initiated mouse cohorts including *TrpV1* mice (#3770, Jackson Laboratory, Bar Harbor, ME) and wildtype *C57BL/6* mice (#0664) in the animal facility at Loma Linda. Breeding pairs were periodically purchased to keep the cohorts genetically consistent with the original source.

b) Acquired and setup lab equipment, including noise exposure instrument and ABR measurement apparatus. One of the ABR system is primarily driven by a TDT-RZ6 system, purchased from Tucker-Davis Technology (Alachua, FL) through the PI's startup fund. In addition, both the noise chamber and the sound delivery component of the ABR system has been calibrated using a ¼'' B&K microphone, to ensure the accuracy of sound levels that are presented to experimental animals.

c) Accumulated adequate number of *TrpV1* mice, and characterized the mutant mice by ABR testing. Newly acquired experimental data are compared to those from PI's previous lab at Oregon Health & Science University (OHSU).

d) Developed genotyping protocols to identify mutant mice and heterozygous mice in the *TrpV1* cohort. We could either use the traditional PCR method or a quantitative PCR system to achieve the genotyping purpose within the lab.

e) Continue to host mouse cohorts including *TrpV1* mice (#3770) and wildtype *C57BL/6* mice (#0664) in the animal facility, and initiated $P2X_2^{-/-}$ (#4603) and $TrpV4^{-/-}$ (#29582) mice. Breeding pairs were purchased from Jackson Laboratory (Bar Harbor, ME). We also initiated and studied a mouse strain named by *Darc*, which is similar to *TrpV1* mice in certain ways including cellular response to noise exposure.

f) Acquired new lab equipment, including a laser scanning confocal microscope and a dissecting microscope (both from Olympus Inc.) through the PI's supporting mechanisms. In addition, a data backup system within the lab has been put into use.

g) Lab staff have been trained and are now proficient in experimental techniques including acoustic and electrophysiological recordings (*e.g.* DPOAEs and ABRs), evaluation on cochlear cytokine levels, and cochlear synaptic ribbon labeling and imaging.

h) Initiated tissue cultural experiments with cochlear explants. An additional dissecting microscope has been acquired and new research staff trained for the aseptic organ culture process and subsequent imaging techniques.

i) Using organotypic culture approach, we have evaluated aminoglycoside candidate channels, including TrpV4 and $P2X_2$ channels.

j) With noise exposure and intratympanic injection of LPS, we investigated the morphology and infiltration of cochlear macrophages. In addition, we studied LPS-induced cochlear uptake of ototoxic aminoglycosides, in the scope of inflammation-enhanced ototoxicity.

k) As our *TrpV1* mouse cohorts getting older, we tested the residual hearing in terms of age-related hearing loss in the background of *C57BL/6*, to increase our understanding of the immunomodulatory role of this multipotent cellular sensor.

l) Investigated the effect of intratympanic LPS on cochlear uptake of ototoxic aminoglycosides, in both wildtype mice and in *TrpV1* mice. We studied the correlation between modulated drug uptake and inflammatory events, including the morphology and infiltration of cochlear macrophages and the variation of immune active cytokines' variation.

m) Longitudinally monitored a small *TrpV1* mouse cohort (as well as a *Darc* mouse cohort) as they are getting older, to reveal the effect of the mutant allele on the systemic aging process.

n) Investigated the dose-dependent effect of gentamicin and furosemide in combination on producing cochlear damage, by 1) characterizing the residual hearing function, 2) distinguishing the morphology of outer and inner hair cells, and ribbon synapses at various cochlear locations, and 3) determination of the synaptic variation in number, and in morphological distribution.

4. KEY RESEARCH ACCOMPLISHMENTS

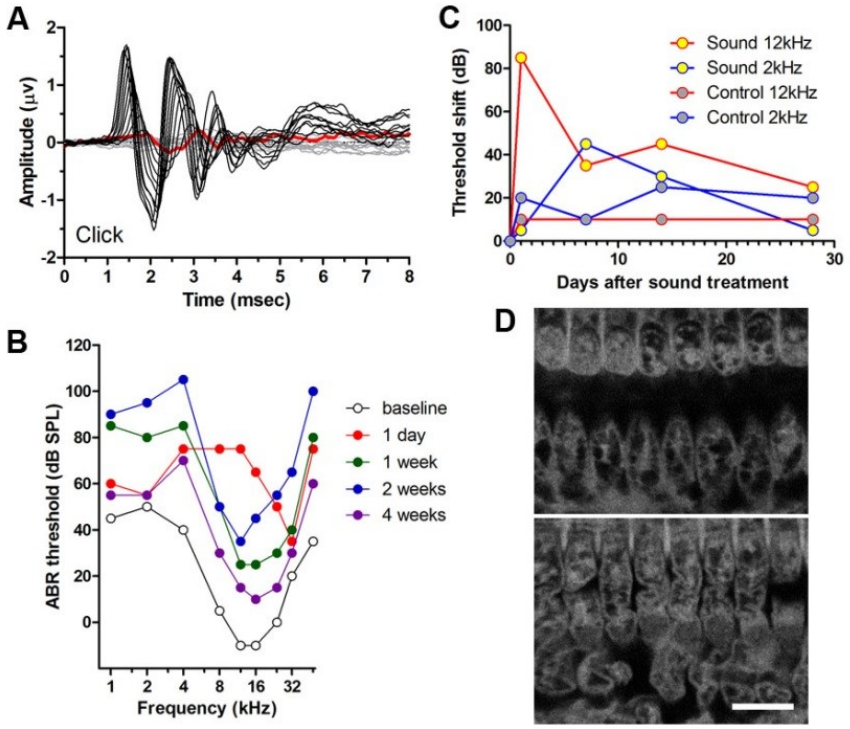

Figure 1. Sound-induced TTS and GTTR uptake by OHCs. A: ABR response traces to click at different sound levels, with 5-dB step. Black traces depict supra-threshold responses while gray traces depict under-threshold responses. The thick red trace depicts the threshold which is 55 dB in this example. B: Tonal ABR thresholds were measured before and after WBN exposure at 96 dB SPL. Different temporal patterns of TTS were observed at lower and higher frequencies, as delineated in C: largest TTS occurred immediately after sound exposure at 12 kHz, while occurred with delay at 2 kHz. In addition, shifts as large as 20-25 dB occurred in control ears without sound exposure. D: GTTR uptake by OHCs was observed in 2 kHz region (upper panel) and in 12 kHz region (lower panel). Scale bar is 20 μm.

a) After WBN exposure at 96 dB SPL of 18 hours (6 hours per day for 3 consecutive days), Dunkin-Hartley guinea pigs exhibit temporary threshold shifts across frequencies (Fig. 1B). However, the most prominent TTS occurred at different time. For instance, at low frequencies such as 2 kHz, the largest TTS occurred 7 days after sound exposure, which was

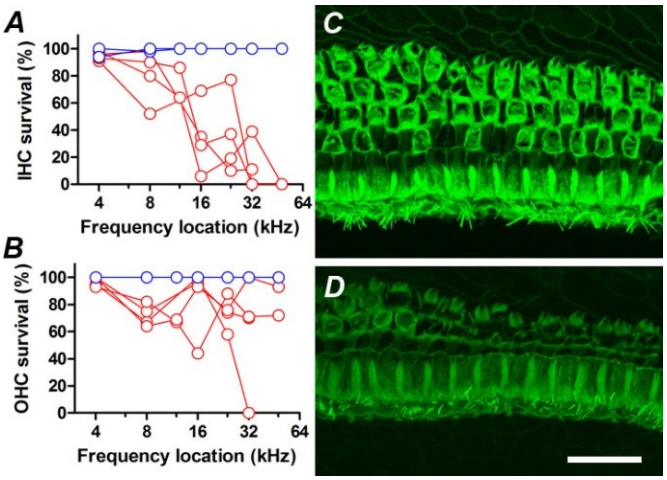

Figure 2. Hair cell loss in adult Myo7a mutant mice. A: Massive OHC loss was observed from 4 individual 5-week-old Myo7a$^{8J/8J}$ mutant mice (red), while little or no cell loss from 2 littermate control Myo7$^{8J/+}$ heterozygous mice (blue). B: Similarly, IHC loss was observed from the same group of mutant mice (red), while no cell from control group (blue). C: With phalloidin labeling, surviving but unhealthy OHCs could be seen from some mouse at 24 kHz cochlear region. The hair bundle of IHCs was identifiable with disarrayed stereocilia. D: In another mouse, OHCs were largely gone at 24 kHz cochlear region. Scale bar = 25 μm.

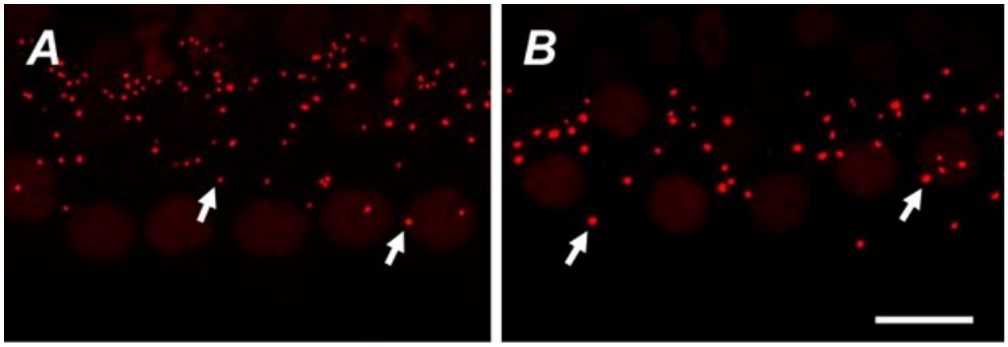

Figure 3. Ribbon synapses from control mice (A) and TrpV1 knockout mice (B). Arrows depict exemplified ribbon synapses that were immunolabeled by anti-CtBP2 IgG. Note that the antibody also labeled the nucleus of inner hair cells. Scale bar is 10 µm.

deviant from higher frequencies, such as 12 kHz, where largest TTS occurred 1 day after sound exposure (Fig. 1C).

b) Unlike wildtype or heterozygous littermate mice, the mutant *Myo7a*$^{8J/8J}$ mice are known of severe hearing loss. Indeed, here we observed massive hair cell loss in 5-week-old young adult mutant mice (Fig. 2A&B). The cell loss was more severe for OHCs compared to IHCs at the same frequency locations; the loss was also more severe at frequencies above 16 kHz, with large variation among individual animals (Fig. 2C&D).

c) We conducted immunofluorescent experiments in which the ribbon synapse of the inner hair cell afferent innervation is evaluated using cochlear micro-dissection and confocal imaging techniques. Our preliminary result in aged mice (~28 weeks of age) suggested that *TrpV1* deficiency appeared to reduce the number of ribbon synapses while enlarged the size of individual ribbons (Fig. 3B), suggesting an incomplete compensatory mechanism. We will study more animals with various ages to confirm this observation.

d) Experiments on *TrpV1* mice from PI's previous lab at OHSU indicated that non-functional TRPV1 protein/subunits were expressed in homozygous mice. The non-functional protein could be detected using anti-TRPV1 sera at the expected channel location (*personal commnuciation with Dr. Steyger*). Assuming the non-functional TRPV1 subunits participate in the channel assembly, a TRPV1 channel (tetramer) with both functional and non-functional TRPV1 subunits can be overall non-functional, unless all four subunits are

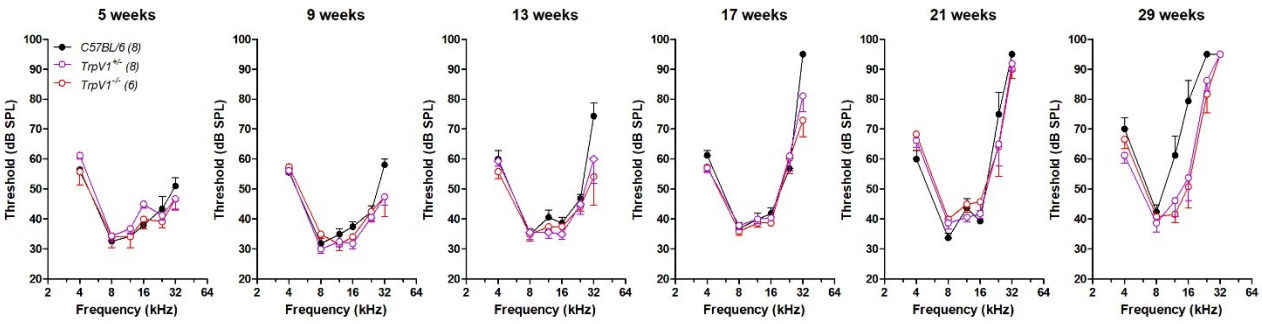

Figure 4. Longitudinal ABR thresholds from TrpV1 heterozygous and homozygous mice, as well as C57BL/6 lab control mice from 5 weeks of age to 29 weeks. Number of mice per group is indicated in the parenthesis.

wildtype (a probability of 1/16). That is, *TrpV1* heterozygous mice predominanently (93.75%) exhibit the phenotypic "dominant negative".

e) Bearing the effect of dominant negative in mind, we revisited the longitudinal ABR data collected in *TrpV1* mice and compared them with *C57BL/6* lab control. As the mice aged, ABR threshold elevation was evident starting from higher frequencies in all tested groups. However, the age-related high frequency hearing loss in *TrpV1* mice (either heterzygotes or homozygotes) trailed *C57BL/6* mice (Fig. 4). For instance, from week 9 to week 17 at 32 kHz. The trailing effect was overt at the age of 29 weeks, exhibiting a clear ABR threshold gap from 12 to 24 kHz, when the threshold at 32 kHz was too high to be detectable in all groups. Although the hearing deterioration in both *TrpV1* groups were very similar, a subtle difference was catchable at the 32 kHz, showing better ABR threshold in homozygous mice, for instance, at week 13 and 17, suggesting a small portion of TRPV1 channels in heterozygotes were still functional, as predicted in b). Overall, the observation of delayed age-related hearing loss in *TrpV1* mice is in accordance with the report of improved longevity in the same mice (Riera et al. 2014). In addition, this experimental approach provides us fundamental knowledge to achieve the goals in Specific Aims 3 and 4, given that the TRPV1 channel is a candidate channel for aminoglycoside uptake by sensory hair cells.

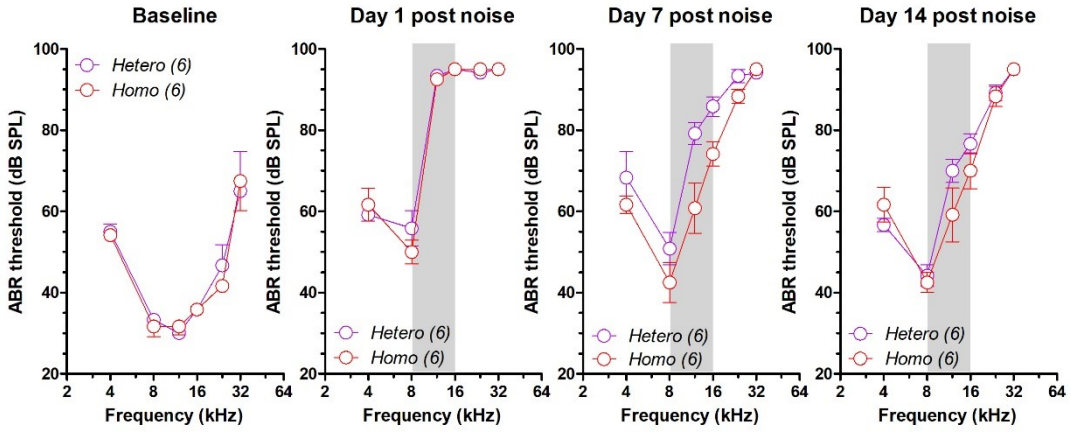

Figure 5. ABR thresholds elevated after the exposure to an octave-wide band noise (8-16 kHz, 106 dB SPL, 2 hours) in TrpV1 mice.

f) We also recruited a small cohort of *TrpV1* mice, including both homozygotes and heterozygotes as littermates, and exposed them to octave-wide band noise (8-16 kHz, 106 dB SPL, 2 hours). The mice started with similar baseline ABR thresholds, and similar thresholds one day after noise exposure (Fig. 5). However, one week after noise exposure, the ABR thresolds in *TrpV1* homozygotes were significantly better than heterozygotes littermate controls (2-way ANOVA, p=0.0011). The improved hearing recovery from noise existed no longer 2 weeks after noise exposure (2-way ANOVA, p=0.67). The results suggested the beneficial effect of TRPV1 deficiency in the cochlea, as shown in the dataset of longitude ABR thresholds (Fig. 4), is likely a local effect to the inner ear, rather than a global effect of improved metablism that was reporeted previsouly in *TrpV1* homozygotes (Riera et al. 2014). It has been known that LPS-induced cochlear inflammation is reduced in *TrpV1* mice (Jiang et al. 2015). Our data from noise exposure in *TrpV1* mice suggested that inflammation suppression alleviated cochlear damage and improved hearing recovery.

g) Immunohistochemisty indicated that TRPV1 channels are located at the organ of Corti, on the cuticular surface constituting hair cells, pillar cells and the phalangeal processes. The expression level is particularly high on the membrane of phalangeal process, suggesting a possible shunt mechanism for endolymphatic cation to sink into supporting cells instead of hair cells upon over-stimulation. To test this hypothesis, we conducted experiment to evaluate temporal threshold shift (TTS) development in *TrpV1* mice (Fig. 6).

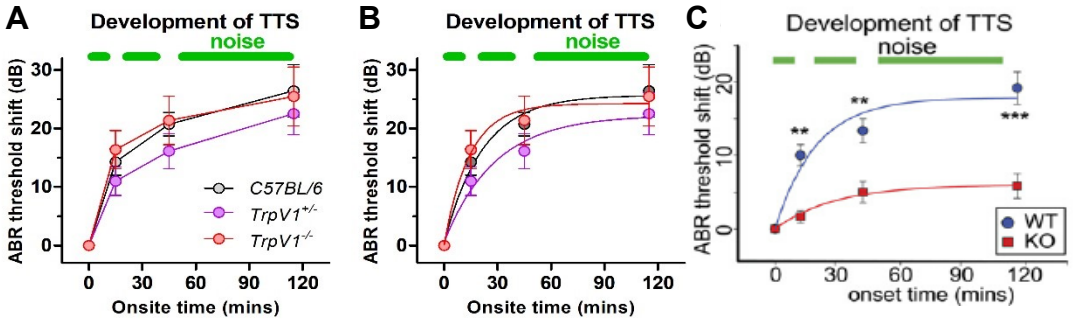

Figure 6. TTS development in TrpV1 mice (A, B) and $P2X_2$ mice (C).

Quick background: Purinergic receptor/subunit $P2X_2$ is a major component of an ATP-stimulated macropore with weakly selective cation permeability, potentially including aminoglycosides. Similar to *TrpV1* and *TrpV4* mice, age-related hearing loss is also reported in *$P2X_2$* mutant mice. Additionally, $P2X_2$ receptor is a major adaptation component that contributes to TTS after acoustic trauma. Using intermittent noise exposure and tonal ABR threshold measurement, it has been reported that the development of TTS is suppressed in *$P2X_2$* mutant mice (Housley et al. 2013). Compromised adaptation is considered the underlying mechanism of age-related hearing loss in *$P2X_2$* mutant mice.

We used a similar experiment protocol: (i) intermittent noise exposure (95 dB SPL, 4-32 kHz, closed-field), (ii) ketamine & xylazine anesthesia, (iii) ABR threshold measurement with 12-kHz tone pips, and observed enhanced TTS development in *$TrpV1^{+/-}$* (n=10), *$TrpV1^{-/-}$* (n=11) and *C57BL/6* (n=7) mice. Two-way ANOVA implicated no difference between any pair of groups in TTS development. Single exponential curve fits for TTS growth; time constants were 19.8, 9.9 and 14.9 min for *$TrpV1^{+/-}$*, *$TrpV1^{-/-}$* and *C57BL/6* mice respectively. Thus, the observation does not suggest that TRPV1 participates the development of TTS or noise-triggered adaptation process.

h) We also examined IHC synaptic ribbon densities in *TrpV1* homozygotes and heterozygotes, after the OBN exposure that is described in d). Exposure to OBN induced great reduction of ribbon density in *TrpV1* heterozygotes compared to *TrpV1* homozygotes at both tested frequencies, 16 and 24 kHz (Fig. 7). Combining loop diuretics to aminoglycoside treatment is an effective approach for accelerating ototoxic damage, especially, in mice, which results in immediate cochlear

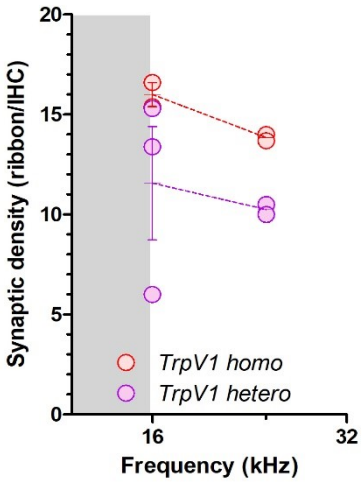

Figure 7. Synaptic ribbon densities from OBN-exposed TrpV1 mice, examined at 16 and 24 kHz. Gray area indicates the frequency range of the OBN (8-16 kHz, 106 dB SPL, 2 hours).

trauma (Hirose and Sato, 2011; Taylor *et al.*, 2008). In this simplified version of a mouse ototoxicity model, the addition of loop diuretics, such as furosemide, disrupts the blood labyrinth barrier thereby greatly elevating the concentration of aminoglycosides, such as gentamicin, in the cochlea (Ding *et al.*, 2016; Taylor *et al.*, 2008). Furosemide, by itself, is not considered directly damaging to the inner-ear components including hair cells (HCs), ribbon synapses or spiral ganglion neurons (SGNs) (Rybak, 1993). In the present study, the dose-dependent effect of gentamicin and furosemide (G/F) in combination was investigated to: 1) characterize the residual hearing function, 2) distinguish the morphology of OHCs and IHCs, and ribbon synapses at various cochlear locations, and 3) determine whether there is a change in the number, or the distribution, of synaptic ribbons.

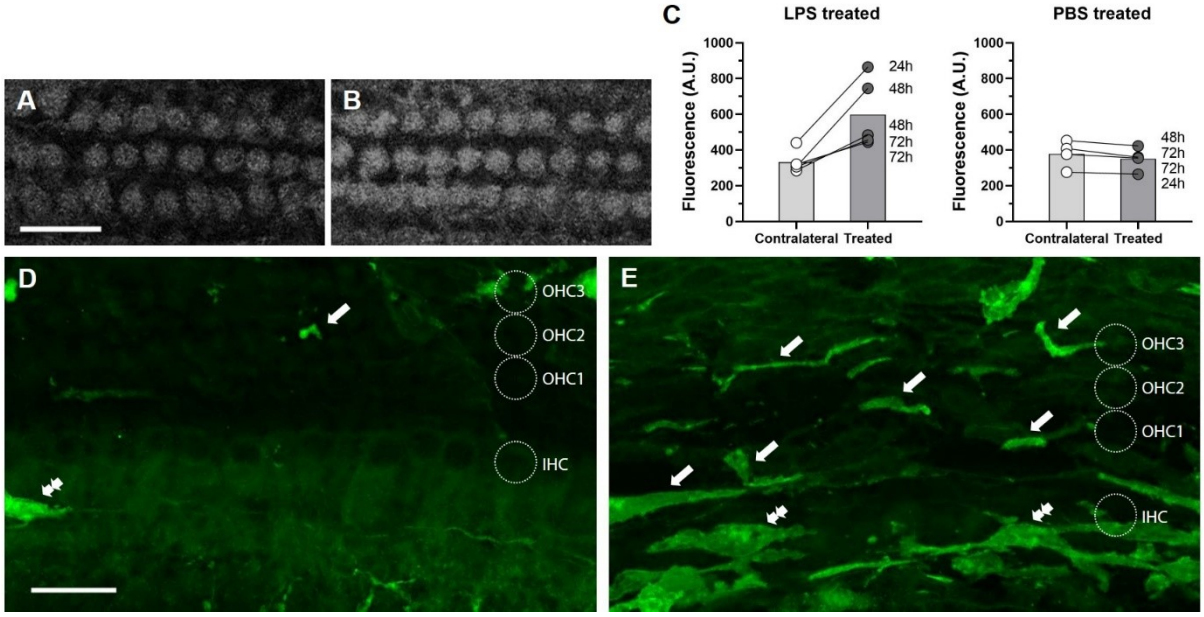

Figure 8. Intratympanic injection of LPS enhanced hair cell uptake of systemically administered GTTR and macrophage infiltration to the cochlea's basilar membrane. A: Baseline uptake of GTTR (2 mg/kg bw, ip, at 1 h) by OHCs in the contralateral ear of an LPS treated subject. B: Elevated GTTR fluorescence in the OHCs from the LPS-treated ear 48 hours after the treatment (it, ~10 µl, 1 mg/ml). Scale bar = 20 µm. C: LPS treatment enhanced OHC uptake of GTTR in the middle cochlear coil of the treated ears compared to the untreated contralateral ears from all tested mice (n=5, p=0.017, paired t-test), while PBS treatment did not (n=4). Systemic GTTR was administered to the mice at 24, 48 and 72 hours after the LPS/PBS treatment. The effect of the time point of post-LPS/PBS treatment was not evaluated, given the limited animal number per time point. A.U. = arbitrary unit. LPS batches were not identical among tested animals, nor the laser power for confocal imaging to quantify GTTR fluorescence, thus, the fluorescent values were not intended to be compared within each group. D: Anti-Iba1 labeling revealed a limited number of macrophages along the basilar membrane (BM) in the contralateral ear of it-LPS treatment. Scale bar=20 µm. E: Increased number of anti-Iba1-identified macrophages were recruited to the BM. These macrophages were either located below OHCs and Deiter's cells (arrow), or located in the osseous spiral lamina, basolateral to inner hair cells (IHCs, double arrows), and appeared in the activated form that lacks fine processes and orientated along the BM.

i) It is known that intensive noise exposure elevates cochlear immune activities, manifested by increased number of tissue specific macrophages in the cochlea. Thus, we rationalized that the prior noise trauma-induced cochlear immune activity includes TRPV1 channel activation

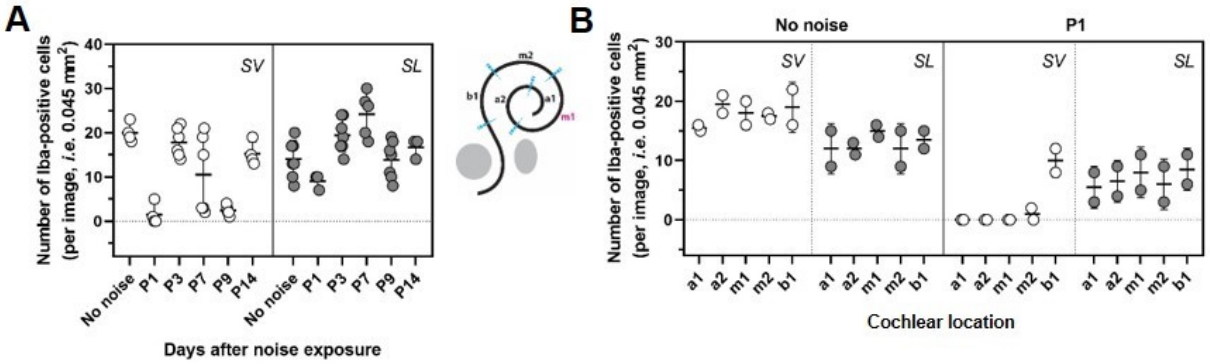

Figure 9. Intense noise exposure (112 dB SPL, OBN) modulated Iba1-positive strial macrophages. A: A significant reduction of Iba1-positive macrophages in the stria vascularis (SV) occurred 1 and 9 days after the noise exposure ($p<0.0001$, unpaired t-tests, n = 3-5 per time point). Iba1-positive macrophages located laterally to the SV, in the spiral ligament (SL) were also examined. The number of these macrophages was also modulated, though to a lesser degree. The middle cochlea coil (m1) was sampled here, as indicated in the diagraph. Mean and s.d. are depicted in whiskers. B: The density of macrophages in the SL was generally lower than that in the SV along the entire length of the cochlea. However, the tendency was reversed one day after noise exposure.

which subsequently enhances aminoglycoside ototoxicity. To test above hypothesis, we induced reliable cochlear inflammation by systemic endotoxemia. In these mice, we observed increased expression of Trp1 in the cochlea and increased uptake of circulating aminoglycosides (GTTR as tracer) by hair cells. Alternatively, we also induced reliable cochlear inflammation by topical lipopolysaccharide (LPS) treatment, and investigated cochlear macrophages by Iba1 labeling. In recent years, Iba1 antibody has been increasingly used in hearing research labs as a cell marker to identify tissue macrophages/microglia. After LPS inoculation, we did observe increased number of Iba1+ cells in many cochlear locations, including the spiral ligament, the basilar membrane (Fig. 8E), the spiral limbus and the spiral lamina, but not in the stria vascularis (SV; Fig. 9).

j) The Iba1+ macrophages in the SV are considered perivascular macrophages, essential for the integraty of the blood labyrinth barrier. In order to understand their behavior after prior noise exposure, we studied Iba1+ labeling in the SV after 2-hour intensive OBN expsoure (112 dB SPL, 8-16 dB). Suprisingly, the number of Iba1+ cells in the SV is modulated with a tendency of reduction instead of increment. The reduction is alarmingly significant 24 hours after noise exposure (Fig. 9A) towards the apex (Fig. 9B). We'd like to further confirm this observation and investigate the functional significance of this SV specific redution.

k) Both noise and bacterial exposure induce cochlear inflammation, and subsequently enhance aminoglycoside ototoxicity. Here, we also question if aminoglycoside treatment itself activates cochlear immune cells, by using tandem intraperitoneal gentamicin and loop diuretic furosemide (G/F) to challenge the inner ear tissue. We did observe increased Iba1-positive activities along the basilar membrane, specially at the spiral laminar, 3-day and 7-day after the G/F treatment (Fig. 10). The Iba1+ activity appears more prominent on 3-day posttreatment compared to 7-day. Although higher gentamicin dose (400 mg) resulted in hair cell loss, but not necessarily more Iba1+ activity.

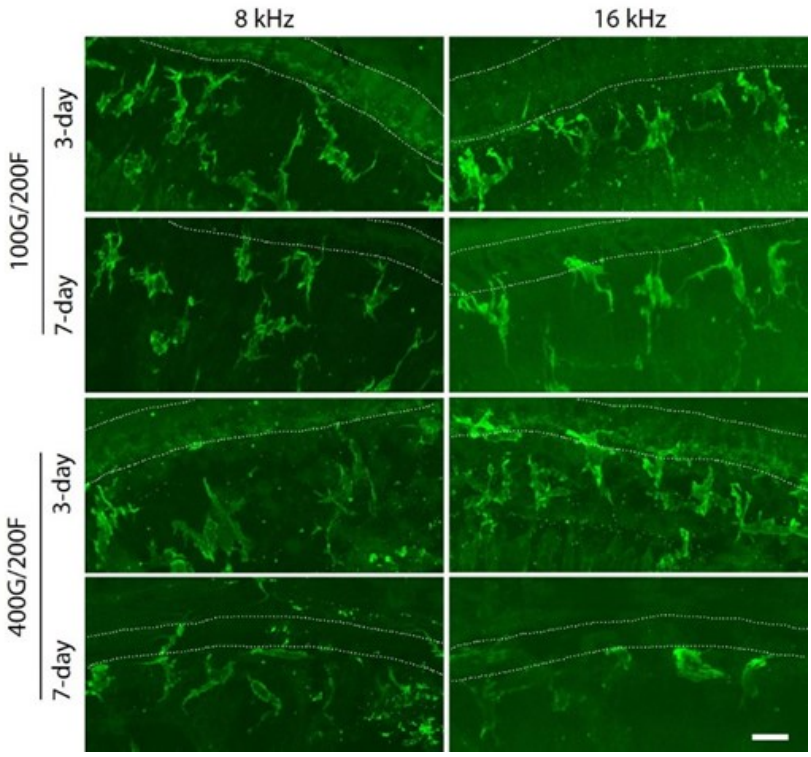

Figure 10. Induction of cochlear macrophages after combined treatment of gentamicin and furosemide. Three days or seven days after the combined treatment using 100 mg/kg gentamicin and 200 mg/kg furosemide (top panels), or 400 mg/kg and 200 mg/kg furosemide (bottom panels), macrophages or microglia cells were immunolabeled by anti-Iba1 antibodies with green fluorescence. Micrographs indicated elevated Iba1+ activity at the cochlear locations equivalent to 8 and 16 kHz in the spiral laminar. Dotted lines depict the location of inner hair cells, and scale bar=20 µm.

l) In the past a few years, we have gained increasing understanding on external factors that agitate the inner ear immune homeostasis, including acoustic overexposure, bacterial inoculation, and aminoglycoside application. All our prior experiments in the project were conducted in *C57BL/6 (BL6)* mice. We already knew that different wildtype mouse strains exhibited varied susceptibility to aminoglycoside ototoxicity, as well as to noise challenge. For instance, *BL6* mice are frequently used as the ototoxicity mouse model, while *CBA/CaJ (CBA)* mice are suggested in other hearing-related studies, given that *BL6* strain harbors the premature and age-related hearing loss gene. Thus, the mouse strain effect on the activation of cochlear immune response is an inevitable scientific question. We performed intratympanic (*i.t.*) injection of LPS in both *BL6* and *CBA* mice, and documented the morphological response of Iba1-positive macrophages in the cochlea, specifically in the organ of Corti, along the basilar membrane (Fig. 11). In sum, *i.t.* LPS inoculation activated Iba1+ macrophages in both wildtype strains, while *BL6* mice exhibited higher responsive features, including the increase of macrophage numbers and extensive arborization. The difference between two strains appeared more significant in the basal region of the cochlea.

m) Likewise, the mouse strain effect on the cochlear vulnerability to combined gentamicin / furosemide (G/F) challenge is a scientifically valuable question. The effect can be evaluated

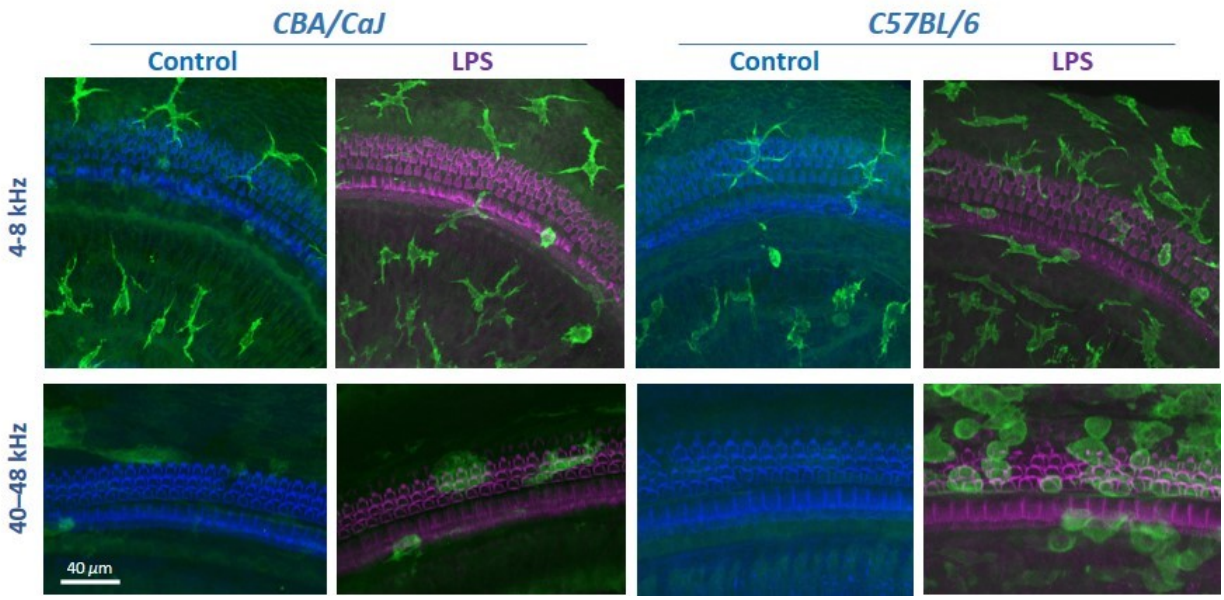

Figure 11. Induction of cochlear macrophages after intratympanic LPS treatment. Two days after the LPS treatment (1 mg/ml, 10 µl), micrographs indicated elevated Iba1+ activity at both the apical and basal cochlear locations. The elevated macrophage activity was more prominent in C57BL/6 mice compared to CBA/CaJ mice. Scale bar=40 µm.

by hair cell survival, ribbon density, and macrophage activation. We found the treatment induced a rapid recruitment of resident macrophages into the damaged basal turn of cochlea of *CBA* mice despite of IHC survival (Fig. 12). This event is hypothetically related to glutamate release after the ototoxic challenge that might directly activates resident cochlear macrophages in the sensory epithelium and protect the synaptic region from further injury in *CBA* mice (Biber et al. 1999; Matsuda et al. 2000). In addition, the G/F treatment also induced the loss of ribbon synapses following OHC loss 15-day posttreatment in both mouse strains; statistical significance was achieved in *BL6* mice only.

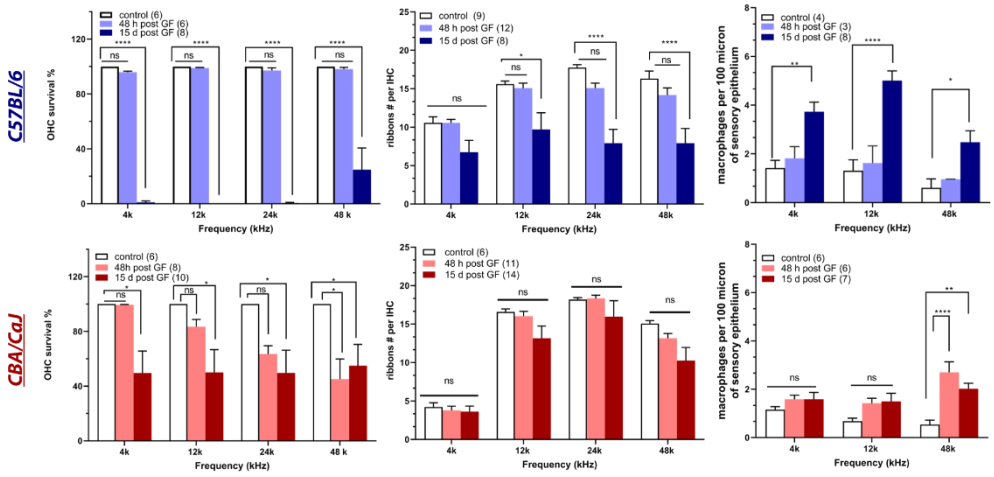

Figure 12. The mouse strain effect on the cochlear vulnerability to combined G/F challenge.

5. CONCLUSION

Cochlear inflammation has gradually become a major research topic in recent years in auditory neuroscience. It is first known that intensive noise exposure elevates cochlear immune activities, manifested by increased number of tissue specific macrophages and elevated cytokine levels in the cochlea. In addition, we recently found that aminoglycosides also trigger cochlear immune response without other extrinsic inflammatory triggers. This finding raised the clinical significance of this line of research, given that aminoglycoside antibiotics are often prescribed to patients with systemic or local infection to suppress a potential or ongoing bacterial presence. The exact role of these cochlear macrophages and their elevated activities is not totally clear. It is known that the function of tissue macrophages is multifaced. We studied the event sequence upon aminoglycoside-induced cochlear damage, including hair cell loss, synaptic damage and macrophage behavior. The recruitment or proliferation of cochlear macrophages appeared as a prelude to hair cell loss, and definitely occurred ahead of synaptic damage. These findings suggest that cochlear macrophages, at least the ones located in the spiral laminar, likely underpin a protective mechanism to the neuronal elements in the cochlea that is essential for a reliable signal transmission, and certainly warrant further investigation.

Over the project period of XW81XWH-14-1-0006, we have successfully identified two molecular targets among a handful candidates that may contribute to an escalated inner ear ototoxicity. One is the Duffy antigen receptor for chemokines (Darc), and the other is the transient receptor potential vanilloid 1 (TrpV1). Understanding their presence in the untreated cochlea and modulation in the inflammatory cochlea are essential in the development of countermeasures to prevent cochlear damage by variety of insults, including but not limited to acoustic overexposure and drug-induced ototoxicity.

6. PUBLICATIONS, ABSTRACTS AND PRESENTATIONS

Peer reviewed publication

1. Meiyan Jiang; Qi Wang; Takatoshi Karasawa; Jawon Koo; Hongzhe Li; Peter S. Steyger (2014). Sodium-glucose transporter-2 (SGLT2; SLC5A2) enhances cellular uptake of aminoglycosides. PLoS ONE 9(9). doi: 10.1371/journal.pone.0108941
2. Lauren Luk; Hongzhe Li; Peter S. Steyger (2014). Perilymphatic Gentamicin Trafficking through Basolateral Channels May Underlie Enhanced Ototoxicity by Noise-Induced Threshold Shifts. Otolaryngology Head and Neck Surgery 151(1 Suppl):P222. doi:10.1177/0194599814541629a268
3. Jianping Liu; Jianping Liu, Allan Kachelmeier, Chunfu Dai, Hongzhe Li, Peter S. Steyger (2015). Uptake of Fluorescent Gentamicin by Peripheral Vestibular Cells after Systemic Administration. PLoS ONE 10(3): e0120612. doi: 10.1371/journal.pone.0120612
4. Yuqin Yang; Fangyi Chen; Takatoshi Karasawa; Ke-Tao Ma; Bing-Cai Guan; Xiao-Rui Shi; Hongzhe Li; Peter S. Steyger; Alfred L. Nuttall; Zhi-Gen Jiang (2015). Diverse Kir expression contributes to distinct bimodal distribution of resting potentials and vasotone responses of arterioles. PLoS ONE 10(5): e0125266. doi:10.1371/journal.pone.0125266

5. Hongzhe Li, Allan Kachelmeier, David N. Furness, Peter S. Steyger (2015). Local mechanisms for sound-enhanced aminoglycoside entry into outer hair cells. Frontiers in Cellular Neuroscience 9. doi: 10.3389/fncel.2015.00130
6. Jawon Koo; Lourdes Qunitanilla-Dieck; Meiyan Jiang; Jianping Liu; Zachary D. Urdang; Hongzhe Li; Peter S. Steyger (2015). Endotoxemia-mediated inflammation enhances cochlear uptake of aminoglycosides and subsequent cochleotoxicity. Sci. Trans. Med. 2015 Jul 29;7(298):298ra118. doi:10.1126/scitranslmed.aac5546.
7. Lina Reiss, Gemaine Stark, Anh Nguyen-Huynh, Kayce Spear, Hongzheng Zhang, Chiemi Tanaka, Hongzhe Li (2015). Morphological Correlates of Hearing Loss after Cochlear Implantation and Electro-Acoustic Stimulation. Hear. Res. doi:10.1016/j.heares.2015.06.007
8. Changquan Wang, Zhenmin Zhong, Peng Sun, Hanbing Zhong, Fangyi Chen, Hongzhe Li (2017). Evaluation of the Hair Cell Regeneration by Measuring and Quantifying the Startle Responses. Neural Plast. 2017 Jan 29. doi: 10.1155/2017/8283075.
9. Qin Yang, Peng Sun, Shi Chen, Fangyi Chen, Hongzhe Li (2017). Behavioral methods for the functional assessment of hair cells. Front. Med. doi: 10.1007/s11684-017-0507-x.
10. Meiyan Jiang, Hongzhe Li, William Meier, Anastasiya Johnson, Yuan Zhang, Farshid Taghizadeh, Allan Kachelmeier, Peter Steyger (2019), "Upregulation of transient receptor potential vanilloid 1 (TRPV1) potentiates aminoglycoside-induced hearing loss", 42nd Midwinter Research Meeting in Otolaryngology, Baltimore, MD.
11. Bouchra Edderkaoui, Liana Sargsyan, Alisa Hetrick, Hongzhe Li (2018). Deficiency of Duffy antigen receptor for chemokines ameliorated cochlear damage from noise exposure. Frontiers in Molecular Neuroscience. doi: 10.3389/fnmol.2018.00173
12. Meiyan Jiang, Hongzhe Li, Anastasiya Johnson, Takatoshi Karasawa, Yuan Zhang, William B. Meier, Farshid Taghizadeh, Allan Kachelmeier, Peter S. Steyger (2019). Inflammation upregulates cochlear expression of TRPV1 to potentiate drug-induced hearing loss. Science Advances 5. 2019 Jul 17; eaaw1836.
13. Xiaoqing Qian, Ziyu He, Yanmei Wang, Binjun Chen, Alisa Hetrick, Chunfu Dai, Fanglu Chi, Hongzhe Li, Dongdong Ren (2021). Hair cell uptake of gentamicin in the developing mouse utricle. Journal of Cellular Physiology, 2020 Dec 13, 236(7), 5235-52. doi: 10.1002/jcp.30228. PMID: 33368220. *Cover image selection.*
14. Liana Sargsyan, Alisa P Hetrick, Jessica G Gonzalez, Marjorie R Leek, Glen K Martin, Hongzhe Li (2021). Effects of combined gentamicin and furosemide treatment on cochlear ribbon synapses. NeuroToxicology, 84, 73-83. PMID: 33667563. doi: 10.1016/j.neuro.2021.02.007.
15. Yongchuan Chai, Weiwei He, Weiqiang Yang, Alisa P Hetrick, Jessica G Gonzalez, Liana Sargsyan, Hao Wu, Timothy TK Jung, Hongzhe Li (2021). Intratympanic lipopolysaccharide elevates systemic fluorescent gentamicin uptake in the cochlea. PMID: 33956344. Laryngoscope. 2021 May 6. doi: 10.1002/lary.29610.

Conference abstracts

1. Jianping Liu, Zachary Urdang, Hongzhe Li, Peter Steyger (2014), "Increased Uptake of Fluorescently-tagged Gentamicin in the Stria Vascularis after Diphtheria Toxin Ablation of Macrophages", 37th Midwinter Research Meeting in Otolaryngology, San Diego, CA.
2. Meiyan Jiang, Takatoshi Karasawa, Qi Wang, Hongzhe Li, Peter Steyger (2014), "Sodium-glucose Transporter-2 (SGLT2; SLC5A2) Enhances the Cellular Uptake of Gentamicin", 37th

Midwinter Research Meeting in Otolaryngology, San Diego, CA.

3. Gemaine Stark, Hongzhe Li, Kayce Spear, Hongzheng Zhang, Chiemi Tanaka, Anh Nguyen-Huynh, Lina Reiss (2014), "Changes in Hearing Thresholds and Hair Cell Synapses after Chronic Electro-Acoustic Stimulation in Guinea Pigs with High-Frequency Hearing Loss", 37th Midwinter Research Meeting in Otolaryngology, San Diego, CA.
4. David Furness, Peter Steyger, Hongzhe Li (2014), "Temporary Threshold Shift Breaks Tip Links in Hair Cells and Enhances Uptake of Gentamicin", 37th Midwinter Research Meeting in Otolaryngology, San Diego, CA.
5. Lauren Luk, Douglas Vetter, Peter Steyger and Hongzhe Li (2014), "Acetylcholine Enhances Aminoglycoside Uptake in Neonatal Hair Cells, via Putative Activation of Nicotinic Acetylcholine Receptors", 37th Midwinter Research Meeting in Otolaryngology, San Diego, CA.
6. Lauren Luk, Hongzhe Li and Peter Steyger (2014), "Perilymphatic Gentamicin Trafficking through Basolateral Channels May Underlie Enhanced Ototoxicity by Noise-Induced Threshold Shifts", Otolaryngology Head & Neck Surgery, September 2014, vol. 151, no. 1, Suppl P222.
7. Jianping Liu, Meiyan Jiang, Zachary Urdang, Hongzhe Li, Peter Steyger (2015), "Conditional macrophage depletion by Diphtheria Toxin affects the macrophage in the cochlear lateral wall", 38th Midwinter Research Meeting in Otolaryngology, Baltimore, MD.
8. Yuqin Yang, Hongzhe Li, Peter Steyger and Zhi-Gen Jiang (2015), "Interleukin-6 Hyperpolarizes Strial Capillary Endothelial Cells by Activation of Stretch-Gated Chloride Channels", 38th Midwinter Research Meeting in Otolaryngology, Baltimore, MD.
9. Hongzhe Li, Jianping Liu, Peter Steyger (2015), "Characterizing the strial capillary dilation in mouse models of sound enhanced intra-cochlear aminoglycoside trafficking", 38th Midwinter Research Meeting in Otolaryngology, Baltimore, MD.
10. Hongzhe Li, Meifang Xiao (2015), "Sound-induced strial capillary dilation and intra-cochlear aminoglycoside trafficking", 21st Annual Blood-Brain Barrier Consortium Meeting in collaboration with the International Brain Barriers Society, Stevenson, WA.
11. Hongzhe Li, Anastasiya Johnson, Meiyan Jiang, Peter Steyger (2016), "Age-related hearing loss in TrpV1 mice", 39th Midwinter Research Meeting in Otolaryngology, San Diego, CA.
12. Alisa Hetrick, Brandon Yeoh, Hongzhe Li (2016), "Vulnerability to Acoustic Trauma in TrpV1 Mice", 5th Joint Meeting of Acoustical Society of America & Acoustical Society of Japan, Honolulu, HI.
13. Alisa Hetrick, Brandon Yeoh, Hongzhe Li (2017), "Noise-induced hearing loss in TrpV1 knockout mice", 40th Midwinter Research Meeting in Otolaryngology, Baltimore, MD.
14. Liana Sargsyan, Alisa Hetrick, Hongzhe Li (2017), "Noise-induced hearing loss in Darc knockout mice", SoCal Hearing Research Conference, UC Riverside, CA.
15. Liana Sargsyan, Alisa Hetrick, Bouchra Edderkaoui, Hongzhe Li (2018), "Darc deficiency ameliorates cochlear damage from noise exposure", 41st Midwinter Research Meeting in Otolaryngology, San Diego, CA.
16. Liana Sargsyan, Ksenia Aaron, Hongzhe Li, John Niparko (2018), "The electrical stimulation of the ear in the USSR in the early 1930's", 15th International Conference on Cochlear Implants and Other Implantable Auditory Technology, Antwerp, Belgium.
17. Liana Sargsyan, Alisa Hetrick, Weiwei He, Glen Martin, Hongzhe Li (2018), "Ribbon synapse distribution correlated with aminoglycoside-induced hearing deficit", SoCal Hearing Research Conference, USC, Los Angeles, CA.

18. Hongzhe Li, Liana Sargsyan, Alisa Hetrick, Bouchra Edderkaoui (2018), "Alleviated Cochlear Damage in an Inflammation Suppressing Model", Joint Meeting 176th Meeting Acoustical Society of America and 2018 Acoustics Week in Canada Canadian Acoustical Association, Victoria, British Columbia, Canada.
19. Meiyan Jiang, Hongzhe Li, William Meier, Anastasiya Johnson, Yuan Zhang, Farshid Taghizadeh, Allan Kachelmeier, Peter Steyger (2019), "Upregulation of Transient Receptor Potential Vanilloid 1 (TRPV1) Potentiates Aminoglycoside-Induced Hearing Loss", 42nd Midwinter Research Meeting in Otolaryngology, Baltimore, MD.
20. Weiwei He, Alisa Hetrick, Liana Sargsyan, Yu Sun, Hongzhe Li (2019), "Modulation of Strial Macrophages after Noise Exposure", 42nd Midwinter Research Meeting in Otolaryngology, Baltimore, MD.
21. Liana Sargsyan, Alisa Hetrick, Weiwei He, Glen Martin, Hongzhe Li (2019), "Distribution of Ribbon Synapses Correlated with Hearing Decline after a Single Dose of Ototoxic Injury", 42nd Midwinter Research Meeting in Otolaryngology, Baltimore, MD.
22. Liana Sargsyan, Alisa Hetrick, Yongchuan Chai, Hongzhe Li (2019), "The Response of Cochlear Microglia-Like Cells to Intratympanic LPS in Different Wildtype Strains", SoCal Hearing Research Conference, UC Irvine, CA.
23. Hongzhe Li, Liana Sargsyan, Alisa Hetrick, Glen Martin (2019), "Alternation of Synaptic-Ribbon Distribution after a Single-Dose Ototoxic Injury", The 2019 NCRAR Conference, Ototoxicity and Noise Damage: Translating Preclinical Findings to Audiological Management, Portland, OR.
24. Yongchuan Chai, Alisa Hetrick, Liana Sargsyan, Weiwei He, Timothy Jung, Hao Wu, Hongzhe Li (2020), "Intratympanic Lipopolysaccharide Induces Inflammatory Responses and Elevates Systemic Gentamicin Uptake in the Cochlea", 43rd Midwinter Research Meeting in Otolaryngology, San Jose, CA.
25. Liana Sargsyan, Alisa Hetrick, Yongchuan Chai, Hongzhe Li (2020), "The Response of Cochlear Microglia-Like Cells to Ototoxic Challenge in Different Strains of Wildtype Mice", 43rd Midwinter Research Meeting in Otolaryngology, San Jose, CA.
26. Liana Sargsyan, Alisa Hetrick, Jessica Gonzalez, Hongzhe Li (2021), "Cochlear Vulnerability After Systemic Gentamicin-Furosemide Treatment in Different Wild Type Mice", 44th Midwinter Research Meeting in Otolaryngology, Virtual.

Podium presentations and book chapters

1. "Ototoxicity under bacterial infection and inflammation", 2nd Hearing Science Symposium: from Hair Cells to Cortex, Shandong ENT Infirmary, Shandong University, Jinan, China, Oct 2016.
2. "Ototoxicity, cochlear synaptopathy and mouse models", 3rd Hearing Science Symposium: from Hair Cells to Cortex, Nanjing University and Southeast University, Nanjing, China, Oct 2017.
3. "A mouse model for inflammation-dependent hearing loss and auditory neuropathy", Shanghai Forum on the Frontier of Hearing Research, Shanghai, China, Dec 2017.
4. "Research progress in vestibular science", 3rd Annual Meeting of Vestibular Disorders Committee of China Medicine Education Association, Shanghai, China, April 2018.
5. Chai, Yongchuan; Li, Hongzhe (2019). Intratympanic gentamicin treatment for Ménière's Disease. In: Meniere's Disease. Ed, Bahmad, Fayez, ISBN 978-1-78923-940-9.

6. "The enigmatic TrpV1 in inflammation-enhanced ototoxicity", Symposium of Advanced Hearing Research, Union Hospital, Tongji Medical College, Huazhong University of Science and Technology, Wuhan, China, April 2019.
7. "Regulate inflammation to reduce cochlear damage", 5th Chinese Hearing Research Conference, Beijing Friendship Hospital, Capital Medical University, Beijing, China, Sept 2019.
8. "The Duffy antigen receptor and inflammation-related hearing loss", Creighton University, Omaha, NE, Jan 2021.

7. INVENTIONS, PATENTS AND LICENSES

Nothing to report.

8. REPORTABLE OUTCOMES

What opportunities for training and professional development has the project provided?

This research project provided opportunities for people with interest and motivation in biomedical research. Project personnel included college students, medical students, and international physicians. Liana Sargsyan, a European trained physician, Yongchuan Chai, an attending doctor from Shanghai, and Weiqiang Yang, a full-feathered ENT doctor from Shenzhen, are all specialized in otology and worked in the PI's lab during the project. Weiwei He, a medical student from Tongji Medical College, Huazhong University of Science and Technology, and Brandon Yeoh, a college student from Brown University, have also contributed to the project. During their tenure in the lab, they accrued hands-on experience in a variety of experimental techniques, including tissue and explant culture, cochlear dissection, image acquisition, biomolecular analysis, and compound synthesis *etc*. Their academic experience acquired by working in this project will certainly provide positive impact on their upcoming career advancement.

What individuals have worked on the project?

Name:	Hongzhe Li, PhD
Project Role:	PI
Nearest person month worked:	40.5

Contribution to Project: Dr. Li has performed work in experimental design, staff training, tissue harvest and processing, confocal imaging, image acquisition and quantification, data analysis, documents, protocols, reports and manuscript preparation.

Name: Peter Steyger, PhD
Project Role: Co-Investigator, Professor
Nearest person month worked: 1.9
Contribution to Project: Dr. Steyger has involved in experimental design, animal protocol compliance and manuscript preparation.

Name: Liana Sargsyan, MSc
Project Role: Research Associate
Nearest person month worked: 53.0
Contribution to Project: Ms. Sargsyan has performed work in animal treatment with aminoglycosides, cochlear microdissection, confocal microscopy, data analysis, and conference presentation, and manuscript preparation.

Name: Alisa Hetrick, BSc
Project Role: Research Technician
Nearest person month worked: 21.0
Contribution to Project: Ms. Hetrick has performed work in ABR and DPOAE recordings, noise and aminoglycoside exposures, and managed mouse cohort with genotyping procedures. She also assisted in acquiring lab equipment and consumables, and protocol development.

Name: Weiwei He, MSc
Project Role: Research Assistant
Nearest person month worked: 12.0
Contribution to Project: Ms. He has performed work of organ culture with cochlear explants, as well as cochlear microdissection, confocal microscopy and molecular biology such as western blot.

Name: Yongchuan Chai, MD, PhD
Project Role: Research Associate
Nearest person month worked: 12.0
Contribution to Project: Dr. Chai has performed work of intratympanic injections in mice, as well as cochlear microdissection, immunohistochemistry, confocal microscopy and data analysis.
Name: Jessica Gonzalez, BSc
Project Role: Research Technician

Nearest person month worked: 11.0
Contribution to Project: Ms. Gonzalez has performed work in ABR and DPOAE recordings, noise and aminoglycoside exposures, and managed mouse cohort. She also assisted in acquiring lab equipment and consumables, and data analysis.

Name: Anastasiya Johnson, MS
Project Role: Research Associate
Nearest person month worked: 10.0
Contribution to Project: Ms. Johnson has performed work in ABR recordings and part of image acquisition.

Name: Weiqiang Yang, MD
Project Role: Research Associate
Nearest person month worked: 7.0
Contribution to Project: Dr. Yang has performed work of cochlear perfusion and intratympanic injections in mice, as well as cochlear microdissection, immunohistochemistry, confocal microscopy and data analysis.

Name: Allan Kachelmeier, MS
Project Role: Research Assistant
Nearest person month worked: 1.9
Contribution to Project: Mr. Kachelmeier has involved in instrument maintenance and document proofreading.

Name: Brandon Yeoh
Project Role: Research Volunteer
Nearest person month worked: 1.0
Contribution to Project: Mr. Yeoh has assisted on ABR recording and data analysis.

How were the results disseminated to communities of interest?

The findings and outcomes of the project have been disseminated by the format of peer-reviewed publications, conference abstracts, and podium presentation etc. Please refer Section 6 for details. There are still certain unpublished data that were acquired from this project valuable to the hearing research community. We'll be actively looking for appropriate settings to have these data published in the future, and certainly acknowledge this funding source when it happens.

9. OTHER ACHIEVEMENTS

Nothing to report.

10. REFERENCES

1. Biber K, Laurie DJ, Berthele A, Sommer B, Tolle TR, Gebicke-Harter PJ, et al. Expression and signaling of group I metabotropic glutamate receptors in astrocytes and microglia. J Neurochem. 1999;72(4):1671-80.
2. Ding D, Liu H, Qi W, Jiang H, Li Y, Wu X, et al. Ototoxic effects and mechanisms of loop diuretics. J Otol. 2016;11(4):145-56.
3. Hirose K, Sato E. Comparative analysis of combination kanamycin-furosemide versus kanamycin alone in the mouse cochlea. Hear Res. 2011;272(1-2):108-16.
4. Housley GD, Morton-Jones R, Vlajkovic SM, Telang RS, Paramananthasivam V, Tadros SF, et al. ATP-gated ion channels mediate adaptation to elevated sound levels. Proc Natl Acad Sci U S A. 2013;110(18):7494-9.
5. Jiang M, Johnson A, Karasawa T, Kachelmeier A, Steyger PS, editors. Role of TRPV1 in the cellular uptake of aminoglycosides. The 38th ARO Midwinter Research Meeting; 2015; Baltimore, Maryland.
6. Matsuda K, Komune S, Tono T, Yamasaki M, Haruta A, Kato E. A role of glutamate in drug-induced ototoxicity: in vivo microdialysis study combined with on-line enzyme fluorometric detection of glutamate in the guinea pig cochlea. Brain Res. 2000;852(2):492-5.
7. Riera CE, Huising MO, Follett P, Leblanc M, Halloran J, Van Andel R, et al. TRPV1 pain receptors regulate longevity and metabolism by neuropeptide signaling. Cell. 2014;157(5):1023-36.
8. Taylor RR, Nevill G, Forge A. Rapid hair cell loss: a mouse model for cochlear lesions. J Assoc Res Otolaryngol. 2008;9(1):44-64.

11. APPENDICES

1. Liana Sargsyan, Alisa P Hetrick, Jessica G Gonzalez, Marjorie R Leek, Glen K Martin, Hongzhe Li (2021). Effects of combined gentamicin and furosemide treatment on cochlear ribbon synapses. NeuroToxicology, 84, 73-83. PMID: 33667563. doi: 10.1016/j.neuro.2021.02.007.
2. Yongchuan Chai, Weiwei He, Weiqiang Yang, Alisa P Hetrick, Jessica G Gonzalez, Liana Sargsyan, Hao Wu, Timothy TK Jung, Hongzhe Li (2021). Intratympanic lipopolysaccharide elevates systemic fluorescent gentamicin uptake in the cochlea. PMID: 33956344. Laryngoscope. 2021 May 6. doi: 10.1002/lary.29610.

Neurotoxicology 84 (2021) 73–83

Contents lists available at ScienceDirect

Neurotoxicology

journal homepage: www.elsevier.com/locate/neuro

Effects of combined gentamicin and furosemide treatment on cochlear ribbon synapses

Liana Sargsyan [a], Alisa P. Hetrick [a], Jessica G. Gonzalez [a], Marjorie R. Leek [a,b], Glen K. Martin [a,b], Hongzhe Li [a,b,*]

[a] Research Service, VA Loma Linda Healthcare System, CA 92357, USA
[b] Department of Otolaryngology - Head and Neck Surgery, Loma Linda University Health, Loma Linda, CA 92354, USA

ARTICLE INFO

Edited by Dr. R. Westerink

Keywords:
Aminoglycosides
Loop diuretics
Cochlea
Hair cells
Synaptopathy
Hidden hearing loss

ABSTRACT

It is well-established that aminoglycoside antibiotics are ototoxic, and the toxicity can be drastically enhanced by the addition of loop diuretics, resulting in rapid irreversible hair cell damage. Using both electrophysiologic and morphological approaches, we investigated whether this combined treatment affected the cochlea at the region of ribbon synapses, consequently resulting in auditory synaptopathy. A series of varied gentamicin and furosemide doses were applied to *C57BL/6* mice, and auditory brainstem responses (ABR) and distortion product otoacoustic emissions (DPOAE) were measured to assess ototoxic damage within the cochlea. In brief, the treatment effectively induced cochlear damage and promoted a certain reorganization of synaptic ribbons, while a reduction of ribbon density only occurred after a substantial loss of outer hair cells. In addition, both the ABR wave I amplitude and the ribbon density were elevated in low-dose treatment conditions, but a correlation between the two events was not significant for individual cochleae. In sum, combined gentamicin and furosemide treatment, at titrated doses below those that produce hair cell damage, typically triggers synaptic plasticity rather than a permanent synaptic loss.

1. Introduction

Cochlear synaptopathy is manifested by a loss of synaptic connections between cochlear inner hair cells (IHCs) and their auditory nerve fiber (ANF) terminals that results in a delayed degeneration of spiral ganglion neurons (SGNs) and their central axonal projections (Moser and Starr, 2016). With noise overexposure, it is possible to create animal models exhibiting a selective and permanent synaptic loss with relatively intact hair cells (HCs) in a phenomenon termed hidden hearing loss (HHL), which has been studied extensively by Kujawa and Liberman (2009, 2015) and Liberman and Kujawa (2017). It is less clear if the synaptopathy that causes HHL (*i.e.*, HHL-type sensitivity) can be induced by other cochlear insults, which often result in considerable plasticity affecting hair-cell synaptic densities (Hong et al., 2018; Liberman and Kujawa, 2017). Using moderate dosing, aminoglycoside antibiotics can produce a specific SGN death without much damage to HCs in genetically modified mice (Oishi et al., 2015), reminiscent of the disease termed auditory neuropathy (AN), which is an umbrella concept of and thus suggesting the likelihood of auditory synaptopathy (Jiang et al., 2017). A chemical model of acoustic synaptopathy in mice is certainly welcomed by the research community to simplify the preparation procedure, while taking advantage of the readily available manipulation of the murine genome. Yet, to date, a convincing synaptopathy indicating HHL has not been demonstrated *in vivo* in mice by any known aminoglycoside treatment (Hong et al., 2018; Liu et al., 2015, 2013).

Prior to the increased attention on synaptopathy, cochlear insults, regardless of whether they are produced by acoustic overstimulation or aging, were believed to first target sensory elements in the mouse cochlea, followed by their associated neural components such as the SGNs (Willott et al., 1998). Moreover, the resulting damage appeared to be more biased toward the sensitive outer hair cells (OHCs) on the sensory epithelium (Spongr et al., 1997; Willott et al., 1998). Intuitively, these outcomes were not expected to occur in an ideal synaptopathy animal model, in which a considerable reduction of synaptic density with intact HC survival assessed by morphological or electrophysiological approaches, is ordinarily anticipated. Intriguingly, Ruan et al. (2014) reported that a single intraperitoneal injection of gentamicin, assisted by a

* Corresponding author at: Research Service (151), VA Loma Linda Healthcare System, 11201 Benton Street, Loma Linda, CA 92357, USA.
E-mail address: Hongzhe.Li@va.gov (H. Li).

https://doi.org/10.1016/j.neuro.2021.02.007
Received 21 July 2020; Received in revised form 24 February 2021; Accepted 25 February 2021
Available online 2 March 2021

loop diuretic, furosemide, induced a SGN loss that could occur before damage to HCs, especially, IHCs. Here, we asked if the ribbon synapse of the IHC could be compromised before HC loss, regardless of the condition of the SGNs. As aforementioned, this would be important, because it would replicate the HHL that is typically observed with noise overexposure or in certain aging animal models. Mechanistically, independent synaptic damage, *i.e.*, HHL, is possible because aminoglycosides are capable of inducing the excitotoxic type of injury at the synaptic level, which is considered to be a major underlying mechanism for noise-induced HHL (Basile et al., 1996; Liberman and Kujawa, 2017; Segal et al., 1999).

Combining loop diuretics with aminoglycoside treatment is an effective approach for accelerating ototoxic damage, especially in mice, which results in immediate cochlear trauma (Hirose and Sato, 2011; Taylor et al., 2008). In this simplified version of a mouse ototoxicity model, the addition of loop diuretics, such as furosemide, disrupts the blood labyrinth barrier thereby greatly elevating the concentration of aminoglycosides, such as gentamicin, in the cochlea (Ding et al., 2016; Taylor et al., 2008). Furosemide, by itself, is not considered directly damaging to the inner-ear components including HCs, ribbon synapses or SGNs (Rybak, 1993). In the present study, the dose-dependent effect of gentamicin and furosemide (G/F) in combination was investigated to: 1) characterize the residual hearing function, 2) distinguish the morphology of OHCs and IHCs, and ribbon synapses at various cochlear locations, and 3) determine whether there is a change in the number, or the distribution, of synaptic ribbons.

The G/F combination treatment is also frequently used to induce cochlear HC loss prior to testing a specific strategy for regenerating HCs (Izumikawa et al., 2005). Excessive damage toward other cochlear components including the ribbon synapse is considered an unfavorable ototoxic event and certainly complicates the assessment of a HC's regeneration capacity. Thus, whether G/F treatment could induce an HHL-type of synaptopathy is an important scientific question, and valuable to the research community with either outcome. We, therefore, examined in detail the effects on the mouse cochlea of this treatment combination using a series of varied doses of G/F.

2. Methods

2.1. Mice and gentamicin/furosemide (G/F) treatment

C57BL/6 (JAX stock #0664) wild-type mice of both sexes, between 6–8 wk of age, were included in the present study. Animals were housed in a Specific Pathogen Free-modified room. Experimental animals were injected intraperitoneally (*i.p.*) with a single dose of gentamicin (Sigma-Aldrich, G1264, Lot #SLBG7734 V) followed within 30 min by furosemide (Fresenius Kabi, Germany). Age-matched mice without any ototoxic treatment served as controls. The dose combination was either a fixed gentamicin injection at 200 mg/kg body weight, with varied furosemide doses (50, 100, 200, 400 mg/kg), or a fixed furosemide dose (200 mg/kg) with varied gentamicin injections (25, 50, 100, 200, 400 mg/kg), as illustrated in Suppl. Fig. 1. The majority of mice underwent distortion product otoacoustic emissions (DPOAE) and auditory brainstem response (ABR) tests prior to, and at several posttreatment time points, *i.e.*, primarily at day 3 and day 7. Seven days after treatment, mice were terminated, and cochlear tissues harvested for morphological examination. Cochlear samples from a subset of mice were collected 2 days after the G/F treatment. Data reported here were collected from a total of 84 mice. The number of mice contributing to each measure is indicated in Tables 1 and 3, or the figures. Nine mice did not survive the treatment, including five which were treated with either 400 mg/kg gentamicin or 400 mg/kg furosemide doses. All animal work was carried out using protocols approved by the Institutional Animal Care and Use Committee of the Jerry L. Pettis VA Medical Center, Loma Linda, CA. Animal-use procedures conformed with federal regulations regarding personnel, supervision, record keeping, and veterinary care.

Table 1
Two-way ANOVA statistics for ABR threshold results. The effect of G/F treatment is delineated. n.s.=not significant.

Dose combo	p value	p value summary	F (DFn, DFd)	n at 7-day
200G/0F	0.3048	n.s.	F (2, 162) = 1.197	10
200G/50F	**<0.0001**	****	F (2, 162) = 10.06	14
200G/100F	**0.0002**	***	F (2, 186) = 8.937	14
200G/400F	**<0.0001**	****	F (2, 138) = 69.64	10

2.2. ABR and DPOAE measurement

Individual anesthetized mice (ketamine 65 mg/kg, xylazine 13 mg/kg, *i.p.*) were stimulated with a closed tube sound-delivery system sealed into the outer ear canal. ABRs to tone-burst stimuli (5-ms duration, 1-ms rise/fall times, n = 512 repeats) at 4, 8, 12, 16, 24 and 32 kHz, at 5-dB steps, ranging from 0 to 90 dB SPL, were recorded using a Tucker-Davis Technologies (TDT) System 3 (Alachua, FL, USA). In particular, thresholds were determined as the lowest signal intensity at which a response could be identified, and wave I peak-to-peak amplitudes were measured from averaged response waveforms at each sound level. A full range of input/output (I/O) functions of wave I amplitudes was typically recorded in response to 12-kHz tone-bursts.

$2f_1$-f_2 DPOAEs were measured to non-invasively assess OHC function (Jimenez et al., 1999). Briefly, the f_1 and f_2 primary tones were generated by a dual-channel synthesizer (Hewlett Packard Model 3326A) and attenuated under the control of in-house customized software. The f_1 and f_2 primary tones (f_2/f_1 = 1.25) were mixed acoustically and delivered to two separate ear-speakers (Tandy Corp, Fort Worth, TX) to avoid artifactual distortion. Ear-canal sound pressure levels were measured by an emissions microphone assembly (Etymotic Research, ER-10B+, Elk Grove Village, IL), embedded in the probe. Sound levels were sampled, synchronously averaged and Fourier analyzed for f_2's ranging from 4.0 to 64.0 kHz in 0.1-octave steps. Corresponding noise floors (NFs) were computed by averaging the levels of the ear-canal sound pressure for five frequency bins above and below the $2f_1$-f_2 frequency bin. Primary tones were presented at L_1=L_2 = 55 dB SPL.

2.3. Tissue-processing, image acquisition and processing

Cochlear samples were immersion-fixed overnight in 4 % paraformaldehyde (pH 7.4), followed by EDTA (10 %, pH 7.4) decalcification at room temperature (RT). To prepare the cochlear whole-mounts, the membranous labyrinth of the cochlea was micro-dissected under a dissecting microscope to remove the softened otic capsule, stria vascularis, Reissner's membrane, and tectorial membrane. After further immersion-fixation in 4 % paraformaldehyde, specimens were permeabilized in 1 % Triton-X solution for 1 h at RT. Then, specimens were incubated at 37 °C overnight with primary antibodies including monoclonal mouse anti-CtBP2 IgG1 (612044, BD Biosciences, 1:200), monoclonal mouse anti-GluR2 IgG2a (MAB397; Millipore; 1:1000), and/or polyclonal rabbit anti-Myo7a antibodies (PA-936, Thermo Fisher, 1:200). After rinsing, the specimens were incubated with the Alexa Fluor 488-, 568-, and/or 647-conjugated secondary antibodies at 1:1000 at 37 °C for 1 h in the dark. Some specimens were also incubated with Alexa Fluor 488 phalloidin at a 1:1000 at RT for 20 min in the dark. After the final wash, the modiolus was removed from the tissue and the epithelia were divided into segments and mounted on slides with the anti-fade fluorescence mounting media VectaShield (Vector Labs, Burlingame, CA) under uniform 60X magnification. Immunolabeled images were acquired using a laser confocal microscope (Fluoview FV3000, Olympus Corp.).

The ribbon density, in the number of ribbons/IHC, was quantified at multiple cochlear locations using ImageJ (NIH, Bethesda, MD). At each location, ribbons from at-least 30 IHCs were counted and averaged to determine the ribbon density, avoiding the need to define the cell

boundary of each IHC. Data were analyzed using Prism (GraphPad Software, La Jolla, CA, USA) software and G*Power (Version 3.1, Germany) software for Windows. Statistical methods included a 2-way ANOVA with Sidak multiple comparisons, unpaired t-tests with Welch's correction, and ANOVA-based sensitivity tests. All tests were two-tailed, and a p value of <0.05 was considered statistically significant.

3. Results

3.1. Gentamicin/furosemide dose response and inter-animal ototoxicity variation

To test whether a single combined dose of ototoxic treatment influenced the ribbon synapse in mouse models of acquired sensorineural hearing loss, we tested *C57BL/6* wild-type mice as an established animal model of HC loss.

In *C57BL/6* mice, when gentamicin dosage was fixed at 200 mg/kg, a dose effect of furosemide was evident in group ABR thresholds measured at 3 and 7 days after G/F treatment, from 0 to 400 mg/kg as illustrated in Fig. 1A–D. For lower furosemide dosages including 50 (200G/50F) and 100 (200G/100F) mg/kg, as shown in Fig. 1B and C, respectively, a marginal but significant treatment effect was observed in average ABR thresholds (2-way ANOVAs, Table 1). For the higher 400 mg/kg furosemide dosage (200 G/400 F) illustrated in Fig. 1D, the average ABR thresholds greatly increased across the entire frequency-test range (2-way ANOVA, $F(2,138) = 69.64$, $p < 0.0001$), indicating severe cochlear injury. A sensitivity test based on the ANOVA statistics was also conducted, and its outcome confirmed the reproducibility of these significant results (Table 2). Although a dose response of furosemide did exist from the group data as indicated in Fig. 1A–D, it is noteworthy that the large inter-animal variation made it impossible to reversely predict G/F dose based on individual ABR thresholds. For instance, an ear with 200G/400F treatment (purple lines in Fig. 1E and F) could present normal ABR thresholds, while an ear with 200G/50F treatment (green line in Fig. 1E and F) presented undetectable ABR thresholds at higher frequencies. When undetectable, a threshold value of 95 dB was assigned for group-averaging purposes. ABR thresholds measured from other G/F dose combinations are illustrated in Suppl. Fig. 2.

DPOAEs were also measured in G/F-treated *C57BL/6* mice,

Table 2
Sensitivity tests based on ABR 2-way ANOVA results. α = 0.05, power = 0.95. MDE = minimum detectable effect.

Dose combo	Total sample size	MDE	Measured effect size	Satisfactory
200G/50F	180	0.2956	0.3525	**yes**
200G/100F	204	0.2773	0.31	**yes**
200G/400F	156	0.3181	1.005	**yes**

Table 3
Two-way ANOVA statistics for DPOAE results. The effect of 7-day post G/F treatment is delineated. n.s.=not significant.

Dose combo	p value	p value summary	F (DFn, DFd)	n at 7-day
200G/0F	0.5016	n.s.	F (1, 656) = 0.4520	10
200G/50F	**<0.0001**	****	F (1, 820) = 48.72	14
200G/100F	**<0.0001**	****	F (1, 1558) = 59.06	22
200G/400F	**<0.0001**	****	F (1, 574) = 190.3	10

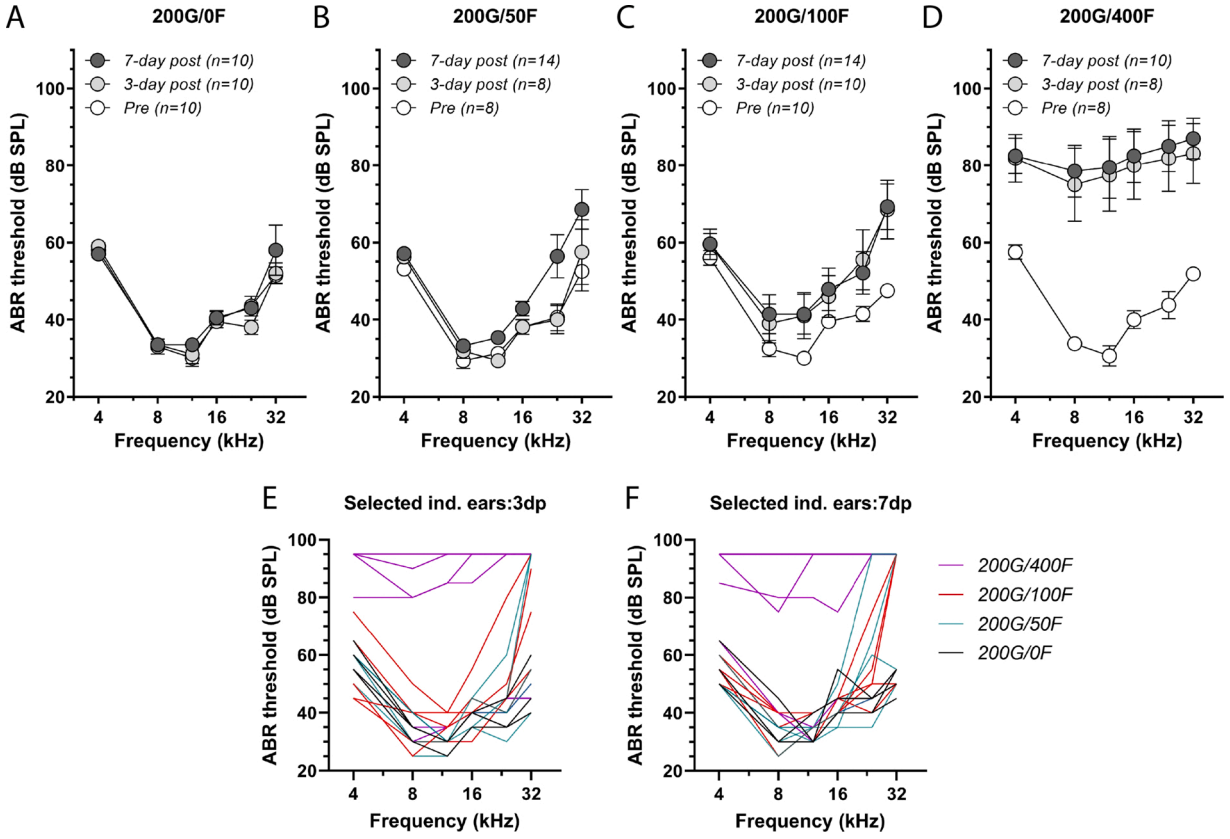

Fig. 1. Dose response of G/F treatment as determined by ABR thresholds. A: Average ABR thresholds with 200G/0F treatment measured before, 3-day and 7-day posttreatment. **B**: 200G/50F. **C**: 200G/100F. **D**: 200G/400F. Error bar = SEM. **E**: Selected ABR thresholds from individual ears measured at 3-day posttreatment, and **F**: at 7-day posttreatment.

providing a sensitive and reliable injury assessment of OHCs in both grouped and individual animals. Average DPOAE responses in the fixed dose of gentamicin groups, to 55-dB SPL primary tones, comparing G/F pretreatment (blue) and 7 days posttreatment (red) conditions are shown in Fig. 2A–D. Gentamicin alone (200 mg/kg) did not result in any DPOAE deficit (Fig. 2A; $F(1,656) = 0.452$, $p = 0.502$), while OHC injury usually occurred at the high-frequency region, and the injury expanded to lower frequency regions as the dose of furosemide increased (Fig. 2B–D), suggesting the overall ototoxic severity escalated (see Table 3 for statistics). This dose-dependent ototoxic principle could also be observed in individual animals (Fig. 2E–I). However, the large, red shaded area indicating the standard deviation of DPOAE responses at 7 days after G/F-treatment (Fig. 2D), suggested the ototoxic OHC injury was highly variable similar to the inter-animal variability observed in ABR thresholds. For example, for one mouse treated with the same 200G/200F dose, severe OHC damage as indicated in Fig. 2K&L was observed, while another mouse might exhibit normal DPOAE responses at 7 days posttreatment (Fig. 2J). Based on the severity of OHC injuries, we categorized G/F-induced cochleotoxicity into three types. In the mild type, OHC damage represented, for example, in Fig. 2F, was limited to the extreme high-frequency range (>30 kHz). In the moderate type shown in Fig. 2G, OHC damage spread into the mid-frequency range (~20 kHz). In the severe type indicated in Fig. 2H, OHC damage was seen throughout the entire frequency range. Among nine mice exhibiting severe DPOAE deficits, seven involved bilateral injuries as shown for mouse #248 in Fig. 2H&I, and mouse #387 in Fig. 2K&L. This observation was in accordance with the consensus that aminoglycoside-induced ototoxicity typically affects both ears equally (Forge and Schacht, 2000). Yet, unilateral mild high-frequency OHC injury was not rare in the present study, as the contralateral ear showed no sign of DPOAE deficit. The upper-frequency limitation of f_2 stimuli was 64 kHz, whereas DPOAE levels were frequently indistinguishable from the noise floor as observed for the data presented in Fig. 2. This technical upper-frequency boundary was very close to, but not adequately reaching the extremity of the basal cochlear location. As a result, OHC injury at the extreme basal cochlear region could not be detected, and an ear could be mis-identified as normal by DPOAE measurements.

The results from ABR thresholds and DPOAE measures, *in toto*, indicated that we have generated a broad spectrum of cochlear injuries based on various G/F dosing combinations, which allowed us to interrogate the ribbon synapse for possible synaptic damage that is independent of HC injuries.

3.2. The wave I I/O curve of ABR responses

ABR wave I amplitude is deemed as a legitimate non-invasive physiological indicator of the functionality of the afferent AN, including the ribbon synapses. As ABR thresholds in G/F-treated mice were measured, the wave I I/O function was also routinely acquired at 12 kHz as illustrated in Fig. 3, given that this is the most sensitive

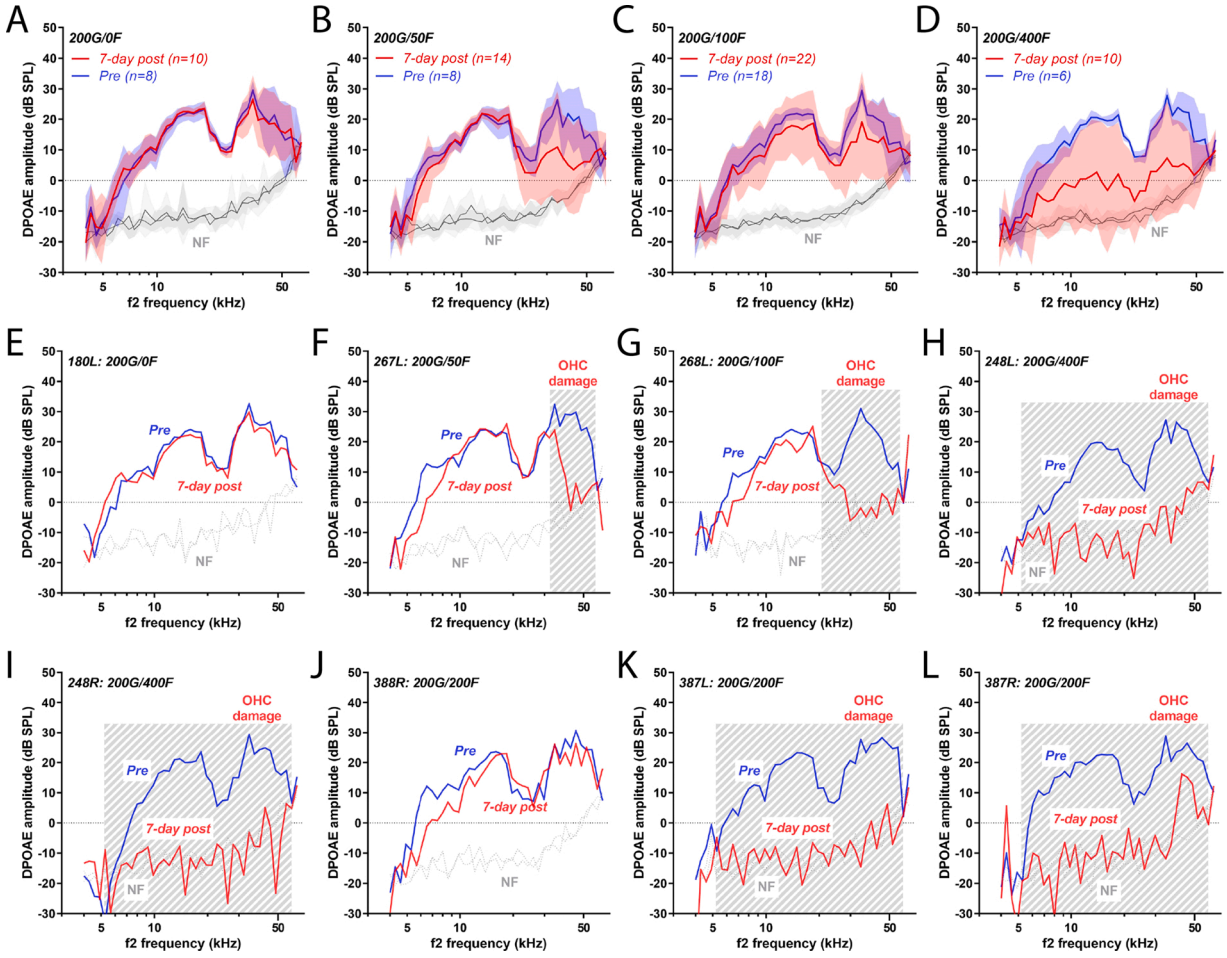

Fig. 2. DPOAE revealed OHC damage from G/F treatment. A-D: In the fixed dose of gentamicin groups, the introduction of furosemide at varied doses generally caused a dose-dependent DPOAE deficit in the cochlea. Shaded area depicts boundaries indicate standard deviation. In individual mice, the severity of DPOAE deficit was diverse, from **E**: no damage, to **F**: mild damage, **G**: moderate damage, and **H** & **I**: severe damage 7-day posttreatment. Considerable inter-animal variation existed with the same treatment regimen. For instance, both with 200G/200F treatment, J: no DPOAE deficit was observed in mouse #388 7-day posttreatment, while **K** & **L**: severe functional damage was observed in mouse #387. Sound levels of the primary tones were equal at L_1=L_2 = 55 dB SPL, f_2/f_1 = 1.25. NF = noise floor.

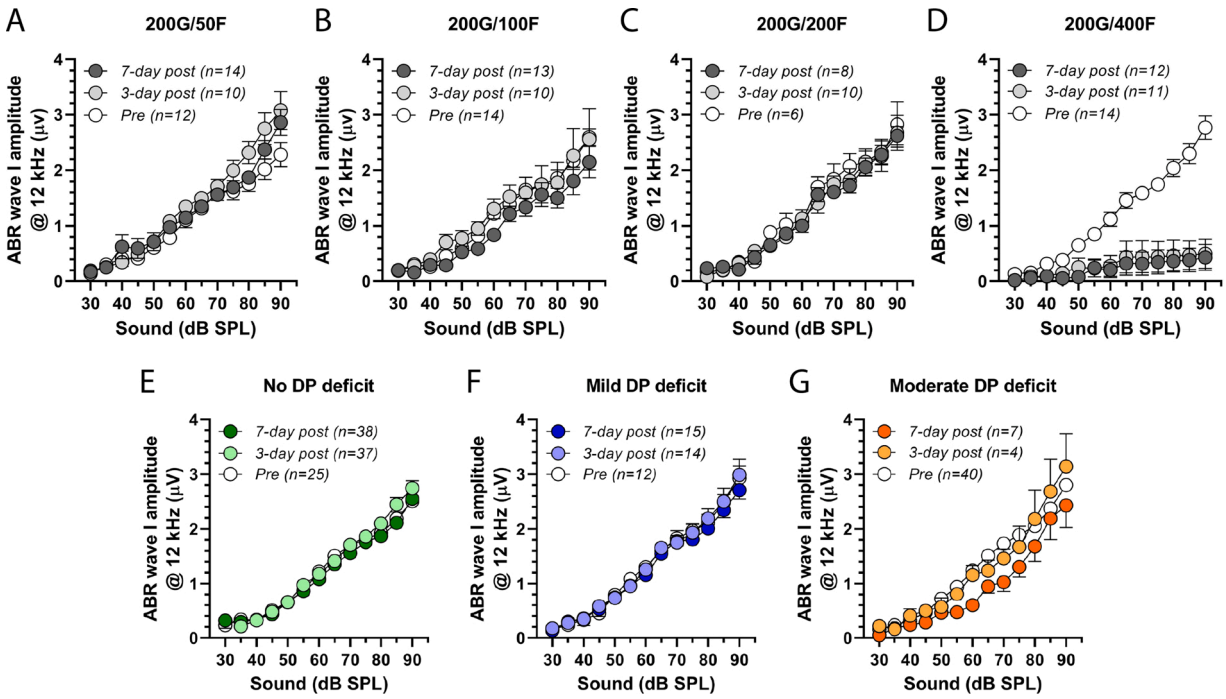

Fig. 3. Input/output functions (I/Os) of wave-I amplitude from ABR to 12-kHz tones. A: Average ABR wave I amplitude I/O functions with 200G/50F treatment measured before, 3-day and 7-day posttreatment. **B**: 200G/100F. **C**: 200G/200F. **D**: 200G/400F. **E**: Average I/O functions from cochleae with no DPOAE deficit, **F**: mild DPOAE decrements, and **G**: moderate DPOAE losses. Error bar = SEM.

frequency location with the lowest threshold, thus, providing the largest dynamic range for the I/O amplitude function. For lower G/F dosages, including the 200G/50F one shown in Fig. 3A, the 200G/100F dose of Fig. 3B and the 200G/200F one in Fig. 3C, no severe OHC injury was observed based on DPOAEs, and the complete range of wave I amplitudes could be acquired as well. The group average of posttreatment wave I I/O functions, at 3 and 7 days, were comparable to their pretreatment control-function counterparts. These data suggested the ribbon synapses, at the tested frequency location, were resistant to G/F treatments. For the 200G/400F dose, for group averaging purposes, wave I amplitudes were assigned by zeros for sub-threshold ABR waveforms. With the contribution of "zero assignments", the average posttreatment wave I I/O curves were lower than the pretreatment curves.

Thus, if hearing sensitivity at the testing frequency of 12 kHz remained after G/F treatment, ABR wave I amplitude was not reduced. Yet, focusing only at the higher-sound levels, wave I amplitudes actually increased for the lowest treatment condition, *i.e.*, 200G/50F, as shown in Fig. 3A (2-way ANOVA, 3-day *vs.* pre, $F(1,250) = 19.51$, $p < 0.0001$; 7-day *vs.* pre, $F(1,287) = 5.482$, $p = 0.0199$). We additionally grouped the wave I I/O functions by the severity of OHC injuries, *i.e.* DPOAE deficit, as shown in Fig. 3E–G. Intriguingly, it was the ears with moderate OHC injury, instead of the ears with mild injury, exhibiting increased wave I amplitudes at higher sound levels as demonstrated in Fig. 3G (2-way ANOVA, $F(2,555) = 2.631$, $p = 0.0729$; Sidak's multiple comparisons test, 3-day *vs.* pre, $p = 0.0077$ at 90 dB, $p = 0.0123$ at 85 dB).

Collectively, results from DPOAE measurements and ABR responses, including both ABR thresholds and wave I amplitudes, indicated that 400 mg/kg furosemide dosing represents an unfavorable dosage to pursue synaptic damage independent of HC loss.

3.3. Morphological alteration of synaptic ribbon after G/F treatment

Seven days after the one-time G/F treatment, synaptic ribbons that were identified by the anti-CtBP2 labeling exhibited various degrees of morphological change. On the *xy* plane at the cochlear location equivalent to 12 kHz (Muller et al., 2005), the ribbon distribution appeared normal for some low-dose G/F treatments, demonstrated by a vacant zone basally located to the IHC nuclei, without a reduction in the number of ribbons, *i.e.*, ribbon density, as illustrated by the micrographs of Fig. 4A1–A4. Among them, Fig. 4A2–A4 are the confocal images reconstructed in the *yz* plane from three adjacent IHCs. Similar to our previous findings in healthy control cochleae, the size of ribbons near the nuclei was relatively small, while those located at the IHC basal pole were larger (Edderkaoui et al., 2018). In addition, it is noteworthy that with the mounting technique used, the IHCs from the apex and the middle coils of the cochlea generally orientate in parallel to the cover slide, which allowed a convenient quantifying of the distance of individual ribbons to the nucleus along the *y* axis, *i.e.*, the main axis of the IHC. Thus, a shape of normal distribution along the main axis was typically anticipated, as indicated in Fig. 4A5 and in Suppl. Fig. 3A. Yet, under most G/F treatment conditions, a certain distribution disorder was observed, for example, in Fig. 4B1–B5 and in Suppl. Fig. 3B, manifested by some ribbons being shifted toward the IHC nucleus without a reduction in the number of ribbons. In addition, the "nucleus-ward or upward" shift appeared predominantly toward the pillar side of the IHC as shown on the left side of Fig. 4B2 and B4. The axial gradient based on the ribbon size was also disturbed. In the extreme ototoxic scenario, the ribbon numbers did decline after some high-dose G/F treatments, with extensive upward shift of the ribbons as illustrated in Fig. 4C2 and in Suppl. Fig. 3C and enlarged ribbons in many cases as demonstrated in Fig. 4C1. Additional examples showing the axial distribution of synaptic ribbons, ranging from normal to extensive upward shift, with and without reduction in ribbon density, can be seen in Suppl. Fig. 3.

3.4. OHC damage occurs in between synaptic plasticity and ribbon density reduction

The ribbon numbers per IHC, *i.e.*, ribbon density, was quantified systemically at the 12-kHz cochlear location and number reduction was rare, only occurring in some cases with the highest G/F dosings at 200

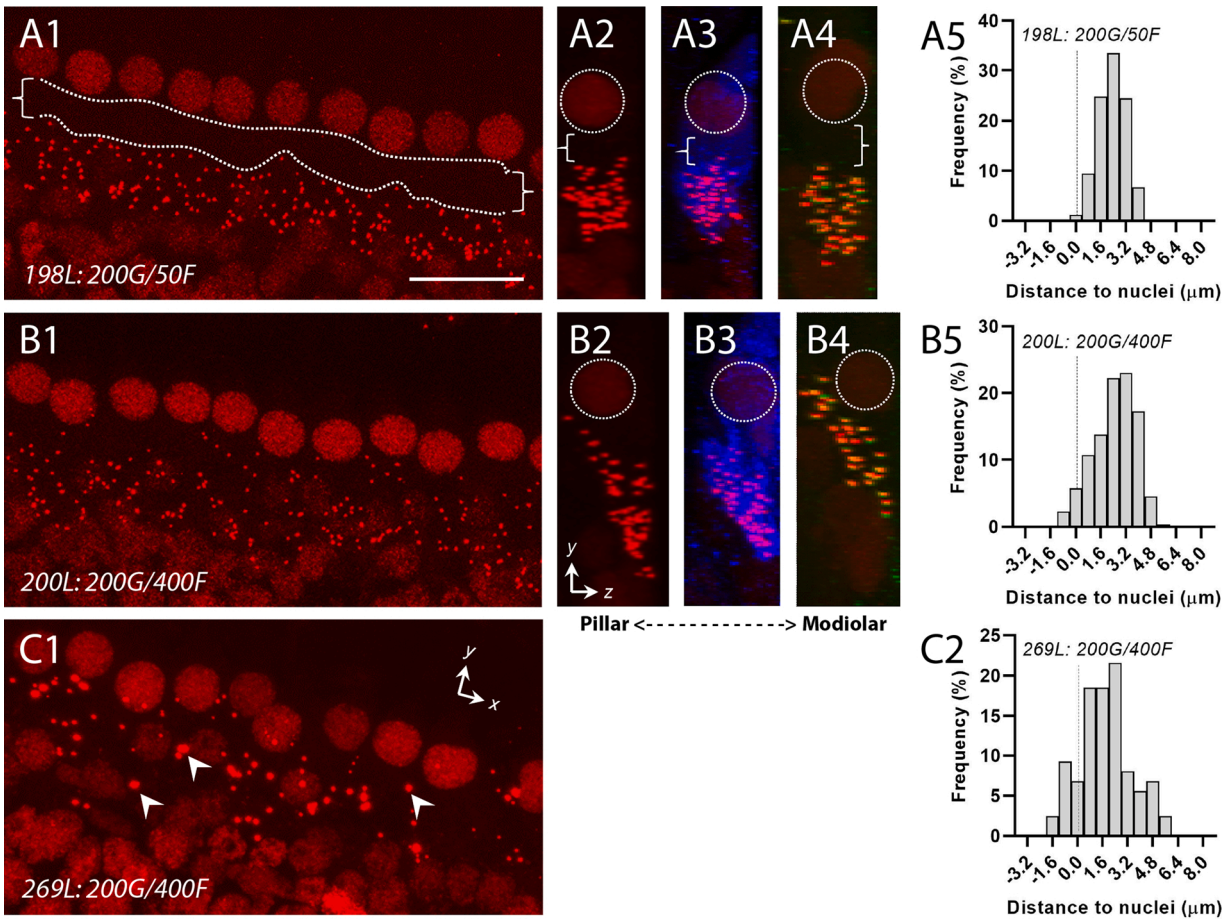

Fig. 4. Alteration of synaptic ribbons after G/F treatment. A: In the apical and middle cochlear locations free of OHC damage, low-dose G/F treatment might not induce any visible change in CtBP2-labeled synaptic ribbons (red puncta), showing a characteristic vacant zone depicted by brackets and dotted lines basal to the IHC nucleus in the *xy* plane (**A1**). Scale bar = 20 μm. Reconstructed images in the *yz* plane from three adjacent IHCs exhibited the distribution of ribbons along the pillar-modiolar axis (**A2**), with identification of the cytoplasm of the IHC by anti-Myo7a immunolabeling (**A3**, blue), and paired postsynaptic AMPA receptors by anti-GluR2 immunolabeling (**A4**, green). A semi-normal distribution of the ribbon along the main cell axis was often observed (**A5**). **B1-4**: Seven days after G/F treatment, at cochlear locations free of OHC damage, a pillar-side upward shift of synaptic ribbons was often seen without a reduction in ribbon number. **B5**: ribbon distribution along the main cell axis was skewed to the nucleus. **C1**: With severe cochlear damage induced by G/F treatment, the ribbon density could be drastically reduced and many individual ribbons enlarged (arrowhead), and again, often exhibiting an upward shift (**C2**). All micrographs were acquired at the cochlear region equivalent to 12 kHz in the middle turn. (For interpretation of the references to colour in this figure legend, the reader is referred to the web version of this article.)

G/400 F (see Fig. 5A) and 400G/200F (see Fig. 5B), although the reduction was not significant in either dosing group due to inter-animal variations. Otherwise, G/F treatment typically resulted in a marginal increase in ribbon density, a hallmark of synaptic plasticity, and the increment was statistically significant for the 200 G/200 F group (Fig. 5A and B; $p = 0.006$, unpaired *t*-test with Welch's correction). Thus, combining the imaging results with the ABR and DPOAE results, the data collectively suggest that the reduction of ribbon density only occurred in the situation with substantial cochlear damage due to G/F treatment, summarized by Fig. 5C. When the ribbon dataset was sorted according to the severity of OHC damage (*i.e.*, DPOAE deficits) that was defined earlier, the reduction became significant with severe DPOAE deficit as shown in Fig. 5D ($p = 0.0022$, unpaired *t*-test with Welch's correction).

Cochlear tissue was typically processed with anti-Myo7a antibodies and/or phalloidin in addition to anti-CtBP2 antibodies, in order to address HC integrity at the same cochlear location where the synaptic ribbons were assessed. With our treatment protocols and doses, G/F-induced IHC loss was extremely rare, while OHC loss frequently was extreme at each imaged cochlear location. That is, the OHC loss was often either complete or none, as shown in Fig. 6A. Thus, the cochlear samples at each examined location could be characterized into one of the two groups, "no OHC loss" group *vs.* "OHC loss" group. As partially reported earlier, 7 days after 200 G/200 F treatment, the overall ribbon density was elevated at examined locations, a sign of synaptic plasticity, including at 12-, 32- and 48-kHz locations as shown in Fig. 6B (2-way ANOVA, $F(1,21) = 9.15$, $p = 0.0064$). Intriguingly, the G/F-induced increment in ribbon density was exclusively contributed by the samples exhibiting "no OHC loss" as illustrated in Fig. 6C (2-way ANOVA, $F(1,17)=44.75$, $p < 0.0001$). Representative cochlear samples at the 12-kHz location from the "no OHC loss" group (see Fig. 6E) and the "OHC loss" group (see Fig. 6F) showed OHC conditions in accordance with the DPOAE results on the same ear measured immediately prior to tissue collection, shown in Fig. 2E and F, respectively. Corresponding values of the ribbon density are depicted in Fig. 6D. Note that without identifiable OHC survival, the ribbon density still fell into the normal range for non-G/F-treated control samples, further confirming that OHC structural damage occurred prior to a ribbon-density reduction.

Postsynaptic AMPA receptors were also identified in a subpopulation of G/F-treated mice, by anti-GluR2 immunolabeling in addition to the presynaptic anti-CtBP2 labeling. While OHCs were survived with G/F treatment, the pre- and post-synaptic pairings were largely maintained (Suppl. Fig. 4A and B, Suppl. Fig. 5A). Incidence of synaptic uncoupling did rise when OHCs failed to survive the G/F treatment (Suppl. Figs. 4C, 5B), and the size of many remaining CtBP2-labeled particles and GluR2 patches were reduced.

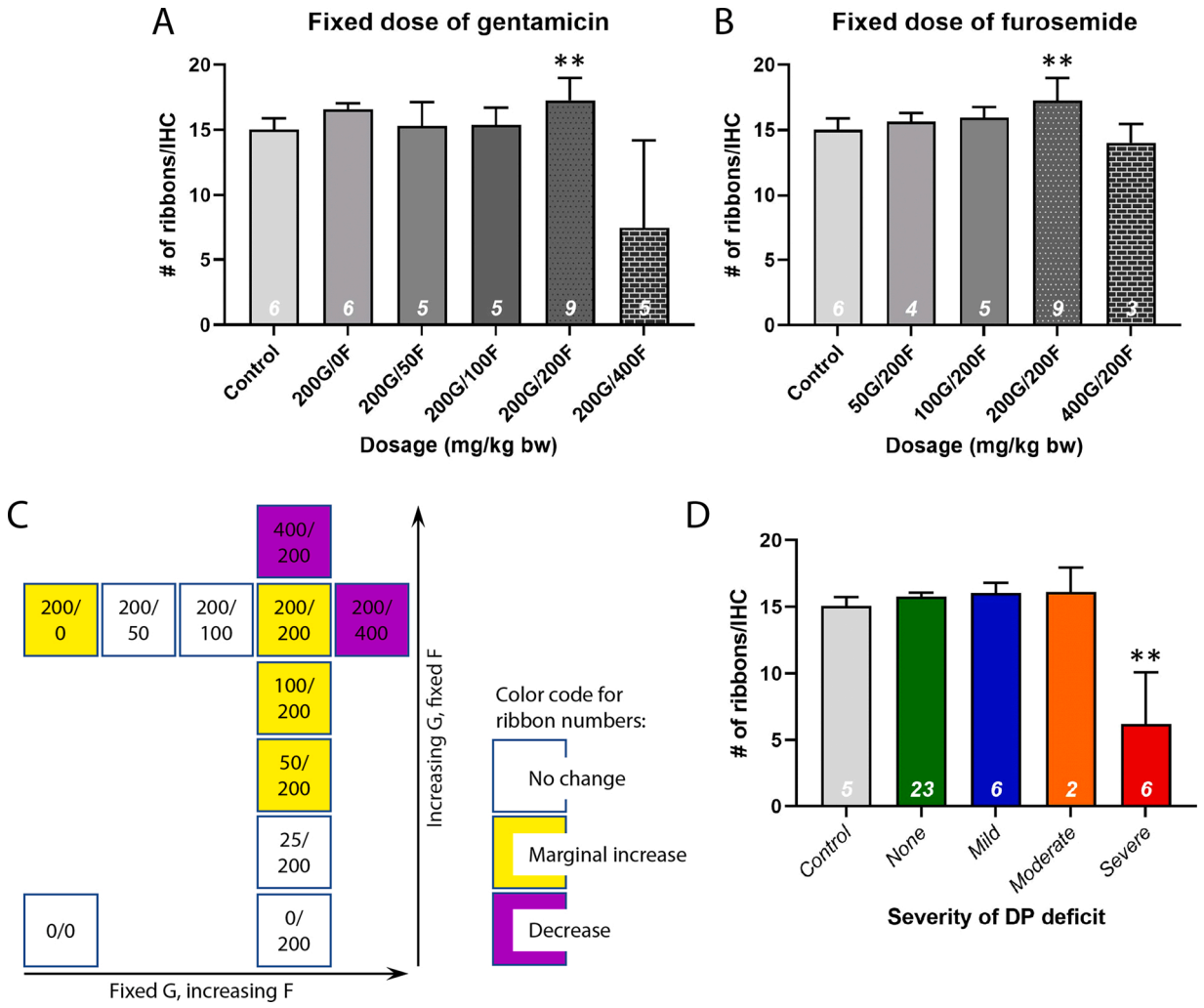

Fig. 5. Group analysis of synaptic ribbon density after G/F treatment. A: Ribbon density with a fixed dose of gentamicin and varied doses of furosemide. In each column, n depicts the number of cochleae studied, and at least 30 IHCs were counted to determine each ribbon density at the cochlear location equivalent to 12 kHz. **B**: Ribbon density with a fixed dose of furosemide and varied doses of gentamicin. **C**: Illustration of G/F treatment dosages that modified the ribbon density. **D**: Ribbon density is categorized based on the severity of DPOAE deficit. ** $p < 0.01$, 2-tailed Welch's t-test. Error bar = SD.

3.5. Gentamicin/furosemide-induced new ribbons unlikely functional

The marginal increase in ribbon density indicated a small number of synaptic ribbons were newly formed after the titrated G/F treatment. The physiological significance of this morphological alteration is unclear. According to the observation that the G/F-induced elevation of the ABR wave I I/O function was slightly more overt by 3 days posttreatment compared to 7 days as indicated in Fig. 3, we speculated that the G/F-enhanced ribbon density also occurred at earlier time points following treatment. Thus, we focused on a subset of *C57BL/6* mice that were administered with 400G/200F doses, and had their cochlear tissue harvested 2 days posttreatment, to better understand the mechanism of the newly generated, G/F-induced synaptic ribbons. The selected group of mice exhibited normal ABR thresholds 2 days after treatment (data not shown), but elevated wave-I amplitudes across the entire range of the tested sound levels as illustrated in Fig. 7A (2-way ANOVA, $F(1, 151) = 6.827$, $p = 0.0099$). In addition, the ribbon density appeared increased at multiple locations throughout the cochlea as indicated in Fig. 7B. However, when we calculated the correlation between the ABR wave-I amplitude and the ribbon density from individual cochleae at the 12-kHz location, the correlation coefficient was low (see Fig. 7C, r = 0.38). This outcome was further confirmed from the larger, 7-day post treatment dataset shown in Fig. 7D. Here, except for the extremely low ribbon numbers (*i.e.*, two incidences) that corresponded to the unidentifiable wave I, the G/F-enhanced ribbon density did not result in increased wave-I amplitudes with a coefficient index near 0. Consequently, the lack of correlation between the electrophysiologic measures and the morphological quantification indicated that the newly G/F-induced ribbons did not directly contribute to the elevated wave-I amplitude, and the synaptic plasticity based on morphological observations did not result in functional synapses in the present study.

4. Discussion

Similar to acoustic overstimulation and aging, it has long been considered that the primary ototoxic target of aminoglycosides including gentamicin is the sensory hair cells in the mammalian cochlea, while the damage to the SGNs is secondary (Forge and Schacht, 2000; Hirose and Sato, 2011). This dogma has recently been challenged (Liberman and Kujawa, 2017; Ruan et al., 2014), particularly with the recent research interest in HHL, a unique form of auditory neuropathy (Starr and Rance, 2015), in which the temporal processing capacity is drastically compromised, while sensitivity to pure tones remains intact.

In the present study, we used DPOAE methods to measure OHC integrity along with morphological counter-labeling agents including phalloidin and anti-Myo7a to identify sensory HCs. DPOAE measures are

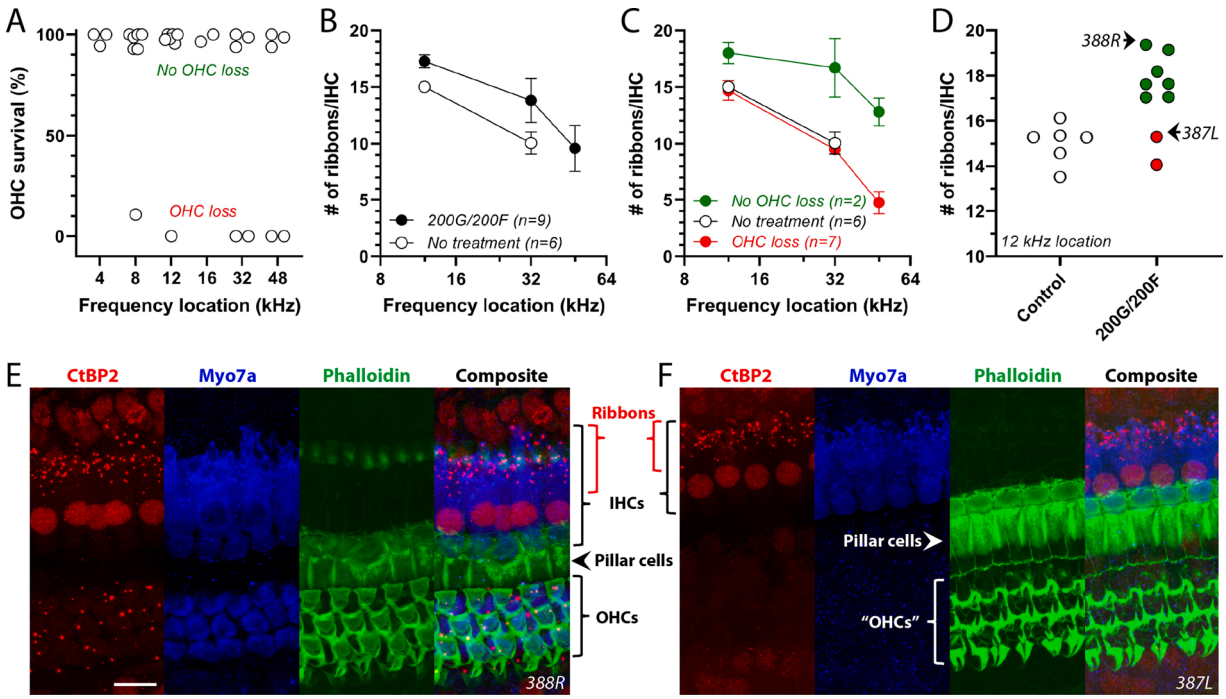

Fig. 6. Synaptic ribbon density after 200G/200F treatment. A: The OHC loss at each cochlear location where a confocal image acquired, was often complete or none. **B**: Average ribbon density from multiple cochlear locations 7 days posttreatment. Error bar = SD. **C**: Ribbon density grouped by whether OHCs were largely survived at the same cochlear location. **D**: Ribbon densities from individual cochleae at the 12-kHz location. Red: showing OHC loss. Green: without OHC loss. **E**: A representative confocal image showing intact OHCs and an elevated number of synaptic ribbons. Scale bar = 10 μm. **F**: A representative confocal image showing a complete loss of OHCs. Phalloidin labeling (green) identified scar formation at the sites of missing OHCs. (For interpretation of the references to colour in this figure legend, the reader is referred to the web version of this article.)

fast and reliable and, more importantly, a non-invasive approach to evaluate OHC function, allowing multiple assessment time points after G/F treatment. Thus, we could readily observe the progress of G/F-induced cochleotoxicity. Together with immunofluorescence techniques, the present study concluded that the G/F treatment did alter the distribution of synaptic ribbons in the IHC, but more likely in a neuroplasticity fashion instead of in association with HHL, prior to damage to the OHCs.

4.1. Gentamicin/furosemide treatment as an effective ototoxicity model in mice

A single dose of gentamicin combined with 400 mg/kg of furosemide is widely used as an effective experimental strategy to ablate OHCs in the inner ear (Kraft et al., 2013; Ruan et al., 2014; Schmitz et al., 2014). In the present study, DPOAE responses confirmed that G/F treatment resulted in HC damage, with equivalent damage severity bilaterally (Forge and Schacht, 2000). Based on our observations, unilateral severe ototoxic damage is extremely rare with only one observed case. This drug-induced cochlear damage has been used as a disease model to study corrective approaches such as cochlear implantation and HC regeneration (Kraft et al., 2013). Since we were keen on producing damage specific to the synaptic ribbon without HC loss, a variety of titrated dose combinations between gentamicin and furosemide were used (see Suppl. Fig. 1). The overall results indicated that the 400 mg/kg dosage was on the high side of dose selection that frequently caused OHC damage. Between the conditions of 200G/400F and 400G/200F, the latter was gentler in terms of stressing OHCs.

From both experimental animal studies and human temporal bone histology, furosemide and other loop diuretics exert reversible damage or edema on the cochlear lateral wall and the stria vascularis within it (Ding et al., 2016; Rybak, 1993; Santos and Nadol, 2017). The edema is typically manifested by the enlargement of the extracellular spaces from the marginal cell tight junctions to the basal cell layer with broadening of the stria vascularis. Diuretics alone do not directly damage HCs in the cochlea and the vestibular system, but, rather, cause a secondary effect from changes in the stria vascularis. Studies in mice suggested that furosemide targets the renin-angiotensin aldosterone system in the stria vascularis and disrupts the blood-cochlear barrier (Ding et al., 2016; Rybak, 1993), which allows ototoxins such as gentamicin to flush into the endolymphatic space many times more than the regular volume, and to quickly enter HCs from there (Li and Steyger, 2011). The effectiveness of furosemide on the stria vascularis likely forms a gradient from the cochlear apex to the base (Hirose and Sato, 2011), while the cochleotoxicity of gentamicin forms a gradient from base to apex. The combined ototoxic efficacy of G/F treatment appears more towards the cochlear base, similar to findings previously reported with kanamycin/furosemide treatment (Hirose and Sato, 2011). Yet, an exception did occur and a few individual cases showed apical-only G/F ototoxicity (DPOAE data not shown). In addition, G/F-induced IHC loss was rare in the present study, given the examination time points were no more than 2 weeks after treatment. Thus, this treatment protocol produces a good model for research efforts on cochlear electrode implantation and regeneration of OHCs.

4.2. Using wave-I amplitude to estimate ribbon density may not be practical shortly after gentamicin/furosemide treatment due to the "edge effect"

Firstly, we did observe a marginal G/F-enhanced wave-I amplitude from group data, and the increment appeared more evident from the ears exhibiting moderate DPOAE deficit as illustrated in Fig. 3G. It is established that a correlation exists between the wave-I ABR amplitude and ribbon density in age-related and/or noise-induced HHL (Kohrman et al., 2020). However, when we pooled data from ears with both ABR wave-I measurement and ribbon quantification at the 12-kHz location,

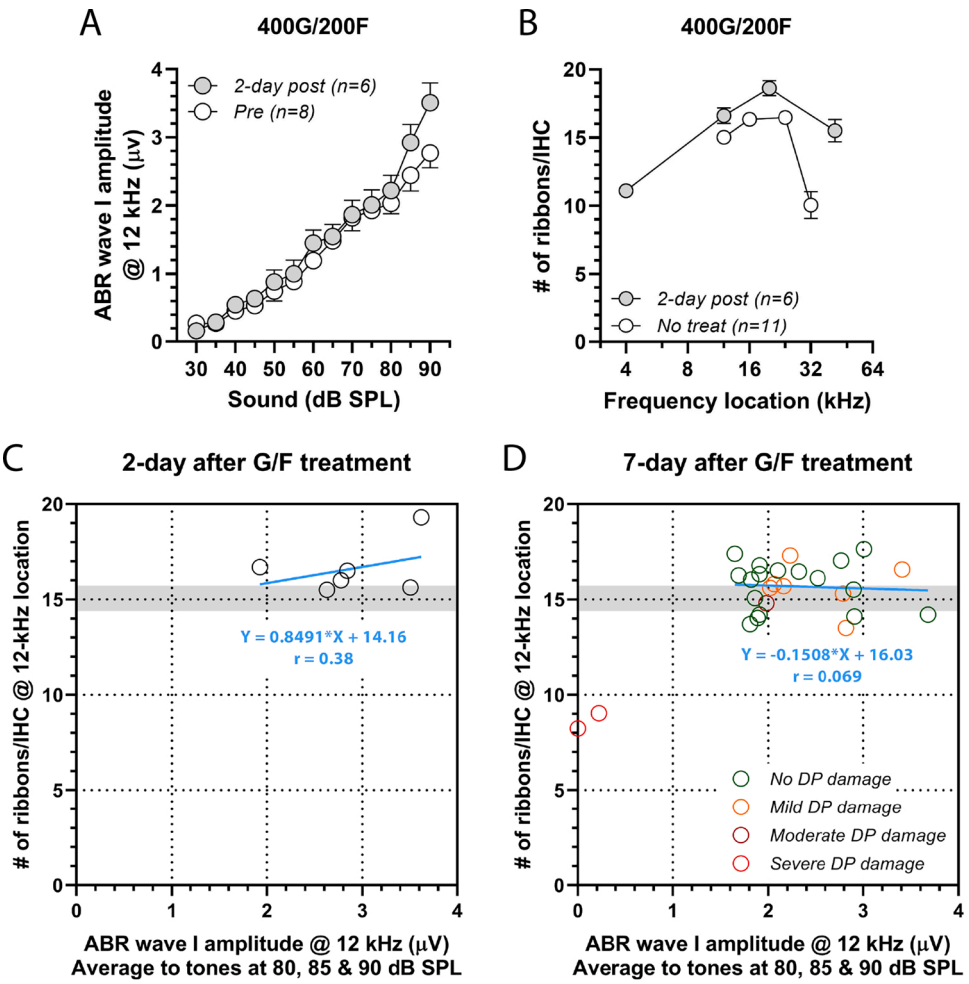

Fig. 7. The lack of correlation between the wave-I ABR amplitudes and ribbon density. **A**: Average ABR I/O-amplitude functions for 400G/200F treatment measured before and 2-day posttreatment. Error bar = SEM. **B**: Average ribbon density from multiple cochlear locations 2-day posttreatment. Error bar = SD. **C**: Scatter plot indicates the lack of correlation between the wave-I ABR amplitude and the ribbon density from individual cochleae for the 400G/200F treatment at 2-day posttreatment. Gray zone indicates the ribbon density from control ears, ±1 SD. **D**: Scatter plot shows poor correlation coefficient between the wave-I ABR amplitude and the ribbon density, from individual cochleae with intact OHCs, treated by 200 mg/kg gentamicin and varied furosemide doses at 7-day posttreatment.

this correlation did not exist for individual G/F-treated ears as seen in Fig. 7C and D as new synaptic ribbons formed. In addition, based on our observations, the prevalence of G/F-enhanced ribbon density was greater than that of G/F-increased wave-I amplitudes. One reason, of course, could be due to the lack of stability of ABR measurements. Or alternatively, the newly formed ribbons were not functional in our protocol and the increased wave-I amplitudes were supported by the augmentation of other functional modalities within the cochlea. For instance, the loss of sensory input from damaged HCs at higher-frequency locations can modify the tuning of succeeding SGNs, resulting in an increased population of SGNs responding to sounds at adjacent lower frequencies, and, consequently, a greater wave-I amplitude. This acute auditory effect is termed the "edge effect" (Snyder et al., 2000). The fact that ears with moderate DPOAE deficit exhibit greater G/F-enhanced wave-I amplitudes at the 12-kHz location supports this explanation, given that the 12-kHz location in these cases were closer to the OHC injury "edge". This acute effect could fade away to a certain extent as the succeeding SGNs gradually lost their function due to the loss of intended input from the corresponding sensory epithelium. Concordantly, the fact that 7-day wave-I amplitude elevations were

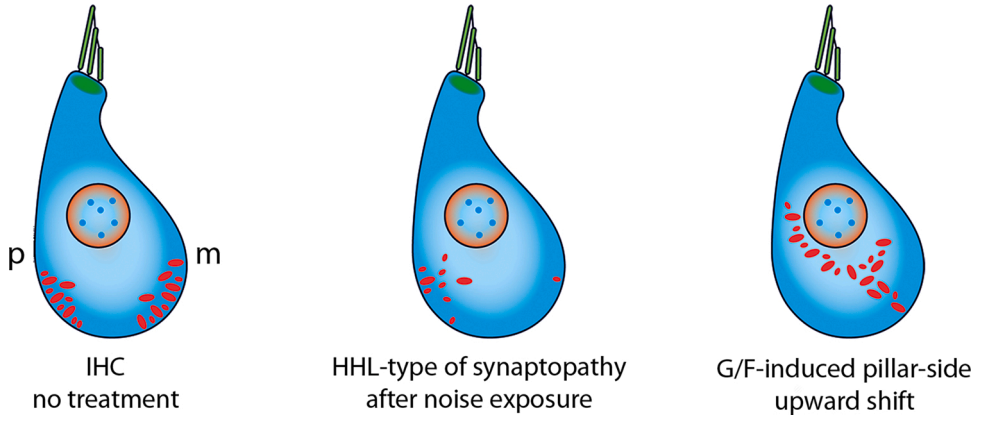

Fig. 8. Illustration demonstrates the pillar-side upward shift of the synaptic ribbons after G/F treatment. Red particles depict individual synaptic ribbons. p = pillar side; m = modiolar side. (For interpretation of the references to colour in this figure legend, the reader is referred to the web version of this article.)

slightly less than that of the 3-day elevations did support the hypothesis.

4.3. Pillar-side upward shift of synaptic ribbons with G/F treatment

After G/F treatment in *C57BL/6* mice, pillar-side upward shift of synaptic ribbons is a prevalent morphological event (Fig. 8). The marginally increased number of ribbons appears not adequate to solely be responsible for their upward shift. That is, the shifted ribbons are unlikely the newly generated synaptic ribbons, but, rather, are the relocated ribbons from the basal pole of IHCs. Specimens without OHC loss and processed with both CtBP2 and GluR2 antibodies confirmed the expected pairing between the presynaptic ribbon and postsynaptic AMPA receptor, which implies that the ribbons are mature, instead of freshly assembled. However, if the overall ribbon density increased significantly with G/F treatment, it is reasonable to hypothesize that some new ribbons are recruited to the cellular membrane not far from the nucleic zone. Ribbons that are located on the pillar side are considered to connect with ANFs with low-threshold and high-spontaneous discharge rates. These fibers also present a narrow dynamic range of discharge rate, meaning less of an increment in the overall discharge rate as the sound level of the acoustic stimulus increased. This could partially explain the marginal, and mostly non-significant increase of the ABR wave-I amplitudes, as well as the lack of a correlation between the wave I amplitudes and ribbon density.

We also observed larger ribbons under certain circumstance after G/F treatment, and the entire z-stack of confocal images were reviewed to determine if the larger size was caused by the overlap of multiple ribbons on the z-direction. It is often not the case. Ribbon enlargement is reminiscent of a similar phenomenon that occurs during neonatal cochlear development, in which a size increment in ribbon synapses occurs between postnatal day 3 and day 10 (Kalluri and Monges-Hernandez, 2017). Ribbon enlargement is possibly associated with functional recovery from noise trauma (Edderkaoui et al., 2018). In these studies, including the present study, due to the resolution of confocal microscopy, we can't rule out the large size was actually due to double ribbons that were located very close, a phenomenon was previously reported by electron microscopy of synapses during early development (Safieddine et al., 2012).

4.4. Why was there not HHL-type of reduction of ribbon density?

Ribbon synaptic transmission between IHCs and SGNs is excitatory and glutamatergic, and the ribbon synapse is susceptible to excitotoxicity, presumably due to excessive glutamate release from IHCs. Intracochlear perfusion of glutamate agonists *in vivo* results in the degeneration of SGN synaptic terminals on IHCs (Pujol et al., 1996, 1985; Ruel et al., 2007). To date, excitotoxicity is the leading underlying mechanism of the HHL-type synaptopathy due to acoustic overexposure (Kujawa and Liberman, 2009, 2015). Intriguingly, excitotoxicity has also been proposed as one of the toxic mechanisms impeding auditory function with aminoglycoside treatment (Duan et al., 2000; Sedo-Cabezon et al., 2014). Given that excitotoxicity primarily targets the synaptic terminals of ANFs, *i.e.*, ribbon synapses, it is legitimate to speculate that aminoglycosides could cause synaptopathy, and more specifically, an HHL-type of synaptopathy with carefully titrated doses of aminoglycosides (Jiang et al., 2017; Liberman and Kujawa, 2017). In the present study, with combined G/F treatment, synaptic ribbons were often reorganized, and ribbon density was rarely reduced, at least, not prior to overt damage at the OHC level. This observation is contrary to a model of aminoglycoside-induced excitotoxicity. Since the cochlear damage by a furosemide-induced ototoxicity is rather rapid (Taylor et al., 2008), we postulate that a chronic situation is necessary for the aminoglycoside to be effectively excitotoxic at the synaptic terminals of the ANF, thus, multiday aminoglycoside treatment might be necessary to encourage an adequate excitotoxicity that results in an HHL-type synaptopathy. Further investigations are thus warranted to confirm such a notion.

4.5. Study limitations

In the present study, we have generated a large dataset to evaluate G/F-induced cochlear synaptic damage, yet, several limitations remain. First, the cochlear morphology was predominantly studied at 7 days posttreatment, missing potential long-term ototoxic effects, while the reported synaptic plasticity could be more evident at earlier posttreatment time points (Fig. 7A). Second, full range I/O functions of ABR wave-I amplitude were only assessed at 12 kHz, except the satellite 200G/200F dosing group (Fig. 6). Third, the concept of newly formed synaptic ribbons was established by an extrapolation from ABR wave-I results and synaptic ribbon morphology. A designated experiment on synaptic plasticity will be instrumental to thoroughly examine this concept. In summary, given the large inter-animal variability after the G/F treatment, a fixed dose of G/F combination can be practically selected, such as 200G/200F, to expand the study and allow research efforts focusing on other experimental parameters in future studies.

CRediT authorship contribution statement

Liana Sargsyan: conceived and designed the project, performed the experiments, analyzed the data. **Alisa P. Hetrick:** performed the experiments, analyzed the data. **Jessica G. Gonzalez:** performed the experiments, analyzed the data. **Marjorie R. Leek:** wrote and revised the paper, provided financial support for the project. **Glen K Martin:** wrote and revised the paper. **Hongzhe Li:** conceived and designed the project, analyzed the data, wrote and revised the paper, provided financial support for the project.

Conflict of Interest

The authors declare no conflict of interest.

Declaration of Competing Interest

The authors report no declarations of interest.

Acknowledgements

This material is the result of work jointly supported by the Office of the Assistant Secretary of Defense for Health Affairs through the Peer Reviewed Medical Research Program under Awards No. W81XWH-14-1-0006 (HL) and No. W81XWH-19-1-0862 (ML), and by the Office of Research & Development of Veterans Health Association under Award No. RX002813 (HL). This work is also supported with resources and the use of facilities at the VA Loma Linda Healthcare System. Opinions, interpretations, conclusions and recommendations are those of the authors and are not necessarily endorsed by the U.S. Department of Defense, the Department of Veterans Affairs or the United States Government. In addition, the authors would like to express their sincere gratitude to Drs. Jonathan Venezia and Brenda Lonsbury-Martin for their consultation.

Appendix A. Supplementary data

Supplementary material related to this article can be found, in the online version, at doi:https://doi.org/10.1016/j.neuro.2021.02.007.

References

Basile, A.S., Huang, J.M., Xie, C., Webster, D., Berlin, C., Skolnick, P., 1996. N-methyl-D-aspartate antagonists limit aminoglycoside antibiotic-induced hearing loss. Nat. Med. 2, 1338–1343.

Ding, D., Liu, H., Qi, W., Jiang, H., Li, Y., Wu, X., Sun, H., Gross, K., Salvi, R., 2016. Ototoxic effects and mechanisms of loop diuretics. J. Otol. 11, 145–156.

Duan, M., Agerman, K., Ernfors, P., Canlon, B., 2000. Complementary roles of neurotrophin 3 and a N-methyl-D-aspartate antagonist in the protection of noise and aminoglycoside-induced ototoxicity. Proc. Natl. Acad. Sci. U. S. A. 97, 7597–7602.
Edderkaoui, B., Sargsyan, L., Hetrick, A., Li, H., 2018. Deficiency of duffy antigen receptor for chemokines ameliorated cochlear damage from noise exposure. Front. Mol. Neurosci. 11.
Forge, A., Schacht, J., 2000. Aminoglycoside antibiotics. Audiol. Neurootol. 5, 3–22.
Hirose, K., Sato, E., 2011. Comparative analysis of combination kanamycin-furosemide versus kanamycin alone in the mouse cochlea. Hear. Res. 272, 108–116.
Hong, J., Chen, Y., Zhang, Y., Li, J., Ren, L., Yang, L., Shi, L., Li, A., Zhang, T., Li, H., et al., 2018. N-methyl-D-aspartate receptors involvement in the gentamicin-induced hearing loss and pathological changes of ribbon synapse in the mouse cochlear inner hair cells. Neural Plast. 2018, 3989201.
Izumikawa, M., Minoda, R., Kawamoto, K., Abrashkin, K.A., Swiderski, D.L., Dolan, D.F., Brough, D.E., Raphael, Y., 2005. Auditory hair cell replacement and hearing improvement by Atoh1 gene therapy in deaf mammals. Nat. Med. 11, 271–276.
Jiang, M., Karasawa, T., Steyger, P.S., 2017. Aminoglycoside-induced cochleotoxicity: a review. Front. Cell. Neurosci. 11, 308.
Kalluri, R., Monges-Hernandez, M., 2017. Spatial gradients in the size of inner hair cell ribbons emerge before the onset of hearing in rats. J. Assoc. Res. Otolaryngol. 18, 399–413.
Kohrman, D.C., Wan, G., Cassinotti, L., Corfas, G., 2020. Hidden hearing loss: a disorder with multiple etiologies and mechanisms. Cold Spring Harb. Perspect. Med. 10.
Kraft, S., Hsu, C., Brough, D.E., Staecker, H., 2013. Atoh1 induces auditory hair cell recovery in mice after ototoxic injury. Laryngoscope 123, 992–999.
Kujawa, S.G., Liberman, M.C., 2009. Adding insult to injury: cochlear nerve degeneration after "temporary" noise-induced hearing loss. J. Neurosci. 29, 14077–14085.
Kujawa, S.G., Liberman, M.C., 2015. Synaptopathy in the noise-exposed and aging cochlea: primary neural degeneration in acquired sensorineural hearing loss. Hear. Res. 330, 191–199.
Li, H., Steyger, P.S., 2011. Systemic aminoglycosides are trafficked via endolymph into cochlear hair cells. Sci. Rep. 1.
Liberman, M.C., Kujawa, S.G., 2017. Cochlear synaptopathy in acquired sensorineural hearing loss: manifestations and mechanisms. Hear. Res. 349, 138–147.
Liu, K., Jiang, X., Shi, C., Shi, L., Yang, B., Shi, L., Xu, Y., Yang, W., Yang, S., 2013. Cochlear inner hair cell ribbon synapse is the primary target of ototoxic aminoglycoside stimuli. Mol. Neurobiol. 48, 647–654.
Liu, K., Chen, D., Guo, W., Yu, N., Wang, X., Ji, F., Hou, Z., Yang, W.Y., Yang, S., 2015. Spontaneous and partial repair of ribbon synapse in cochlear inner hair cells after ototoxic withdrawal. Mol. Neurobiol. 52, 1680–1689.
Moser, T., Starr, A., 2016. Auditory neuropathy–neural and synaptic mechanisms. Nat. Rev. Neurol. 12, 135–149.
Muller, M., von Hunerbein, K., Hoidis, S., Smolders, J.W., 2005. A physiological place-frequency map of the cochlea in the CBA/J mouse. Hear. Res. 202, 63–73.
Oishi, N., Duscha, S., Boukari, H., Meyer, M., Xie, J., Wei, G., Schrepfer, T., Roschitzki, B., Boettger, E.C., Schacht, J., 2015. XBP1 mitigates aminoglycoside-induced endoplasmic reticulum stress and neuronal cell death. Cell Death Dis. 6, e1763.
Pujol, R., Lenoir, M., Robertson, D., Eybalin, M., Johnstone, B.M., 1985. Kainic acid selectively alters auditory dendrites connected with cochlear inner hair cells. Hear. Res. 18, 145–151.
Pujol, R., Gervais d'Aldin, C., Saffiedine, S., Eybalin, M., Puel, J.L., 1996. Repair of inner hair cell-auditory nerve synapses and recovery of function after an excitotoxic injury. In: RJS (Ed.), Auditory Plasticity and Regeneration. Thieme Medical Publishers Inc, New York, pp. 100–107.
Ruan, Q., Ao, H., He, J., Chen, Z., Yu, Z., Zhang, R., Wang, J., Yin, S., 2014. Topographic and quantitative evaluation of gentamicin-induced damage to peripheral innervation of mouse cochleae. Neurotoxicology 40, 86–96.
Ruel, J., Wang, J., Rebillard, G., Eybalin, M., Lloyd, R., Pujol, R., Puel, J.L., 2007. Physiology, pharmacology and plasticity at the inner hair cell synaptic complex. Hear. Res. 227, 19–27.
Rybak, L.P., 1993. Ototoxicity of loop diuretics. Otolaryngol. Clin. North Am. 26, 829–844.
Safieddine, S., El-Amraoui, A., Petit, C., 2012. The auditory hair cell ribbon synapse: from assembly to function. Annu. Rev. Neurosci. 35, 509–528.
Santos, F., Nadol, J.B., 2017. Temporal bone histopathology of furosemide ototoxicity. Laryngoscope Investig. Otolaryngol. 2, 204–207.
Schmitz, H.M., Johnson, S.B., Santi, P.A., 2014. Kanamycin-furosemide ototoxicity in the mouse cochlea: a 3-dimensional analysis. Otolaryngol. Head. Neck Surg. 150, 666–672.
Sedo-Cabezon, L., Boadas-Vaello, P., Soler-Martin, C., Llorens, J., 2014. Vestibular damage in chronic ototoxicity: a mini-review. Neurotoxicology 43, 21–27.
Segal, J.A., Harris, B.D., Kustova, Y., Basile, A., Skolnick, P., 1999. Aminoglycoside neurotoxicity involves NMDA receptor activation. Brain Res. 815, 270–277.
Snyder, R.L., Sinex, D.G., McGee, J.D., Walsh, E.W., 2000. Acute spiral ganglion lesions change the tuning and tonotopic organization of cat inferior colliculus neurons. Hear. Res. 147, 200–220.
Spongr, V.P., Flood, D.G., Frisina, R.D., Salvi, R.J., 1997. Quantitative measures of hair cell loss in CBA and C57BL/6 mice throughout their life spans. J. Acoust. Soc. Am. 101, 3546–3553.
Starr, A., Rance, G., 2015. Auditory neuropathy. Handb. Clin. Neurol. 129, 495–508.
Taylor, R.R., Nevill, G., Forge, A., 2008. Rapid hair cell loss: a mouse model for cochlear lesions. J. Assoc. Res. Otolaryngol. 9, 44–64.
Willott, J.F., Turner, J.G., Carlson, S., Ding, D., Seegers Bross, L., Falls, W.A., 1998. The BALB/c mouse as an animal model for progressive sensorineural hearing loss. Hear. Res. 115, 162–174.

The Laryngoscope

Intratympanic Lipopolysaccharide Elevates Systemic Fluorescent Gentamicin Uptake in the Cochlea

Yongchuan Chai, MD, PhD; Weiwei He, MD; Weiqiang Yang, MD; Alisa P. Hetrick, BS; Jessica G. Gonzalez, BS; Liana Sargsyan, MD; Hao Wu, MD, PhD; Timothy T. K. Jung, MD, PhD; Hongzhe Li, PhD

Objectives/Hypothesis: Lipopolysaccharide (LPS), a key component of bacterial endotoxins, activates macrophages and triggers the release of inflammatory cytokines in mammalian tissues. Recent studies have shown that intratympanic injection of LPS simulates acute otitis media (AOM) and results in morphological and functional changes in the inner ear. Here we established an AOM mouse model with LPS to investigate the uptake of ototoxic gentamicin in the inner ear, and elucidated the underlying mechanism by focusing on cochlear inflammation as a result of AOM.

Study Design: Preclinical rodent animal model.

Methods: Fluorescently tagged gentamicin (GTTR) was systemically administered to mice with AOM. Iba1-positive macrophage morphology and inner ear cytokine profile were evaluated by immunofluorescence technique and a mouse cytokine array kit, respectively.

Results: We observed characteristic symptoms of AOM in the LPS-treated ears with elevated hearing thresholds indicating a conductive hearing loss. More importantly, the LPS-induced AOM activated cochlear inflammatory responses, manifested by macrophage infiltration, particularly in the organ of Corti and the spiral ligament, in addition to the up-regulation of proinflammatory cytokines. Meanwhile, GTTR uptake in the stria vascularis and sensory hair cells from all the LPS-treated ears was significantly enhanced at 24, 48, and 72-hour post-treatment, as the most prominent enhancement was observed in the 48-hour group.

Conclusion: In summary, this study suggests that the pathological cochlea is more susceptible to ototoxic drugs, including aminoglycosides, and justified the clinical concern of aminoglycoside ototoxicity in the AOM treatment.

Key Words: Acute otitis media, lipopolysaccharide, aminoglycosides, gentamicin, inflammation, macrophage, cytokine, drug uptake, hearing loss.

***Laryngoscope*, 00:1–10, 2021**

INTRODUCTION

Otitis media (OM) is arguably the most prominent pathology that is associated with acquired hearing deficits, after excluding factors such as genetic predisposition, aging, and history of exposure to noise and ototoxic agents.[1] Regardless of treatment selection, significant short- and long-term adverse effects are expected, and treatment plans for acute otitis media (AOM) typically include the application of antibiotics.

Aminoglycoside is a group of antibiotics that is critical for treating life-threatening Gram-negative bacterial infections.[2] However, aminoglycosides also induce cytotoxicity in the cochlea, the vestibular system, and the kidney. All cells appear to take up aminoglycosides after systemic administration, and while most cells clear the drug rather quickly, inner ear sensory hair cells (HCs) selectively retain the drug.[3] Previous studies have used Texas Red-conjugated gentamicin (GTTR) as a powerful tool to study drug trafficking kinetics in the cochlea. Serum levels of GTTR rapidly increase following intraperitoneal injection and GTTR preferentially accumulates in the stria vascularis (SV).[4] GTTR has a broad fluorescence (dynamic) range with increasing dose, providing a reliable sensitivity to determine the differential uptake of the marker as experimental condition varies.[5]

Inflammation caused by OM is thought to alter the permeability of cochlear membranes that face the middle ear cavity, allowing bacterial toxins and inflammatory

From the Research Service (Y.C., W.H., W.Y., A.P.H., J.G.G., L.S., T.T.K.J., H.L.), VA Loma Linda Healthcare System, Loma Linda, California, U.S.A.; Department of Otolaryngology Head and Neck Surgery (Y.C., W.H., H.W.), Shanghai Ninth People's Hospital Affiliated Shanghai Jiaotong University School of Medicine, Shanghai, China; Ear Institute, Shanghai Jiaotong University School of Medicine (Y.C., W.H., H.W.), Shanghai, China; and the Department of Otolaryngology Head and Neck Surgery (Y.C., W.H., W.Y., T.T.K.J., H.L.), Loma Linda University Health, Loma Linda, California, U.S.A.

Additional supporting information may be found in the online version of this article.

Editor's Note: This Manuscript was accepted for publication on April 26, 2021

Y.C., W.H., and W.Y. contributed equally to this work.

The research was conducted in the absence of any commercial relationship that could be construed as a potential conflict of interest.

The authors have no other funding, financial relationships, or conflicts of interest to disclose.

Send correspondence to Hongzhe Li, PhD, Research Service, 11201 Benton Street, Loma Linda, CA 92357.

E-mail: hongzhe.li@va.gov or hongzhe@gmail.com

DOI: 10.1002/lary.29610

substances to more readily enter into the inner ear.[6,7] In this study, we explored the effect of Lipopolysaccharide (LPS)-induced AOM on aminoglycoside uptake, as well as the other aspects of the inflammatory response in the cochlea. Following stimulation in the middle ear, fibrocytes in the spiral ligament are responsive to immunogenic signals and subsequently release cytokines, as a relay to initiate immune responses in the inner ear.[8] In previous studies, systemic LPS-induced endotoxemia caused elevation of ototoxic aminoglycoside uptake by cochlear tissues including sensory HCs.[9] This observation is suggestive that similar effects are likely to occur after intratympanic LPS injection, an iconic animal model of OM without live bacterial infection.

Clinically, topical treatment of OM with aminoglycosides, such as neomycin, is effective, but also controversial and many otolaryngologists are concerned that aminoglycoside eardrops may be ototoxic if they enter the middle ear through a ruptured tympanic membrane (TM).[10] Scientific evidence for this specific concern is scarce and clinicians often take precaution and best practice, avoiding the ototopical use of aminoglycosides. The present study also provides the needed justification to support the ototoxic concern upon drug selection in OM treatment in the presence of TM perforation or tympanostomy tube allowing ototoxic ear drops to land in the middle ear.

MATERIALS AND METHODS

Mice

C57BL/6 mice (aged 6–8 weeks, JAX stock #0664) were housed in a Specific Pathogen Free-modified room, without any sound treatment besides the ambient noise. All animal work was carried out using protocols approved by the Institutional Animal Care and Use Committee of the Jerry L. Pettis VA Medical Center, Loma Linda, CA. Animal use procedures conform with federal regulations regarding personnel, supervision, record keeping, and veterinary care.

LPS or PBS Treatment and Tissue Preparation

To perform minimally invasive intratympanic (*i.t.*) injection, a small puncture was initially made by an insulin syringe needle at the anteroinferior quadrant of the TM. Then, another syringe needle, which was connected to a fine flexible polyurethane tube (Fig. 1A), was used to perform the *i.t.* injection. In each animal, 10 μl LPS (Invitrogen, Cat# 00-4976, 1 mg/ml, dissolved in 0.01 M PBS) or phosphate-buffered saline (PBS) was injected into the right ear. At different times after LPS/PBS treatment, mice were cardiac perfused with PBS, then 4% formaldehyde. Cochleae were excised and post-fixed for 2 hours, then proceeded to immunolabeling. For cytokine detection, cochleae from mice not-cardiac perfused were flash-frozen in liquid nitrogen and stored.

Auditory Testing

An auditory brain-stem response (ABR) test was selected to evaluate the hearing function. Briefly, each ear was tested with a closed tube sound delivery system sealed into the ear canal. The ABRs to tone burst stimuli (5-ms duration, 1-ms rise/fall) at 4, 8, 12, 16, 24, and 32 kHz, with 5-dB steps, were recorded using a TDT System 3 (Tucker-Davis Technologies, Alachua, FL). The threshold was determined by the lowest stimulus level that produces a minimally visible response.

Systemic GTTR Application and Cochlear Uptake

After LPS/PBS treatment, fluorescently (Texas Red) tagged gentamicin (GTTR, m.w. = ~1,100 g/mol) was systemically (2 μg/g body weight, *i.p.*) administered to mice 1 hour before cardiac perfusion. Purified GTTR conjugate was produced as previously described.[5] In the present study, GTTR was solely used as a molecular tracer to study its intracochlear uptake, and at a dose greatly lower than that induces ototoxicity when gentamicin (C2, m.w. = 463.6 g/mol) is administered.

The same confocal settings were used to compare bilateral images from individual mice, with two acquisitions per location to guarantee data consistency. GTTR fluorescent pixel intensities were obtained by the histogram function of the ImageJ software (Fiji, National Institutes of Health, Bethesda, MD) after the removal of nucleic pixels using Adobe Photoshop. Pixel intensities were statistically compared within each set of images per experiment and not directly compared between different experiments. To normalize data among multiple experimental sets, the mean intensity was ratioed against the control standard and graphed.[11]

Immunolabeling of Iba1-Positive Macrophages

Immunofluorescence labeling was performed using anti-Iba1 rabbit IgG to identify the macrophage. After perfusion and fixation, cochlear tissues were isolated and dissected without decalcification, then processed for immunohistochemical labeling. Tissue was rinsed with 0.5% Triton X-100 in PBS for 30 min and incubated at room temperature for 2 hours in blocking solution (5% normal horse serum; 1% Triton X-100 in PBS). Tissue was then incubated overnight at 37°C with anti-Iba1 rabbit IgG (Cat# ab178846, Abcam; 1:200) in antibody incubation solution (1% normal horse serum; 1% Triton X-100 in PBS). Then specimens were incubated for 2 hours with secondary antibody conjugated to AlexaFluor-647 (Cat# A21245, Invitrogen; 1:500) and phalloidin-488 (Cat# A12379, Invitrogen; 1:1,000) at 37°C. All specimens were rinsed before mounting and microscopic imaging (Olympus FV3000).

Cytokine Array Kit Analysis

A mouse cytokine array kit (R&D systems, Cat #ARY006) was used to simultaneously detect 40 mouse cytokines in LPS-treated cochlear samples, according to the manufacturer's instructions. The chemiluminescent signal on each membrane was collected using an Amersham Imager 600 (GE Healthcare Life Sciences, Pittsburgh, PA). The intensity (pixel density) of each spot on the membrane was quantified using ImageJ software, and corrected for background intensity and normalized to the positive control on the same membrane. The experimental group and the control group each contained five cochlear samples.

Statistical Analyses

Specific statistical methods were chosen based on the data being analyzed. The Student's paired *t*-test was used for GTTR fluorescence intensity analyses. The Mann–Whitney test was used for the assessment of the thickness of TM. For ABR

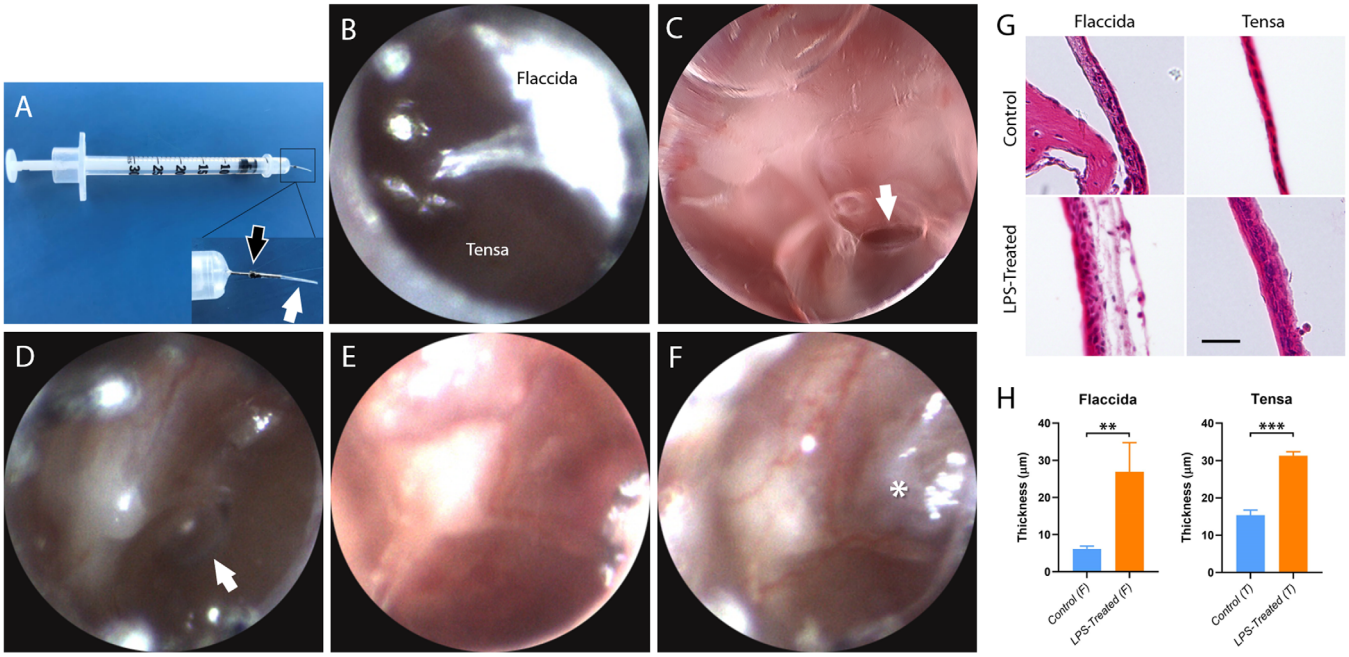

Fig. 1. Mouse model of acute otitis media by intratympanic injection of lipopolysaccharide (LPS). A, To achieve minimally invasive *i.t.* injection, a syringe needle of 31-gauge (black arrow) was connected to a fine polyurethane tube (white arrow, *o.d.* = 0.15 mm). B, Endoscopic findings of a normal tympanic membrane (TM) with Pars tensa and Pars flaccida identified. C, A puncture (arrow) was made at the anteroinferior quadrant of the mouse TM and the middle ear filled with LPS solution immediately after the *i.t.* injection. D–F, Endoscopic findings 48 hours after *i.t.* LPS injection comprised membrane opacity and middle ear effusion (D–F), air pocket (arrow in D), redness and thickening of the membrane with visible vasodilation (E, F), and pseudo-membrane (asterisk in F) at the puncture site. G, H&E staining revealed leukocyte infiltration and epithelial thickening of the TM. Middle ear cavity was located toward the right side of each panel. Error bar = 100 μm. H, Thickness comparison between LPS-treated TMs (n = 9, 10) and non-treated membranes (n = 6, 7). Mann–Whitney tests indicated significant LPS-induced thickening. $^{**}P < .01$, $^{***}P < .001$. [Color figure can be viewed in the online issue, which is available at www.laryngoscope.com.]

analyses, we used two-way analysis of variance (ANOVA) with Sidak's multiple comparisons. $P < .05$ was considered significant. Sensitivity tests were performed for statistical evaluation of the datasets based on GTTR fluorescence so as to confirm the reproducibility (Table S1).

RESULTS

Establishment of the LPS-Induced Mouse AOM Model

Intratympanic injection of LPS has been widely adopted to establish animal AOM models.[12–14] In our AOM mouse model, empirical clinical manifestations were detected by otic endoscopy as well as histological hematoxylin and eosin (H&E) staining (Fig. 1). The normal appearance of the TM was thin and transparent with light reflection (Fig. 1B). Immediately after the *i.t.* LPS injection, an aperture in the membrane could be seen, and the middle ear cavity was filled with translucent liquid (Fig. 1C). After 48 hours, the TM became congested and thickened, light reflection disappeared, the middle ear cavity was filled with turbid liquid (Fig. 1D–F), membrane perforation healed, and a healing pseudomembrane covered on the prior perforation (Fig. 1F). Microscopic images of H&E-stained samples confirmed the thickening of TM (Fig. 1G,H). The membrane thickening appeared more prominent at the inner mucosal epithelial layer facing the middle ear cavity (Fig. 1G).

LPS Treatment Enhanced GTTR Uptake by Cochlear Tissues

Three treatment groups were initially tested for 24, 48, and 72-hour post-injection, to determine the effective time of *i.t.* LPS injection on GTTR uptake, by outer hair cells (OHC) and by the SV. After LPS treatment, the SV GTTR uptake increased by 71%, 32%, and 18% in the 24, 48, and 72-hour groups, respectively (Fig. 2A). In comparison, the increase of OHC GTTR uptake was 32%, 43%, and 27%, respectively (Fig. 2B). A significant correlation existed between the SV and OHC GTTR uptake for each post-treatment time point, manifested by a significant non-zero slope of the linear regression (Figs. 2C, S1 and Table S2). Given the greatest OHC GTTR uptake enhancement, 48-hour LPS post-treatment was selected for the following experiments, and we expanded the sample size in this group to detect treatment effect in detail in terms of region-specific GTTR uptake. In all ears (n = 8) with LPS treatment for 48 hour, more intensive OHC GTTR fluorescence was observed among all three cochlear turns (Fig. 3).

As to the GTTR uptake by cochlear lateral wall tissues, a similar trend was observed. GTTR fluorescence intensity in marginal cells, intermediate cells (interstitial space), basal cells, and fibrocytes (including spiral ligament) was more intense than that of the contralateral control ear, and the increase of immunofluorescence intensity in intermediate cells was the most obvious

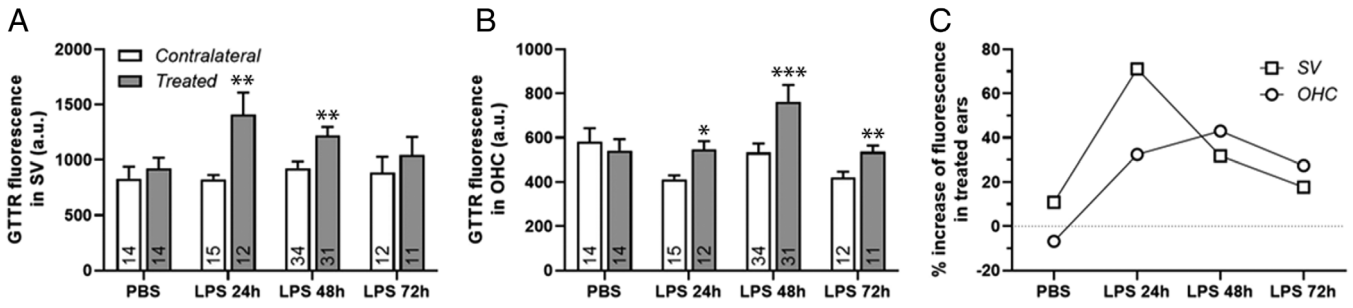

Fig. 2. GTTR uptake in the stria vascularis (SV) and by outer hair cells (OHC) from non-treated contralateral ears, or ears treated with lipopolysaccharide (LPS) or PBS. A, Compared with the contralateral control ears, GTTR uptake in the SV was significantly enhanced at all three LPS post-treatment time points, but not in the control group with *i.t.* PBS treatment. B, Similarly, GTTR uptake by the OHCs increased by 32.5%, 43.1%, and 27.4% in *i.t.* LPS groups at 24, 48, and 72 hours post-treatment, respectively. The number of examined cochlear locations was denoted in each bar, with 3–5 locations from each mouse. (PBS group, 4 mice; LPS-24 hour group, 4 mice; LPS-48 hour, 8 mice; LPS-72 hour group, 4 mice. ***$P < .0001$, **$P < .001$, *$P < .05$, and *t*-tests). C, Bilateral comparison of GTTR uptake was represented in the format of % increase of fluorescence intensity in the treated ear, for the SV and OHCs.

(Fig. 4A,B). The enhancement of GTTR fluorescence intensities in intermediate cells in the middle and basal turns and the whole cochlea including all three turn locations was significant (Fig. 4C). These results indicated the *i.t.* LPS elevated the GTTR uptake in HCs and lateral wall tissues of the cochlea.

LPS Treatment Activated Iba1-Positive Macrophages in the Fibrocyte Layer of the Lateral Wall but not That in the SV

In the untreated contralateral control ear, a certain number of Iba1-positive macrophages with ramified shape were present in the fibrocyte layer of the cochlear lateral wall (Fig. 5A; first column). Forty-eight hour after *i.t.* LPS, these immune cells were activated. The number of macrophages in the fibrocyte layer increased drastically in all three turns, and the morphology of Iba1-positive macrophages greatly altered. In brief, the change could be described by vigorous branching and enlarged cell volume (Fig. 5A; second column). As previously reported,[15] Iba1-positive macrophages were also detectable in the SV but appeared rather inactive after LPS treatment as we observed no change in either number or morphology (Fig. 5B).

LPS Treatment Also Activated Iba1-Positive Macrophages in the Organ of Corti

In the absence of LPS treatment, and distinguishable from the morphology of macrophages in the cochlear lateral wall, Iba1-positive macrophages exhibited various shapes in the organ of Corti depending on their locations. The shape of Iba1-positive macrophages in the apex is typically dendritic while macrophages in the base are predominantly amoeboid. The shape of macrophages in the middle turn is between these two extremities, typically a partially arborized shape (Fig. 6A).[16] At 48-hour post-treatment, the number of macrophages increased throughout the organ of Corti, and the apical macrophages changed from the typical dendritic shape to a more arborized shape (Fig. 6B).

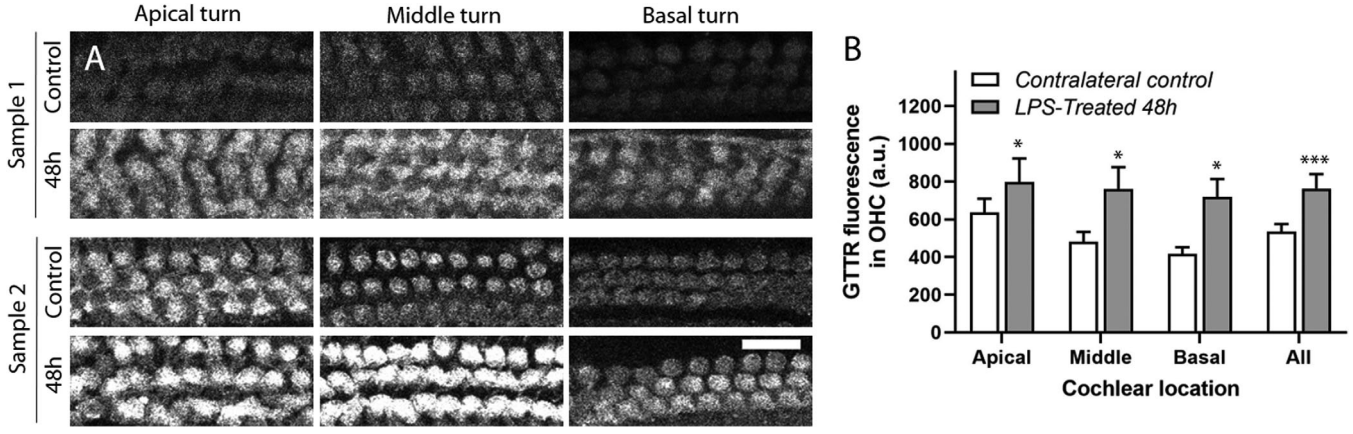

Fig. 3. Lipopolysaccharide (LPS) significantly enhanced GTTR uptake by outer hair cells (OHCs). GTTR (2 mg/kg) was injected *i.p.* 1 hour after *i.t.* LPS treatment for 48 hours. A, Representative images demonstrated increased GTTR fluorescence intensity in OHCs at various longitudinal cochlear locations, compared to the contralateral control ears without any treatment. Scale bar = 20 μm. B, The fluorescence intensity of the sub-cuticular zone of individual OHCs was scored from each confocal stack. Six stacks were imaged from each cochlea, either LPS-treated or control, with two stacks per location from the apical turn, middle turn, or basal turn. The Student's paired *t*-test indicated that *i.t.* LPS treatment exerted a statistically significant effect on GTTR fluorescence in the OHC sub-cuticular zone in all three different turn locations compared to the control ($n = 8$ mice, ***$P < .001$, *$P < .05$). Error bars, SD. a.u., arbitrary unit.

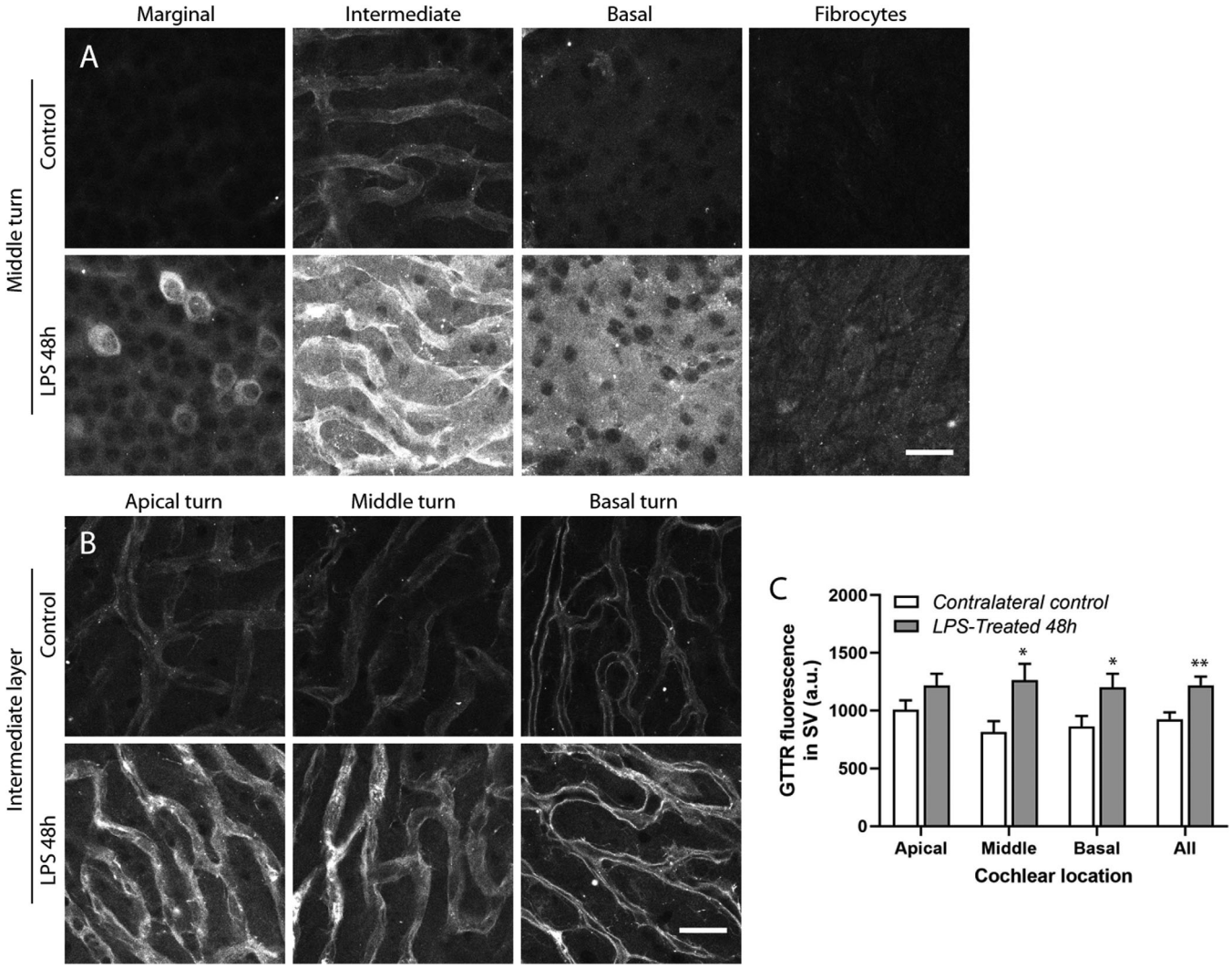

Fig. 4. Lipopolysaccharide (LPS) significantly enhanced GTTR uptake in the cochlear lateral wall. GTTR (2 mg/kg) was injected *i.p*. for 1 hour after *i.t*. LPS treatment for 48 hours. A, In wholemounts of the *i.t*. LPS-treated and control cochlear lateral wall, disparate levels of GTTR fluorescence were observed in the marginal cell layer, the intermediate cell layer, the basal cell layer, and the fibrocyte layer (spiral ligament) in the contralateral control ear (four images in the first row), among which the fluorescence intensity in the intermediate cell layer and the basal cell layer was relatively high. Compared to the control ears, GTTR fluorescence intensity was more robust in the respective cell layers in the LPS-treated ears (four images in the second row), and the increase of fluorescence intensity in the intermediate cell layer was the most noticeable. Scale bar = 20 μm. B, Increased GTTR fluorescence intensities were observed in the intermediate cell layer along the longitudinal axis from the basal turn to the apical turn in the LPS-treated ear compared to the control ear. Scale bar = 20 μm. C, GTTR fluorescence intensity was quantified from the intermediate cell layer, and significantly higher intensity was found in middle and basal turns, and in the entire cochlear combining the three turn locations in the LPS-treated ear ($n = 8$ mice, $^{**}P < .01$, $^{*}P < .05$). Error bars, SD. a.u., arbitrary unit.

LPS Treatment Induced the Change of Multiple Cytokines in Cochleae

To test if the cochlear cytokine levels also altered by *i.t*. LPS, paired whole cochlear lysates from pooled samples ($N = 7$) were processed to evaluate the cochlear cytokine profile at 48-hour post-treatment, using mouse cytokine arrays (Fig. 7A). Images of array membrane incubated with the LPS samples and the untreated controls (Fig. 7B) showing six references (A1-2, A23-24, and F1-2) exhibited the most intense immunoblotting signals, whereas the negative control (F23-24) and all the blanks (on rows E&F) exhibited undetectable signals. Seventeen cytokines were present in both LPS-treated and control samples (Fig. 7B,C). Of these, the expression of 10 cytokines, including both pro-inflammatory and anti-inflammatory, was significantly up-regulated in the LPS-treated cochlear tissues (Fig. 7C).

LPS Treatment Induced Conductive Hearing Loss

Intratympanic LPS resulted in elevated ABR thresholds at all tested frequencies. The hearing threshold increased by 11.7 to 20.8 dB at 48-hour post-treatment (Fig. 8A). The parallel threshold elevation indicated a dominant conductive hearing loss, rather than sensorineural hearing loss, in accordance with previous findings.[14,17] HC survival was evaluated according to

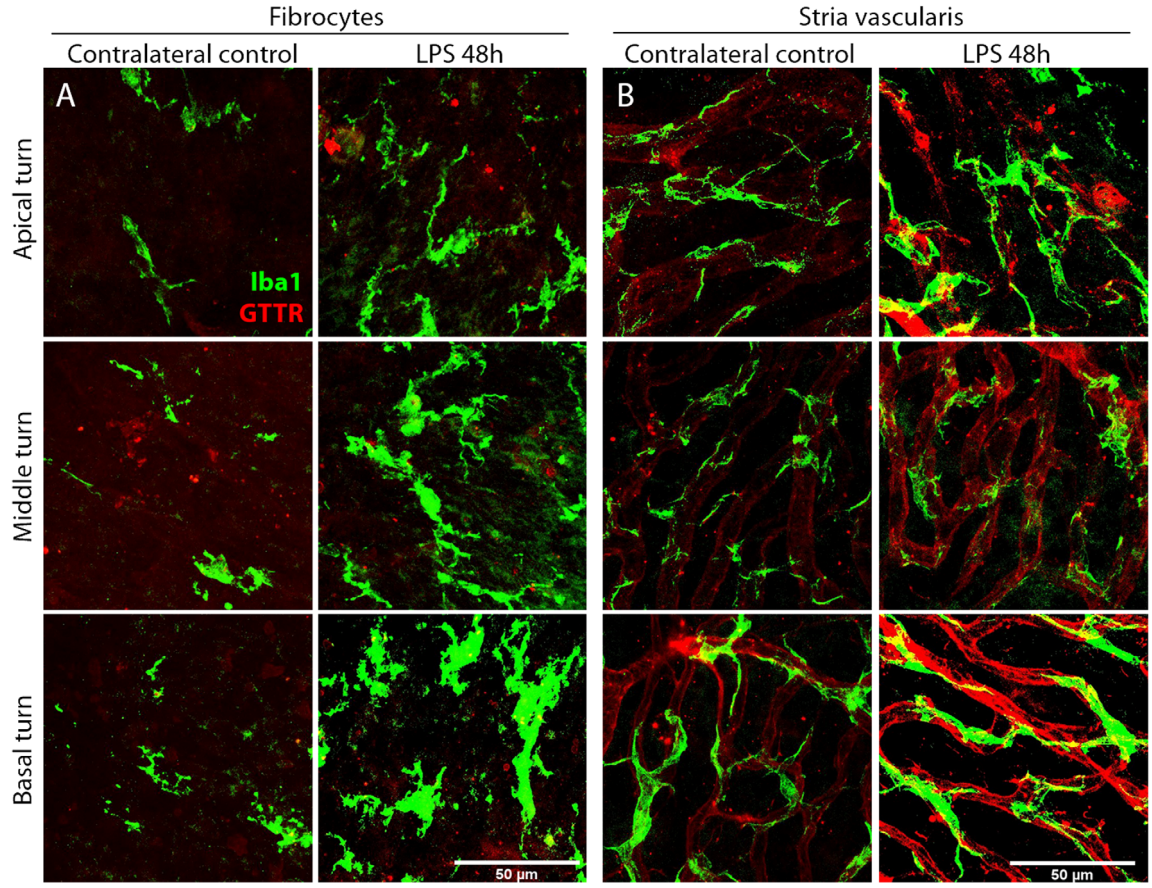

Fig. 5. Lipopolysaccharide (LPS) treatment modified Iba1-positive macrophages morphologically and numerically in the spiral ligament but not in the stria vascularis. After *i.t.* LPS treatment for 48 hours, GTTR (2 mg/kg) was administered (*i.p.*) for 1 hour prior to cochlear tissue collection including the LPS-treated ear and the contralateral control ear. GTTR fluorescence signals (red) in the cochlear lateral wall facilitated the identification of the layered anatomy. Each panel represented a z-projection confocal image through a segmented depth of the lateral wall, at various cochlear locations from the apex to the base. A, Compared to the contralateral control ear, a significant increase of Iba1-positive macrophages (green) in the spiral ligament was observed in all three turns with LPS treatment, meanwhile, the morphology of Iba1-positive macrophages also changed greatly, including enlargement and additional branching. B, In contrast, this distribution and morphology change of Iba1-positive macrophages was negligible in the SV. Scale bar = 50 μm fits all panels. [Color figure can be viewed in the online issue, which is available at www.laryngoscope.com.]

phalloidin labeling at 24, 48, and 72-hour post-injection. Consistent with the ABR result, both OHCs and inner hair cells (IHCs) largely survived and the degree of survival was comparable between LPS-treated and control ears (Fig. 8B), with the exception of 24-hour time point, at which *i.t.* LPS resulted in an OHC loss in the middle turn.

DISCUSSION

Previous studies have shown that *i.t.* LPS can cause inflammatory cell infiltration and the release of inflammatory factors in tympanum and middle ear mucosa.[12–14] Results from the present study indicate that similar inflammatory responses can also be induced in the cochlea.

OM and Sensorineural Hearing Loss

OM is arguably the most prevalent disease in humans and a major public health concern. Here, we studied the pathological responses of LPS treatment and their effect on hearing in an AOM mouse model. Our results indicated that there is no loss of OHC, up to 72 hour after LPS treatment. In contrast, the observed ABR threshold shift was an indicator of conductive hearing loss, presumably due to the middle ear effusion upon AOM. However, this does not strictly mean that AOM does not result in impairment of sensorineural function in the cochlea. As our initial focus was on the uptake of GTTR by OHCs, the experimental design inevitably included a bias toward selecting cochlear locations with intact OHC morphology. HC loss is typically considered to proceed with the damage of spiral ganglion neurons and their dendrite fibers that innervate corresponding inner HCs.[18,19] Recent work on cochlear synaptopathy suggested that this is not always true.[20–22] For instance, moderate noise exposure can result in suprathreshold hearing deficit without obvious HC loss.[21,23] Furthermore, the cochlear immune activity likely has a unique role in cochlear synaptopathy.[24,25] Thus, it is a legitimate

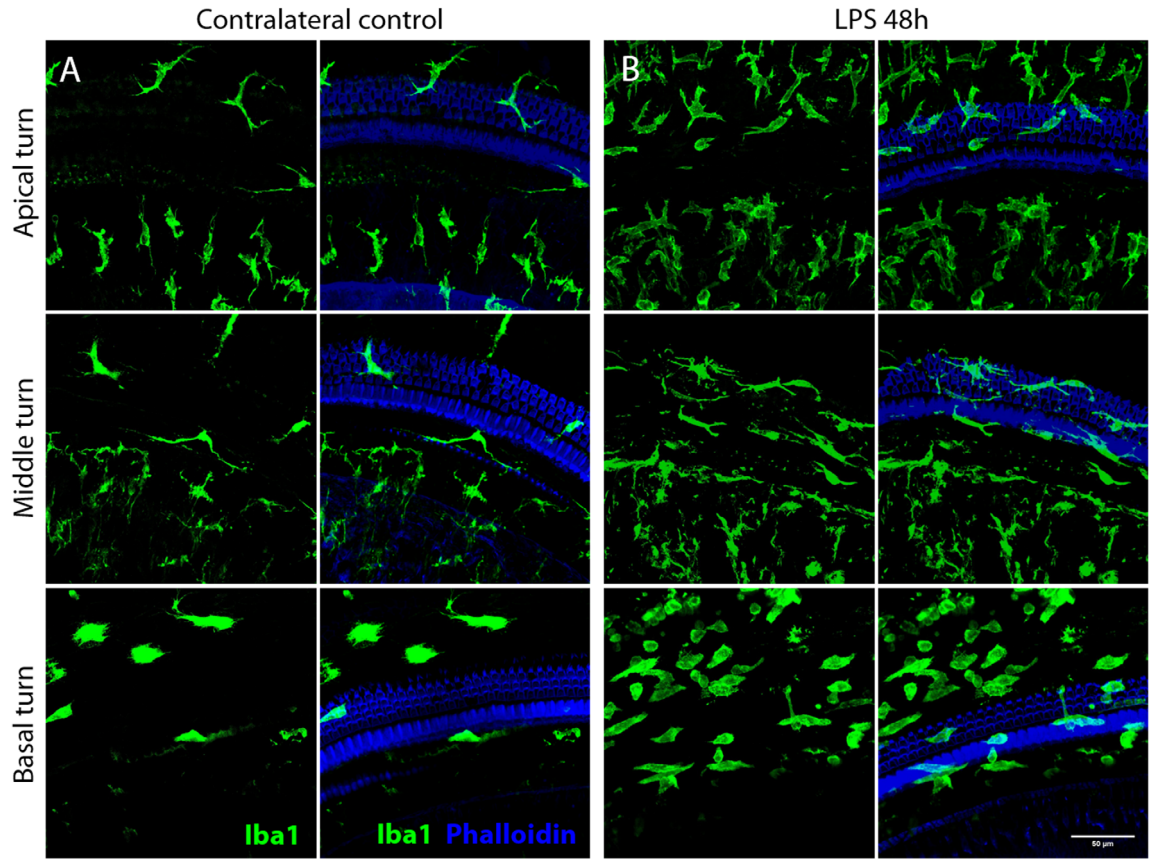

Fig. 6. Lipopolysaccharide (LPS) treatment stimulated morphological change of Iba1-positive macrophages in the organ of Corti. Cochlear tissues were collected after LPS treatment for 48 hours, then immunolabeled with anti-Iba1 antibody (green) and phalloidin (blue) to identify Iba1-positive macrophages and the structure of organ of Corti, respectively. Each panel represented a z-projection confocal image through the depth of sensory epithelium. A, In the organ of Corti of the contralateral control ear, a small number of macrophages were identified in the apical turn, the middle turn, and the basal turn. The characteristic morphology of apical macrophages was dendritic, in comparison, amoeboid shapes in the basal turn. The macrophage morphology in the middle turn was between the two extremities, exhibiting an arborized. B, After LPS treatment, the number of macrophages increased significantly in all three turns, and the apical macrophages changed from the typical dendritic shape to a more arborized form. Scale bar = 50 μm fits all panels. [Color figure can be viewed in the online issue, which is available at www.laryngoscope.com.]

question whether *i.t.* LPS could lead to synaptic damage to some extent, though subsequent work is warranted.

Although AOM did not directly cause structural damage in the inner ear, it did elevate the cochlear susceptibility to an ototoxic drug if administered during the morbidity period. The results of the present study also validated the concerns of many clinicians with respect to the potential ototoxicity when aminoglycoside drops are used to treat AOM.[10]

Activated Immune Activity in the Cochlea Under AOM

A key finding in the present study is that cochlear macrophages and inflammatory factors respond to LPS treatment. Previous findings on inner ear gene expression were reported for acute and chronic OM models using inflammatory gene arrays.[26,27] These studies together with our results suggest similar inflammatory pathways are involved in the escalated aminoglycoside ototoxicity.

In our AOM model, the boundary of the inflammatory microenvironment expanded to the cochlea from the middle ear. In the cochlea, LPS treatment altered the number and distribution of Iba1-positive macrophages, as well as their morphology in the spiral ligament and in the organ of Corti. Some macrophages changed from the typical dendritic shape to a more arborized form with an enlarged cell body. These morphological changes indicate the activation of macrophages and potential participation in nonspecific immune responses. The number and morphology of macrophages in the SV showed little modification in response to AOM, consistent with previous report.[6] Upon inflammatory stimulation, macrophages migrated from the vasculature to the spiral ligament and the spiral limbus, through capillaries embedded in these perilymph-filled regions of the mammalian cochlea.[28–30] However, the capillary environment of the SV[31–34] does not typically allow chemotactic migration of leukocytes into the intrastrial space. The number of macrophages in the SV demonstrates little variation even in conditions of severe inflammation.[14,15]

Cytokines and chemokines are extracellular signaling molecules that mediate cell–cell communication and have critical roles in many biological processes. Previous

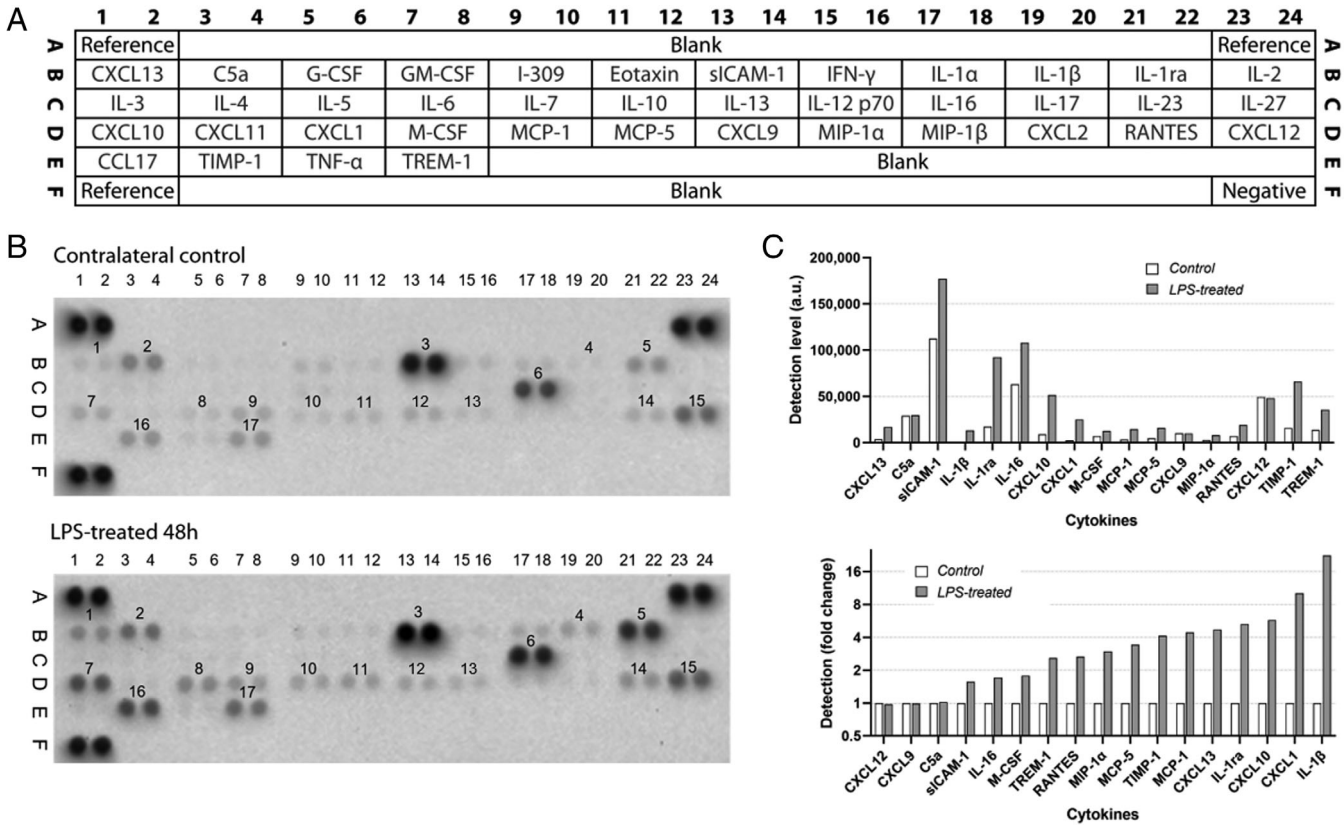

Fig. 7. Cytokine Array detection of multiple analytes in mouse cochlear tissues with *i.t.* Lipopolysaccharide (LPS) treatment. A, The alignment of 40 cytokines in duplicates on the mouse cytokine array. Reference, reference spots; Negative, negative control. B, Cytokine array blots probed with pooled, untreated contralateral control samples and *i.t.* LPS samples at 48 hours post-treatment ($N = 7$ each). Each blot represents immunoreactive labeling against the respective antibodies. The blots marked with digits are the cytokines that were clearly expressed in cochlear tissues or significantly regulated between the paired samples. 1:CXCL13; 2:C5a; 3:sICAM-1; 4:IL-1β; 5:IL-1ra; 6:IL-16; 7:CXCL10; 8: CXCL1; 9:M-CSF; 10:MCP-1; 11:MCP-5; 12:CXCL9; 13:MIP-1α; 14:RANTES; 15:CXCL12; 16:TIMP-1; 17:TREM-1. Note the absence of labeling of the negative control and blank slots. C, The detection level of marked cytokines was presented in the format of paired comparison (top) and in ranked fold change due to LPS treatment (bottom). The relative expression levels of each cytokine were determined by the average pixel intensity between the corresponding duplicates on the array, and the respective signals on the two arrays were compared after signal correction using the pixel intensity of the reference spots. Compared to the untreated control ears, the expression of various cytokines including IL-1β, CXCL1, CXCL10, IL-1ra, CXCL13, MCP-1, and TIMP-1 was significantly increased in the cochlear tissues after *i.t.* LPS treatment. a.u., arbitrary unit.

studies demonstrated that inflammatory cytokines following bacterial stimulation in the middle ear were released by resident fibrocytes,[35,36] while cochlear macrophages also release many cytokines to participate in immunity. A variety of chemokines, adhesion molecules, and other inflammation-related factors were detected previously,[37] in accordance with the increased interleukins and chemokines found in our study. It is expected that some of these cytokines activate immune cell proliferation and extend the inflammatory response, while others could be involved in processes related to inner ear tissue remodeling.

Altered Aminoglycoside Ototoxicity Under AOM

Aminoglycoside ototoxicity is a complex process occurring in a dose-dependent manner,[2] primarily affecting sensory HCs in the cochlea and vestibular labyrinth. Additional factors further predispose patients to enhanced ototoxicity, including noise exposure and individual genetic susceptibility.[38–41] Here we also observed AOM-altered aminoglycoside uptake. Modified OHC uptake of aminoglycoside in vivo or in vitro has been documented by many investigators,[5,42–45] the systemic aminoglycosides are trafficked from the strial capillaries across the SV into endolymph,[4,46,47] then cochlear HCs primarily take up aminoglycosides in endolymph across their apical membranes by mechanoelectrical transduction (MET) channels.[3,4,47–49] Aminoglycosides could also enter cells via an endocytosis pathway,[48,50–52] or via nonselective cation channels, including transient receptor potential (TRP) channels.[4,49,53–56]

Previous studies reported that systemic LPS increased the expression of acute-phase inflammatory markers in cochlear tissues, and it increased cochlear concentrations of GTTR and gentamicin.[9] This endotoxemia-induced inflammation was deemed to associate with the physiological modification of the SV and subsequently enhanced cochlear loading with gentamicin.

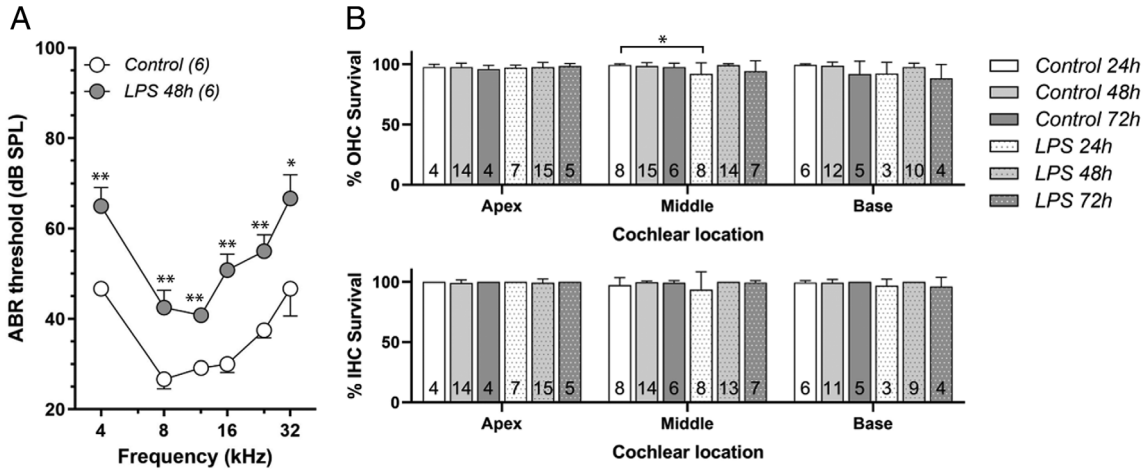

Fig. 8. Intratympanic lipopolysaccharide (LPS) injection caused conductive hearing loss. A, LPS-treated ears exhibited parallel ABR threshold elevation 48 hours later, in the degree of 15–20 dB at all tested frequencies, a characteristic indicator of conductive hearing loss. Control group, $n = 6$; LPS group, $n = 6$; $^{*}P < .05$, $^{**}P < .01$. Error bars, SD. B, Hair cell survival was not altered by *i.t.* LPS treatment examined 24, 48, and 72 hours post-treatment, suggesting the ears were free of sensorineural hearing loss. Hair cells were quantified based on phalloidin labeling along the length of the cochlea, including apex, middle, and base. LPS did not cause hair cell loss in either OHC population (top) or IHC population (bottom), except the 24 hours time point at the middle cochlear turn for OHCs (F [1,30] = 7.325, $P = .011$; Sidak's multiple comparisons test, $P = .025$). $N = 4$–8 mice per group, and 1–2 sites at each cochlear location per mouse were examined. $^{*}P < .05$. Error bars, SD.

Our results indicated that LPS-induced local acute inflammation also increased GTTR uptake in the inner ear. In the AOM model, systemic GTTR could enter the inner ear via the inflamed, and often fluid-filled middle ear. However, the observation of the uniform increase of GTTR uptake throughout the cochlea is more consistent with a local enhancement mechanism pertaining to the blood-labyrinth barrier.

Although AOM raises the cochlear susceptibility to aminoglycosides, the direct relationship between the middle ear inflammation and the inner ear sensitivity of aminoglycosides remains unclear. We speculated that increased chemokines could directly modulate the activity of endocytosis, and sensitize the expression of selected aminoglycoside-permeant channels, such as MET and TRP channels within the cochlea.[49,54,55,57] For instance, TRPV1 expression could be upregulated in the scenario of inflammation[58–60] and translocated from the vesicular reservoir to the plasma membrane via exocytosis.[61] Besides, aminoglycoside antibiotics are commonly used by a topical approach in the context of AOM with or without tympanic perforation in the clinic setting, while the aminoglycoside analog, GTTR, was systemically administered in the present study. Given the rapid middle-ear tissue remodeling and membrane thickening upon the LPS-induced inflammation, it is not straightforward to predict how the efficacy of transtympanic aminoglycosides is modulated. Thus, further studies with local aminoglycoside treatment are warranted, possibly using a variety of OM animal models. Regardless, the results of this study suggest that the pathological cochlea is more susceptible to ototoxic aminoglycosides, providing a novel aspect in searching for ototoxicity countermeasures without compromising their beneficial anti-bacterial properties.

CONCLUSION

LPS-induced AOM rendered the cochlea more susceptible to ototoxicity from aminoglycosides. Cochlear inflammation altered the permeability of the blood-labyrinth barrier, allowing substance in the vasculature to readily enter the inner ear. Thus, the ototoxic risk is elevated in the pathological cochlea, and the clinical concern of aminoglycoside ototoxicity in the AOM treatment is justified.

Acknowledgment

This material is the result of work that was partly supported by the Office of the Assistant Secretary of Defense for Health Affairs through the Peer-Reviewed Medical Research Program No. W81XWH-14-1-0006 (H.L.), by the Office of Research and Development of Veterans Health Association No. RX002813 (H.L.), by the Precision Talent Training Project of Shanghai 9th People's Hospital No. JC201904 (Y.C.), by the Visiting Program for Young and Middle-Aged Scholars of Shanghai Municipal Education Commission (Y.C.), by the Shanghai Key Laboratory of Translational Medicine on Ear and Nose Diseases No. 14DZ2260300 (H.W.), and by the Innovative Research Team of High-Level Local Universities in Shanghai. This work is also supported with resources and the use of facilities at the VA Loma Linda Healthcare System. Opinions, interpretations, conclusions, and recommendations are those of the authors and are not necessarily endorsed by the U.S. Department of Defense, the Department of Veterans Affairs, or the United States Government.

REFERENCES

1. Rovers MM, Schilder AG, Zielhuis GA, Rosenfeld RM. Otitis media. *Lancet* 2004;363:465–473.
2. Forge A, Schacht J. Aminoglycoside antibiotics. *Audiol Neurotol* 2000;5: 3–22.
3. Dai CF, Mangiardi D, Cotanche DA, Steyger PS. Uptake of fluorescent gentamicin by vertebrate sensory cells in vivo. *Hear Res* 2006;213:64–78.
4. Wang Q, Steyger PS. Trafficking of systemic fluorescent gentamicin into the cochlea and hair cells. *J Assoc Res Otolaryngol* 2009;10:205–219.
5. Li H, Wang Q, Steyger PS. Acoustic trauma increases cochlear and hair cell uptake of gentamicin. *PLoS One* 2011;6:e19130.
6. Shi X. Pathophysiology of the cochlear intrastrial fluid-blood barrier (review). *Hear Res* 2016;338:52–63.
7. Hirose K, Li SZ, Ohlemiller KK, Ransohoff RM. Systemic lipopolysaccharide induces cochlear inflammation and exacerbates the synergistic ototoxicity of kanamycin and furosemide. *J Assoc Res Otolaryngol* 2014;15:555–570.
8. Moon SK, Park R, Lee HY, et al. Spiral ligament fibrocytes release chemokines in response to otitis media pathogens. *Acta Otolaryngol* 2006; 126:564–569.
9. Koo JW, Quintanilla-Dieck L, Jiang M, et al. Endotoxemia-mediated inflammation potentiates aminoglycoside-induced ototoxicity. *Sci Transl Med.* 2015;7:298ra118.
10. Harris AS, Elhassan HA, Flook EP. Why are ototopical aminoglycosides still first-line therapy for chronic suppurative otitis media? A systematic review and discussion of aminoglycosides versus quinolones. *J Laryngol Otol* 2016;130:2–7.
11. Jiang M, Wang Q, Karasawa T, Koo JW, Li H, Steyger PS. Sodium-glucose transporter-2 (SGLT2; SLC5A2) enhances cellular uptake of aminoglycosides. *PLoS One.* 2014;9:e108941.
12. Guo H, Li M, Xu LJ. Apigetrin treatment attenuates LPS-induced acute otitis media though suppressing inflammation and oxidative stress. *Biomed Pharmacother* 2019;109:1978–1987.
13. Ishihara H, Kariya S, Okano M, Zhao P, Maeda Y, Nishizaki K. Expression of macrophage migration inhibitory factor and CD74 in the inner ear and middle ear in lipopolysaccharide-induced otitis media. *Acta Otolaryngol* 2016;136:1011–1016.
14. Zhang J, Chen S, Hou Z, Cai J, Dong M, Shi X. Lipopolysaccharide-induced middle ear inflammation disrupts the cochlear intra-strial fluid-blood barrier through down-regulation of tight junction proteins. *PLoS One.* 2015; 10:e0122572.
15. He W, Hetrick A, Sargsyan L, Sun Y, Li H. Modulation of strial macrophages after noise exposure. Paper presented at: *The 42nd ARO Midwinter Research Meeting*. Baltimore, MD. 2019
16. Chen P, Chai Y, Liu H, et al. Postnatal development of microglia-like cells in mouse cochlea. *Neural Plast* 2018;2018:1970150.
17. Choi CH, Jang CH, Cho YB, Jo SY, Kim MY, Park BY. Matrix metalloproteinase inhibitor attenuates cochlear lateral wall damage induced by intratympanic instillation of endotoxin. *Int J Pediatr Otorhinolaryngol* 2012;76:544–548.
18. Spongr VP, Flood DG, Frisina RD, Salvi RJ. Quantitative measures of hair cell loss in CBA and C57BL/6 mice throughout their life spans. *J Acoust Soc Am* 1997;101:3546–3553.
19. Willott JF, Turner JG, Carlson S, Ding D, Seegers Bross L, Falls WA. The BALB/c mouse as an animal model for progressive sensorineural hearing loss. *Hear Res* 1998;115:162–174.
20. Kujawa SG, Liberman MC. Adding insult to injury: cochlear nerve degeneration after "temporary" noise-induced hearing loss. *J Neurosci* 2009;29: 14077–14085.
21. Kujawa SG, Liberman MC. Synaptopathy in the noise-exposed and aging cochlea: primary neural degeneration in acquired sensorineural hearing loss. *Hear Res.* 2015;330:191–199.
22. Liberman MC, Kujawa SG. Cochlear synaptopathy in acquired sensorineural hearing loss: manifestations and mechanisms. *Hear Res* 2017;349:138–147.
23. Fernandez KA, Jeffers PW, Lall K, Liberman MC, Kujawa SG. Aging after noise exposure: acceleration of cochlear synaptopathy in "recovered" ears. *J Neurosci* 2015;35:7509–7520.
24. Edderkaoui B, Sargsyan L, Hetrick A, Li H. Deficiency of Duffy antigen receptor for chemokines ameliorated Cochlear damage from noise exposure. *Front Mol Neurosci.* 2018;11
25. Kaur T, Clayman AC, Nash AJ, Schrader AD, Warchol ME, Ohlemiller KK. Lack of Fractalkine receptor on macrophages impairs spontaneous recovery of ribbon synapses after moderate noise trauma in C57BL/6 mice. *Front Neurodegener* 2019;13.
26. MacArthur CJ, Pillers DA, Pang J, Kempton JB, Trune DR. Altered expression of middle and inner ear cytokines in mouse otitis media. *Laryngoscope* 2011;121:365–371.
27. Ghaheri BA, Kempton JB, Pillers DA, Trune DR. Cochlear cytokine gene expression in murine chronic otitis media. *Otolaryngol Head Neck Surg* 2007;137:332–337.
28. Fredelius L, Rask-Andersen H. The role of macrophages in the disposal of degeneration products within the organ of corti after acoustic overstimulation. *Acta Otolaryngol* 1990;109:76–82.
29. Hirose K, Discolo CM, Keasler JR, Ransohoff R. Mononuclear phagocytes migrate into the murine cochlea after acoustic trauma. *J Comp Neurol* 2005;489:180–194.
30. Tan BT, Lee MM, Ruan R. Bone-marrow-derived cells that home to acoustic deafened cochlea preserved their hematopoietic identity. *J Comp Neurol* 2008;509:167–179.
31. Goodall AF, Siddiq MA. Current understanding of the pathogenesis of autoimmune inner ear disease: a review. *Clin Otolaryngol* 2015;40:412–419.
32. Fujioka M, Okano H, Ogawa K. Inflammatory and immune responses in the cochlea: potential therapeutic targets for sensorineural hearing loss. *Front Pharmacol* 2014;5:287.
33. Malik MU, Pandian V, Masood H, et al. Spectrum of immune-mediated inner ear disease and cochlear implant results. *Laryngoscope* 2012;122: 2557–2562.
34. Iwai H, Baba S, Omae M, Lee S, Yamashita T, Ikehara S. Maintenance of systemic immune functions prevents accelerated presbycusis. *Brain Res* 2008;1208:8–16.
35. Oh S, Woo JI, Lim DJ, Moon SK. ERK2-dependent activation of c-Jun is required for nontypeable Haemophilus influenzae-induced CXCL2 upregulation in inner ear fibrocytes. *J Immunol* 2012;188:3496–3505.
36. Woo JI, Pan H, Oh S, Lim DJ, Moon SK. Spiral ligament fibrocyte-derived MCP-1/CCL2 contributes to inner ear inflammation secondary to nontypeable H. influenzae-induced otitis media. *BMC Infect Dis* 2010;10:314.
37. Hu BH, Cai Q, Hu Z, et al. Metalloproteinases and their associated genes contribute to the functional integrity and noise-induced damage in the cochlear sensory epithelium. *J Neurosci* 2012;32:14927–14941.
38. Li H, Steyger PS. Synergistic ototoxicity due to noise exposure and aminoglycoside antibiotics. *Noise Health* 2009;11:26–32.
39. Govaerts PJ, Claes J, van de Heyning PH, Jorens PG, Marquet J, De Broe ME. Aminoglycoside-induced ototoxicity. *Toxicol Lett* 1990;52: 227–251.
40. Triggs E, Charles B. Pharmacokinetics and therapeutic drug monitoring of gentamicin in the elderly. *Clin Pharmacokinet* 1999;37:331–341.
41. Selimoglu E. Aminoglycoside-induced ototoxicity. *Curr Pharm des* 2007;13: 119–126.
42. Aran JM, Erre JP, Lima da Costa D, Debbarh I, Dulon D. Acute and chronic effects of aminoglycosides on cochlear hair cells. *Ann N Y Acad Sci* 1999; 884:60–68.
43. Imamura S, Adams JC. Distribution of gentamicin in the Guinea pig inner ear after local or systemic application. *J Assoc Res Otolaryngol* 2003;4: 176–195.
44. Steyger PS, Peters SL, Rehling J, Hordichok A, Dai CF. Uptake of gentamicin by bullfrog saccular hair cells in vitro. *J Assoc Res Otolaryngol* 2003;4: 565–578.
45. Zhai F, Zhang R, Zhang T, Steyger PS, Dai CF. Preclinical and clinical studies of unrelieved aural fullness following intratympanic gentamicin injection in patients with intractable Meniere's disease. *Audiol Neurootol* 2013;18:297–306.
46. Li H, Steyger PS. Systemic aminoglycosides are trafficked via endolymph into cochlear hair cells. *Sci Rep.* 2011;1
47. Dai CF, Steyger PS. A systemic gentamicin pathway across the stria vascularis. *Hear Res* 2008;235:114–124.
48. Hashino E, Shero M. Endocytosis of aminoglycoside antibiotics in sensory hair cells. *Brain Res* 1995;704:135–140.
49. Marcotti W, van Netten SM, Kros CJ. The aminoglycoside antibiotic dihydrostreptomycin rapidly enters mouse outer hair cells through the mechano-electrical transducer channels. *J Physiol* 2005;567:505–521.
50. Hiel H, Schamel A, Erre JP, Hayashida T, Dulon D, Aran JM. Cellular and subcellular localization of tritiated gentamicin in the Guinea pig cochlea following combined treatment with ethacrynic acid. *Hear Res* 1992;57: 157–165.
51. Sandoval RM, Dunn KW, Molitoris BA. Gentamicin traffics rapidly and directly to the Golgi complex in LLC-PK(1) cells. *Am J Physiol Renal Physiol* 2000;279:F884–F890.
52. Nagai J, Komeda T, Yumoto R, Takano M. Effect of protamine on the accumulation of gentamicin in opossum kidney epithelial cells. *J Pharm Pharmacol* 2013;65:441–446.
53. Li H, Kachelmeier A, Furness DN, Steyger PS. Local mechanisms for loud sound-enhanced aminoglycoside entry into outer hair cells. *Front Cell Neurosci* 2015;9:130.
54. Myrdal SE, Steyger PS. TRPV1 regulators mediate gentamicin penetration of cultured kidney cells. *Hear Res* 2005;204:170–182.
55. Tanaka R, Muraki K, Ohya S, et al. TRPV4-like non-selective cation currents in cultured aortic myocytes. *J Pharmacol Sci* 2008;108:179–189.
56. Alharazneh A, Luk L, Huth M, et al. Functional hair cell mechanotransducer channels are required for aminoglycoside ototoxicity. *PLoS One.* 2011;6:e22347.
57. Karasawa T, Wang Q, Fu Y, Cohen DM, Steyger PS. TRPV4 enhances the cellular uptake of aminoglycoside antibiotics. *J Cell Sci* 2008;121:2871–2879.
58. Engler A, Aeschlimann A, Simmen BR, et al. Expression of transient receptor potential vanilloid 1 (TRPV1) in synovial fibroblasts from patients with osteoarthritis and rheumatoid arthritis. *Biochem Biophys Res Commun* 2007;359:884–888.
59. Cho WG, Valtschanoff JG. Vanilloid receptor TRPV1-positive sensory afferents in the mouse ankle and knee joints. *Brain Res* 2008;1219: 59–65.
60. Akbar A, Yiangou Y, Facer P, Walters JR, Anand P, Ghosh S. Increased capsaicin receptor TRPV1-expressing sensory fibers in irritable bowel syndrome and their correlation with abdominal pain. *Gut* 2008;57: 923–929.
61. Planells-Cases R, Valente P, Ferrer-Montiel A, Qin F, Szallasi A. Complex regulation of TRPV1 and related thermo-TRPs: implications for therapeutic intervention. *Adv Exp Med Biol* 2011;704:491–515.